Telomerase a prognostic marker and therapeutic target

By

Dipti S. Thakkar

A thesis submitted to the University of Central Lancashire in partial fulfilment of the requirements for the degree of Doctor of Philosophy

Month Year submitted: June 2010

Declaration

I declare that while registered as a candidate for this degree I have not been registered as a candidate for any other award from an academic institution. The work present in this thesis, except where otherwise stated, is based on my own research and has not been submitted previously for any other award in this or any other University.

DIPTI THAKKAR

Signed

Abstract

Malignant glioma is the most common and aggressive form of tumours and is usually refractory to therapy. Telomerase and its altered activity, distinguishing cancer cells, is an attractive molecular target in glioma therapeutics. The aim of this thesis was to silence telomerase at the genetic level with a view to highlight the changes caused in the cancer proteome and identify the potential downstream pathways controlled by telomerase in tumour progression and maintenance. A comprehensive proteomic study utilizing 2D-DIGE and MALDI-TOF were used to assess the effect of inhibiting two different regulatory mechanisms of telomerase in glioma. RNAi was used to target hTERT and Hsp90α.

Inhibition of telomerase activity resulted in down regulation of various cytoskeletal proteins with correlative evidence of the involvement of telomerase in regulating the expression of vimentin. Vimentin plays an important role in tumour metastasis and is used as an indicator of glioma metastasis. Inhibition of telomerase via si*hTERT* results in the down regulation of vimentin expression in glioma cell lines in a grade specific manner. While, 9 of 12 glioblastoma tissues (grade IV) showed vimentin to be highly expressed, its expression was absent in lower grades and normal tissues. This suggests that vimentin can be potentially used as a glioma progressive marker. This is the first study to report the potential involvement of telomerase in the regulation of vimentin expression. This study also identified that combination therapy, comprising siRNA targeted towards telomerase regulatory mechanisms and the natural product Epigallocatechin-3-gallate (ECGC), results in decreased cell viability producing comparable results to that of other chemotherapeutic drugs.

List of publications:

This thesis has led to the following publications:

1. Cruickshanks, N., Shervington, L., Patel, R., Munje, C., Thakkar, D., Shervington, A. Can hsp90alpha-Targeted siRNA Combined With TMZ Be a Future Therapy for Glioma? Cancer Invest. 2010. DOI: 10.3109/07357901003630967.

2. Shervington, A., Pawar, V., Menon, S., Thakkar, D., Patel, R. The sensitization of glioma cells to cisplatin and tamoxifen by the use of catechin. Mol. Biol. Rep. 2009;36(5):1181-1186.

3. Thakkar, D, Shervington, A. Proteomics: the tool to bridge the gap between the facts and fables of telomerase. Crit Rev Oncog. 2008;14(4):203-215.

4. Thakkar, D., Shervington, L., Shervington, A. Insight into glioma metastasis mechanism by regulation of vimentin via telomerase: the unnamed soldier identified by proteomic studies. Submitted to Cancer Investigations (accepted manuscript).

To My Loving Family

Contents

List of Figures

List of Tables

ACKNOWLEDGEMENT

I owe my gratitude to all the people in my life who have made this research possible by supporting me in different ways and because of whom my graduate experience has been one that I will cherish forever.

First and foremost I would like to thank my supervisor Dr. Amal Shervington for her constant support and guidance. She encouraged me to not only grow as an experimentalist but also as an independent thinker. I cannot thank Dr. Shervington enough for her incessant patience and support especially during the revisions of this manuscript. She not only guided me with my research but also taught me how to put your best foot forward when life does not go your way. I have been amazingly fortunate to have an advisor whose mentorship was paramount in providing a well rounded experience consistent with my long-term career goals. For everything you've done for me, Dr. Shervington, I thank you.

I would like to thank all my colleagues, especially Dr. Rahima Patel, Chinmay Munje and Zarine Khan for helping me on a daily basis with all my difficulties and for some much needed humour and entertainment in what could have otherwise been a somewhat stressful laboratory environment. I am very grateful to them for going out of their way and removing time to help me during the writing of this thesis. Thanks especially to Dr. Leroy Shervington, who has read through my draft copies, for encouraging the use of correct grammar and consistent notation in my writings and for carefully reading and commenting on countless revisions of this manuscript.

Many friends have helped me stay sane through these difficult years. I would like to especially thank Krupa Shah, Krunal Khamkar, Chinmay Munje and Saif Khan for listening to all my moaning and complaining and yet supporting and encouraging me and bringing me food in the middle of the night to keep me going. Their support and care helped me overcome setbacks and stay focused on my graduate study. I also would like to thank GHS for making me feel close to home in a foreign country and providing me the much needed cultural relief.

I owe my deepest gratitude to my family who mean the world to me. I appreciate everything that they have done for me. Their support, encouragement, quiet patience and unwavering love are the pillars of my life. I would also like to thank my immediate family, who has been a constant source of love, concern, support and strength all these years. I would like to dedicate this thesis to my father Shailesh Thakkar, Mother Prafulla Thakkar, my brother Divyesh Thakkar and my sister-in-law Binal Thakkar. I deeply value their belief in me and allowing me to be as ambitious as I wanted

Last but not the least I would like to thank GOD for blessing me and making me fortunate and giving me a chance to fulfil my ambitions. May your name be exalted, honoured, and glorified.

ABBREVIATIONS

2D-DIGE	Two-dimensional differential in-gel electrophoresis
2DE	Two-dimensional electrophoresis
2D-PAGE	Two-Dimensional Polyacrylamide Gel Electrophoresis
67LR	67kDA laminin receptor
ACTB	Beta-actin
ALT	Alternative lengthening of telomeres
AMV	Avian Myeloblastosis Virus
ANXA1	Annexin 1
AP1	Activator protein 1
AP2	Activator protein 2
ATF	Activating transcription factor
BTNW	Brain Tumour Northwest
CB	Cajal body
CDK4	Cyclin dependent kinase 4
cDNA	Complementary deoxyribonucleic acid
CFLI	Cofilin 1
CNS	Central nervous system
CpG	Cytidine-phosphate-guanosine
CREB	cAMP-responsive element binding protein
Ct	Cycle threshold
Cy	Fluorescent cyanide
dbSNP	Database of Single Nucleotide Polymorphisms
DCK1	Dyskerin
DMSO	Dimethyl sulphoxide
DNA	Deoxyribonucleic acid
DNMT1	DNA methyltransferase 1

dsDNA	Double stranded ribonucleic acid
DTT	Dithiothreitol
E2F-1	E2F transcription factor 1
ECACC	European collection of cell cultures
ECGC	Epigallocatechin-3-gallate
EF2	Elongation factor 2
EGFR	Epidermal growth factor receptor
Egr-1	Early growth response 1
EMBL	European molecular biology laboratory
EMT	Epithelial-mesenchymal transition
ER	Endoplasmic reticulum
ESI	Electrospray ionization
FBS	Fetal bovine serum
FITC	Fluorescein Isothiocyanate
FTIC	Fourier transform ion cyclotron
GAPDH	Glyceraldehyde-3-phosphate dehydrogenase
GBM	Glioblastoma multiforme
GSTP1	Glutathione S-transferase P1
H&E	Hematoxylin and eosin
hMSCs	Human bone marrow mesenchymal stem cells
hnRNPs	Heterogeneous nuclear ribonucleoproteins
HOP	Hsp-organizing protein
HPRD	Human protein research database
hRAP1	Human repressor activator protein 1
Hsp40	Heat shock protein 40
Hsp70	Heat shock protein 70
Hsp90	Heat shock protein 90
hStau	Human staufen

hTERT	Human telomerase reverse transcriptase
hTR	Human telomerase RNA
ICAT	Isotope-coded affinity tag
IEF	Isoelectric focusing
IgG	Immunoglobulin G
IgM	Immunoglobulin M
IK2	Ikaros2
Ilk signaling	Integrin linked kinase signaling
IPA	Ingenuity Pathway Analysis
IPGs	Immobilized pH gradients strips
iTRAQ	Isobaric tagging for relative and absolute quantitation
kDa	KiloDalton
MALDI-TOF	Matrix-assisted laser desorption/ionization time-of-flight
MLCK	Myosin light chain kinase
MRCL3	Myosin regulatory light chain variant 3
MRN complex	Mre11/Rad50/Nbs1 complex
mRNA	Messenger ribonucleic acid
MudPIT	Multidimensional protein identification technology
MW	Molecular weight
MYOD	Myoblast determining factor
MZF-2	Myeloid specific zinc finger protein 2
NCBI	National Centre for Biotechnology Information
NCBInr	National Center for Biotechnology Information non-redundant
NF1	Nuclear factor 1
OD	Optical density
p53	Protein 53
PAGE	Polyacrylamide gel electrophoresis
PARP	Poly(ADP-ribose) polymerase

PCR	Polymerase chain reaction
PI	Propidium iodide
pI	Iso-electric point
PML	Promyelocytic leukaemia
POT1	Protection of telomere protein 1
PR	Progesterone receptor
qRT-PCR	Quantitative real-time polymerase chain reaction
RAN	Ras-related nuclear protein
Rb	Retinoblastoma
RISC	RNA-Induced Silencing Complex
RNA	Ribonucleic acid
RISC	RNA induced silencing complex
RNH1	Ribonuclease inhibitor
RRP0	Ribosomal protein P0 variant
SDS-PAGE	Sodium dodecyl sulphate polyacrylamide gel electrophoresis
SILAC	Stable isotope labelling with amino acids in cell culture
siRNA	Small interference ribonucleic acid
SNP	Single nucleotide polymorphisms
Sp1	Stimulating protein 1
ssRNA	Single stranded ribonucleic acid
T3R α	Thyroid hormone receptor α
TAE	Tris-acetate-EDTA
TBE	Tris-borate-EDTA
TCAB1	Telomerase cajal body protein 1
TEP1	Human telomerase-associated protein 1
TIN2	TRF1-interacting protein 2
T_m	Melting temperature
TNKS	Tankyrase

TRAP	Telomeric repeat amplification protocol
TRF1	Telomere repeat binding factor 1
TRF1	Telomere repeat factor 1
TRF2	Telomere repeat binding factor 2
TRF2	Telomere repeat factor 1
U87-MG-sihsp90α	U87-MG cells after silencing hsp90α
U87-MG-sihTERT	U87-MG cells after silencing hTERT
USF 1	Upstream stimulatory factor
USF 2	Upstream stimulatory factor
UV	Ultra violet
V	Volts
v/v	Volume/Volume
w/v	Weight/Volume
WHO	World Health Organisation
WT1	Wilms' tumour suppressor 1

CHAPTER 1

INTRODUCTION

1. Introduction

Cancer is a perversion of cellular genotype and phenotype marked by unrestrained and invasive growth of genetically transformed cells. These genetically transformed cells cause disruption of the complex and interdependent condominium of cells which otherwise leads to multicellularity in a healthy body. The incidence of cancer is expected to double on a global scale over the next decade (Eaton, 2003). In England it is estimated that by 2020 the incidence of cancer will increase by 33 % thereby accounting for 299 000 cases in 2020 in contrast to 224 000 in 2001 (Moller *et al*., 2007). Cancer results in the deregulation of a number of signal transduction pathways, molecules involved in DNA repair, cell cycle checkpoints, cellular apoptosis and invasion. This makes cancer a very complex and dynamic disease.

1.1 Hallmarks of cancer

Hanahan and Weinberg succinctly summarised the essential alterations in the cellular physiology that collectively dictates the malignant transformation of cells into six hallmarks of cancer. Each of these hallmarks breach the anticancer mechanism, hardwired in the cells, and are commonly shared in almost all types of cancers (Hanahan and Weinberg, 2000). These hallmarks are shown in Fig 1.1 and can be described as follows:

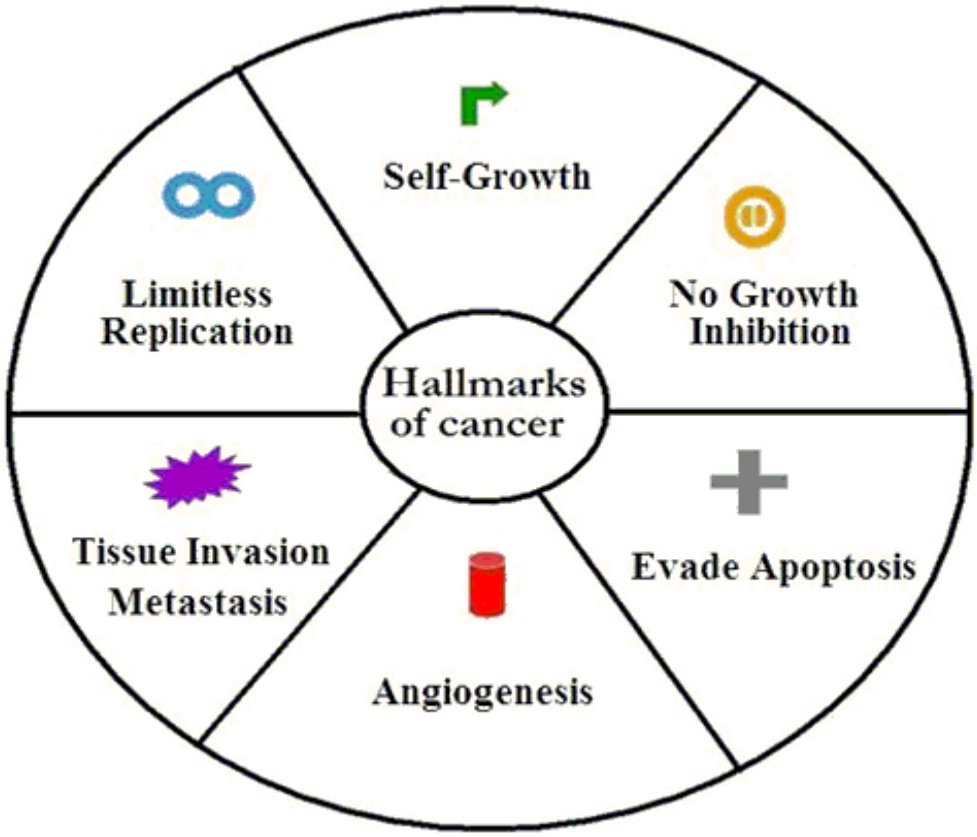

Figure 1.1 Hallmarks of cancer as described by Hanahan and Weinberg (2000).

1.1.1 Self-sufficiency in growth signals

Cell proliferation is rigidly controlled by signaling molecules, bound to transmembrane receptors, which prompt cellular growth and division. Mutations in cancer cells results in over expression of growth factors or their receptors causing hypersensitivity to growth signals which in turn imparts self-sufficiency in growth signals. An example of this mechanism is the activation of H-Ras oncogene which encodes proteins involved in regulating cell division when stimulated by growth factor (Hanahan and Weinberg, 2000).

1.1.2 Insensitivity to growth-inhibitor signals

Cellular growth and development is regulated by an intricate network of positive and negative feedback loops. Cancer cells ignore the anti-growth signals and continue to proliferate maintaining replicative potential. An example of this process is the loss the retinoblastoma protein (pRB), a tumour suppressor gene, which makes the cancer cells insensitive to the growth-inhibitory signals (Hanahan and Weinberg, 2000).

1.1.3 Evasion of apoptosis

Factors such as DNA damage, insufficiency of cell survival factors, imbalanced signaling, over expression of oncogenes and hypoxia act as sensors and initiate programmed cell death in normal cells. In cancerous cells this mechanism is violated, cells evade apoptosis and continue to divide. A classic example of a mechanism that aids to evade apoptosis is the expression of a muatated p53 tumour suppressor gene in over 50% of human cancer (Hanahan and Weinberg, 2000).

1.1.4 Sustained angiogenesis

Angiogenesis is necessary for tumour invasion and metastasis. In cancer cells the process of angiogenesis is deregulated causing an over-production of angiogenic inducers and a lack of angiogenic inhibitors or both. The over-production of vascular endothelial growth factor which stimulates the growth of new blood vessels is an example of how cancer cells sustain angiogenesis.

1.1.5 Tissue Invasion and Metastasis

Metastasis is the ultimate stage of cancer development. Tumour cells migrate from their primary site of development and invade distant locations in the body. Following invasion, cancer cells transit the extracellular matrix, intravasate and traverse the blood vessels, extravasate and grow at secondary sites. Metastasis can be characterised by disruption of cell adhesion molecules and integrins and increased proteolysis which facilitates tissue invasion. An example of this mechanism is the inactivation of transmembrane proteins E-cadherin, which regulates cell adhesion in normal cells (Hanahan and Weinberg, 2000).

1.1.6 Limitless replicative potential

Normal cells undergo senescence after a fixed number of divisions known as the Hayflick Limit. DNA polymerase is unable to completely replicate the chromosome due to the end replication problem. This result in progressive loss of the chromosomal end called telomere (section 1.2). With each division the repetitive telomere sequence loses 50-100 base pairs which ultimately results in the exposure of chromosomal DNA, senescence and cell death. Tumour cells develop a mechanism to overcome this problem by expressing the enzyme telomerase which protects the telomeres from shortening. Telomeres can also be lengthened through homologous recombination. As a result, tumour cells never grow old and continue to replicate (Hanahan and Weinberg, 2000).

1.2 Telomere and telomerase

Telomerase plays a key role in the acquisition of cancer phenotype by aiding the unlimited replicative potential which as explained earlier is a hallmark of cancer. Telomeres have been defined as the functional chromosomal ends by H.J. Muller and identified by Barbara McClintock, six years before the identification of DNA as hereditary material by Oswald Avery (McClintock, 1939; Muller, 1938).

Human telomeres are tracts of repetitive hexameric DNA sequences (TTAGGG), around 15-20 kilobase in size at birth, and are followed by a 3' single-strand, G-rich overhang (Shay and Gazdar, 1997). They are located at the end of chromosomes, and their maintenance is essential for cell survival as they provide a buffer of potentially expendable DNA that protects the chromosomes from degradation and loss of essential genes that could be lost during cell division (Pendino *et al*., 2006). They protect the cell from end to end fusion by forming special t-loop like structures, thereby allowing the cell to distinguish between double-strand breaks and natural chromosome ends, thus maintaining chromosomal integrity (Griffith *et al*., 1999).

During cell division, DNA dependent DNA polymerase cannot replicate the extreme ends of the chromosome on the lagging strand due to the putative 5' to 3' exonuclease effect of the conventional DNA polymerases. Since no primer is bound at the extreme 5' end of each chromosome, there is a gap in replication, leading to a progressive shortening of daughter strands with each round of DNA replication (Olovnikon, 1973). This is known as the 'end replication problem' and results in the loss of telomeric material with each division. When

a critical telomere length is reached the cells exit the cell cycle and undergo senescence marked by growth arrest during the GI phase. These cells are in an irreversible arrest phase whereby they are unable to undergo further cell divisions. Though senescent cells are unable to divide they can continue metabolic activities (Dimri *et al*., 1995; Shay and Roninson, 2004).

Telomerase, a multi-subunit, ribonucleoprotein holoenzyme, plays a pivotal role in telomere maintenance (Shay and Gazdar, 1997, Pendino *et al*., 2006). In human cells, telomerase functions as a reverse transcriptase to add multiple copies of the 5'-GGTTAG-3' motif to the end of the G-strand of the telomere, thereby compensating the end replication problem. Telomerase is composed of two core subunits; telomerase reverse transcriptase hTERT, the catalytic subunit and a functional RNA subunit hTR which serves as a template for telomeric DNA synthesis as shown in Fig 1.2.

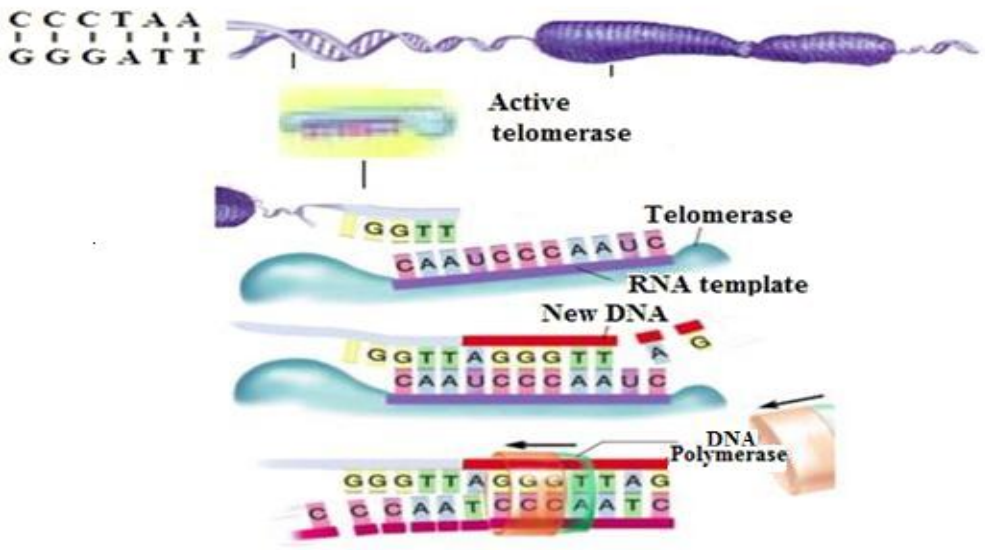

Figure 1.2 Telomere length regulation by telomerase solving the end replication problem (adapted from stemcells.nih.gov/info/scireport/appendixC.asp accessed on 15 April 2010).

hTERT gene is present as a single copy on chromosome 5 at 5p15.3 and encodes for a 127 kDa protein with a net basic charge and c-terminal reverse transcriptase motifs. The hTERT adds hexameric repeats using its intrinsic RNA as a template for reverse transcription (Fan *et al*., 2003). The *hTR* gene is present as a single copy on chromosome 3 at 3q26.3. The RNA moiety is 445 nucleotides long with a 5'-CUAACCCUAAC-3' template sequence (Collins and Mitchell 2002; Keith *et al*., 2002). By reverse transcription, telomerase makes a DNA copy of its own RNA sequence, which is then fused to the 3' terminus of the chromosome.

Telomerase activity is repressed in most somatic cells and telomeres progressively shorten, leading to proliferative senescence. Exceptions to these are male germ line cells, activated lymphocytes, proliferating progenitor cells hematopoietic proliferating stem-like cells, the common feature of these telomerase positive cells being their high regenerative capacity. Literature has shown considerable evidence proving that telomerase activity is regulated by cellular proliferation (Shay and Gazdar, 1997; Hiyama and Hiyama, 2003, Dome *et al*., 1999 and Elenitoba-Johnson, 2001). Tumours bypass cellular senescence by abrogating important cell-cycle checkpoints like p53, p21, $p16^{INK4a}$ and pRb. This leads to extended growth which leads to crisis (Wright *et al*., 2001; Cong *et al*., 2002) eventually leading to activation or upregulation of telomerase. Telomerase is found to be activated in approximately 85% of human cancer tissues which makes it an attractive target for anti-cancer therapy. Furthermore, the biology of telomere and the telomerase holds substantial promise in uncovering the molecular process of the treatment of cancers (Shay and Gazdar, 1997; Hiyama and Hiyama, 2003).

Some immortal cells can maintain telomere length even in the absence of telomerase via an alternative lengthening of telomere (ALT) mechanism. ALT is a non-conservative telomere lengthening pathway implicating homologous recombination and transfer of telomere tandem repeats between sister-chromatids wherein one telomere terminus is invaded by another single-stranded DNA telomere which uses it as a copy template (Henson *et al*., 2002; Nittis *et al*., 2008). ALT can be characterized by heterogeneous telomere length and presence of abundant of promyelocytic leukaemia (PML) nuclear bodies at the telomeric level (Nittis *et al*., 2008). These ALT-associated PML bodies (APBs) contain extrachromosomal telomeric DNA, telomere-specific binding proteins, and proteins involved in DNA recombination and replication. The mechanism for the regulation of ALT has not yet been fully elucidated and much remains to be identified. ALT adds complexity to the regulation of the telomere and poses a challenge for the development of anti-cancer therapies targeting the telomere (Henson *et al*., 2005; Jeyapalan *et al*., 2005; Jiang *et al*., 2005). ALT, however, is a minor pathway and has been reported to be present in only 10% of the tumours and is not the focus of the current thesis.

1.2.1 Regulation of telomerase by telomerase associated proteins

Telomerase is composed of two core subunits, telomerase reverse transcriptase hTERT which is the catalytic subunit of telomerase and a functional RNA subunit hTR which serves as a template for telomeric DNA synthesis (Elenitoba-Johnson, 2001). hTR is expressed in all tissues irrespective of telomerase activity, with cancer cells generally exhibiting a five fold higher expression than normal cells (You *et al*., 2006). Antisense

hTR experiments have shown to repress telomerase activity and mRNA levels of both *hTR* and *hTERT* thereby making it an important target in cancer therapy (You *et al*., 2006).

hTERT is generally repressed in normal cells and upregulated in immortal cells, suggesting that hTERT is the primary determinant for the enzyme activity (Avilion *et al*., 1996). On average, *hTERT* mRNA is estimated to be present between 1 to 30 copies per cell and is closely associated with telomerase activity (Yi *et al*., 2001; Shervington and Patel, 2008). Both, hTR and hTERT are required for the function of the telomerase enzyme (Cairney and Keith, 2008), and due to the complexity of hTR and hTERT regulations, this project mainly focused on the catalytic subunit (hTERT).

Telomerase activity is regulated at multiple levels, one of which is the association of telomerase with various proteins such as human telomerase-associated protein 1, dyskerin, tankyrase, pontin and Hsp90. These proteins mediate and/or regulate the association of telomerase with the telomere. They also play a role in the assembly of the holoenzyme (Elenitoba-Johnson, 2001; Keith *et al*., 2007; Toogun *et al*., 2008). The human telomerase-associated protein 1 (hTEP1), is the functional equivalent of the p80 component of *Tetrahymena* telomerase and associates with both hTR as well as hTERT (Harrington, 1997). The precise mechanism and significance of this subunit still remains unclear, with only a few investigations suggesting that disruption of the protein has no effect on telomerase activity *in vivo* (Liu *et al*., 2000). Dyskerin is a crucial component of telomerase and is required for the stabilization of the RNA component of telomerase (Cong *et al*., 2002). A complex of hTERT, hTR and dyskerin has been proposed to be the protein composition of the catalytically active human telomerase in immortal cells (Cohen *et al*., 2007). ATPases pontin and reptin have been recently identified as telomerase components

playing a role in the assembly of telomerase. Pontin interacts with both hTERT and dyskerin (Venteicher *et al*., 2008). In addition, L22 and human staufen (hStau) have also been reported to be associated with telomerase. The precise role of these proteins is still unclear, however it has been suggested that they play a role in the assembly of telomerase and in the processing and localization of hTR (Le *et al*., 2000). Recent findings have shown that La autoantigen interacts with hTR and influences telomere length *in vivo* (Ford *et al*., 2001). Furthermore, TCAB1 (telomerase Cajal body protein 1) has been reported to act as a regulatory subunit of the telomerase holoenzyme by controlling telomerase trafficking. TCAB1 is required for telomerase synthesis and cajal body localization (Venteicher *et al*., 2009). Results from our laboratory have shown the presence of hTEP1, dyskerin, Tankyrase (Shervington *et al*., 2007) and Hsp90 (Shervington *et al*., 2006) in glioma cell lines and tissues.

Several telomere associated proteins influence telomerase which poses an additional step in the regulation of telomerase activity. These proteins play a part in regulating the recruitment and accessibility of the telomere to telomerase. These includes proteins such as telomere repeat factor 1 (TRF1) and factor 2 (TRF2) which negatively regulates telomere length; over expression of these proteins leads to telomere shortening (Smogorzewska *et al*., 2000). Tankyrase 1 and 2 are positive regulators of telomere length; they bind to TRF1 and ADP-ribosylate, thereby inhibiting its binding to the telomere (Seimiya, 2006). In contrast, TRF1-interacting protein 2 (TIN2) protects TRF1 from being modified by tankyrase and negatively regulates telomere length (Kim *et al*., 2002). The protection of telomere protein 1 (POT1) acts as a negative as well as a positive regulator of telomerase. As a negative regulator, it binds to the 3'overhang thereby inhibiting access of telomerase

to the telomere and inhibits telomere elongation; as a positive regulator it stabilizes the open structure of the chromosome and helps in the recruitment of telomerase onto the telomere (Liu, 1999; Cong *et al*., 2002; Colgin *et al*., 2003). Besides these, TRF2 interacts with repressor activator protein 1 (hRap1) and the MRN complex Mre11/Rad50/Nbs1 DNA repair complex (Karlseder *et al*., 1999). Also, heterogeneous nuclear ribonucleoproteins (hnRNPs), and poly(ADP-ribose) polymerase (PARP) have been reported to influence telomere length (Liu, 1999; Ford *et al*., 2001).

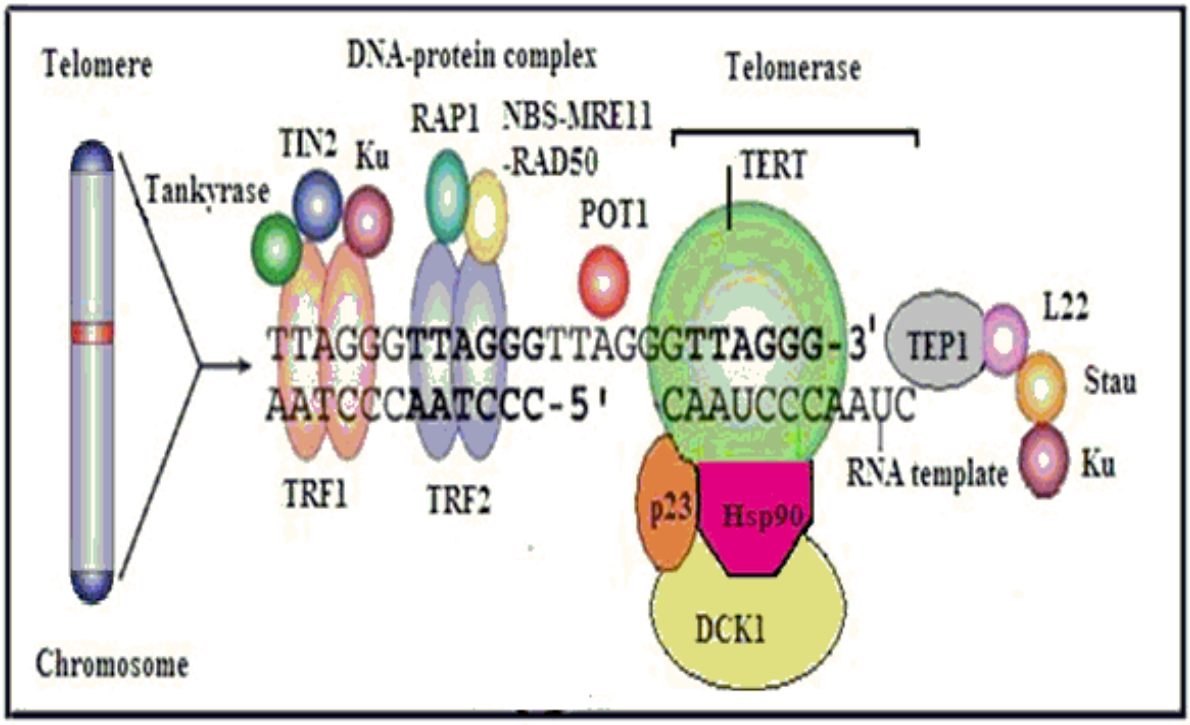

Figure 1.3 Schematic representation of the composition of telomeric complexes, telomerase and their regulatory proteins (adapted from Hodes *et al.*, 2002).

1.2.2 Regulation of hTERT by transcriptional factors

There is numerous data that provides evidence that transcriptional regulation is one of the key regulating mechanisms of telomerase (Horikawa and Barrett, 2003). *hTERT* gene is composed of 16 exons and 15 introns spanning more than 40 kb. Cloning of the *hTERT* promoter has revealed a GC-rich promoter which contains several sites for transcriptional binding factors and has no detectable TATA or CAAT boxes (Cong *et al*., 1998). The 330 bp upstream has been reported to be the core promoter regulating *hTERT* activity (Takakura *et al*., 1999). In addition, *hTERT* promoter has also been shown to contain GC boxes that are potential binding sites for stimulating protein 1 (Sp1), a general transcription factor that binds to the promoter GC-box, enhancer and locus control regions to activate a large number of genes (Takakura *et al*., 1999; Janknecht, 2004). The presence of several E boxes (CACGTG), which are the binding sites for the Myc/Max/Mad network and upstream stimulatory factor (USF 1 / 2) have been reported. Myc/Max heterodimers and USF 1 / 2 act as activators (Cong *et al*., 1998; Janknecht, 2004; Flores *et al*., 2006) in contrast with Mad/Max which act as a repressor complex (Cong *et al*., 1998, Cong *et al*., 2002). Sequence analyses of the *hTERT* promoter have also revealed the presence of E2F transcription factor 1 (E2F-1) (Cong *et al*., 1998; Crowe *et al*., 2001) and two potential estrogen response elements (Janknecht, 2004). Estrogen activates telomerase in hormone sensitive tissues through a direct transcriptional regulation of *hTERT* (Cong *et al*., 1998; Janknecht, 2004). The Wilms' tumour suppressor 1 (WT1) (Cong *et al*., 2002; Oh *et al*., 1999), myeloid specific zinc finger protein 2 (MZF-2) (Cong *et al*., 1998; Fujimoto *et al*., 2000) and a novel transcription factor binding element MT box (Tzukerman *et al*., 2000) have also been identified within the *hTERT* promoter. Moreover, transcription factors such

as activator protein 1 (AP1), activator protein 2 (AP2), activating transcription factor (ATF), cAMP-responsive element binding protein (CREB), Ikaros2 (IK2), myoblast determining factor (MYOD), nuclear factor 1 (NF1), progesterone receptor (PR), and thyroid hormone receptor α (T3R α) have all been identified using MatInspector software (Cong *et al*., 2002; Horikawa *et al*., 1999). The presence of all the above listed transcriptional factors suggests that *hTERT* expression is controlled at multiple levels. While oncogenes such as *SV40*, *K-ras*, *Akt*, protein kinase C, bcl-2, 2c-Abl, and oncogenic variants of HPV E6 proteins and C-MYC induce *hTERT* expression, tumour suppressor genes such as pRB, autocrine transforming growth factor, p21 and Waf-131 actually suppress it (Elenitoba-Johnson, 2001; Cong *et al*., 2002; Horikawa and Barrett, 2003).

1.2.3 Regulation of telomerase by epigenetic, post-transcriptional and post-translation modifications

The highly GC-rich CpG island has been identified within the *hTERT* promoter suggesting an allowance for epigenetic modulation via promoter methylation. Depending on the cellular context of the study undertaken, the CpG island methylation of the *hTERT* promoter is associated with either enhancing or repressing telomerase activity (Guilleret and Benhattar, 2003; Patel *et al*., 2008). Guilleret and Benhattar`s data demonstrated an upregulation of hTERT activity due to methylation (Guilleret and Benhattar, 2003), in contrast to the results obtained from our laboratory showing that inhibition of the DNA methyltransferase gene *DNMT1* using siRNA, reduces telomerase activity (Patel *et al*., 2008).

In addition to methylation, epigenetic modifications such as the modulation of nucleosome histones, play key roles in the regulation of the *hTERT* promoter (Kyo *et al*., 2008). Dynamic histone methylation mediated by histone methyltransferases and demethylases regulate chromatin structure and *hTERT* transcription (Kyo *et al*., 2008).

Telomerase activity can also be regulated by post transcriptional mechanisms. Kilian and colleagues were among the first to suggest that alternative splicing of *hTERT* transcripts may be an important regulatory mechanism of the telomerase activity (Kilian *et al*., 1997).

To date, six alternative splicing sites have been proposed which includes two deletion sites and four insertion sites. These variants produce mRNA that lacks the critical reverse transcriptase motif. Out of the six splice variants, four insertion variants and one deletion (β site) variant result in premature termination of the translation process. The second deletion (α site) splice variant causes a 36 bp deletion within the reverse transcriptase motif and has been shown to inhibit telomerase activity causing telomere shortening and cell death. However, none of the splice variants have been able to reconstitute telomerase activity. It has also been demonstrated that cells can shift their expression from a full-length active variant to a β-splice variant which is inactive (Ulaner *et al*., 1998; Yi *et al*., 2001).

Post-translation modifications such as protein phosphorylation, can also regulate telomerase activity via mediators such as *Akt* and various isoforms of protein kinase C (Kang *et al*., 1999). Post-translational modifications of telomerase may also involve the interaction of hTERT with accessory proteins, chaperones, and polypeptide modifiers (Lee *et al*., 2004; Holt *et al*., 1999).

Increasing the complexity of telomerase regulation, a senescence-inducing gene on chromosome 3 has also been reported to suppress the telomerase activity in breast and renal carcinomas. Two regions on the short arm of chromosome 3 (3p21.3-p22 and 3p12-21.1) where these regulatory genes may be located have been proposed, however the nature of these 3p genes still remains to be identified (Cuthbert *et al*., 1999).

1.2.4 Regulation of telomerase by chaperone Hsp90

The Hsp90 chaperone complex is the first known set of proteins that physically and functionally interact with human telomerase (Cong *et al*., 2002). They play a role in regulating the assembly and formation of an active telomerase by binding to hTERT, thereby influencing its assembly with hTR. Hsp90 chaperone complex is composed of at least Hsp90, p23, Hsp70, Hsp-organizing protein (HOP) and Hsp40. Hsp90 and p23 are found to bind hTERT protein to promote the assembly of the active telomerase complex *in vivo*. Hsp70 and its counterpart, Hsp40, are known to provide energy to the Hsp90/p23 complex and their physical interaction is facilitated by a unique co-chaperon, HOP (Cong *et al*., 2002; Holt and Shay, 1999). There are contrasting views about the requirement of these other chaperones as pre-requisites for telomerase activity (Forsythe *et al*., 2001; Shervington *et al*., 2006). Thus, Hsp90 plays a key role in telomerase regulation and is essential for efficient telomerase assembly (Forsythe *et al*., 2001; Shervington *et al*., 2006). The Hsp90 inhibitor, geldanamycin, has been shown to prevent the assembly of active telomerase (Shervington *et al*., 2006; Ford *et al*., 2001). Results from our laboratory have

shown that siRNA directed towards *hsp90α* not only completely silences *hsp90α* but also results in almost 90% silencing of *hTERT* (unpublished data).

Hsp90 is an abundantly expressed and highly conserved protein belonging to the family of the heat shock proteins. It is a molecular chaperone and helps in the folding of several client proteins. It is involved in cell cycle progression, apoptosis, and plays a role in malignant phenotypes associated with invasion, angiogenesis and metastasis (Yi *et al*., 2001). There are over 100 known Hsp90 client proteins which include many kinases, like epidermal growth factor receptor (EGFR) and cyclin dependent kinase 4 (CDK4), transcription factors such as estrogen and androgen receptors, Hypoxia inducible factor 1, p53, survivin and hTERT (Workman *et al.*, 2007). Since Hsp90 client proteins have an effect on such a diverse range of cellular proteins, the therapeutic potential of targeting Hsp90 may be best appreciated by considering the possibility of simultaneously targeting the six hallmarks of a cancer cell. Hsp90 inhibition alters the various cancer dependencies and antagonizes all of the hallmark pathological traits of malignant cells (Xu and Neckers, 2007) (Fig.1.4). Hence in this study silencing of *hsp90* was selected as the indirect regulatory mechanism for inhibiting the activity of telomerase.

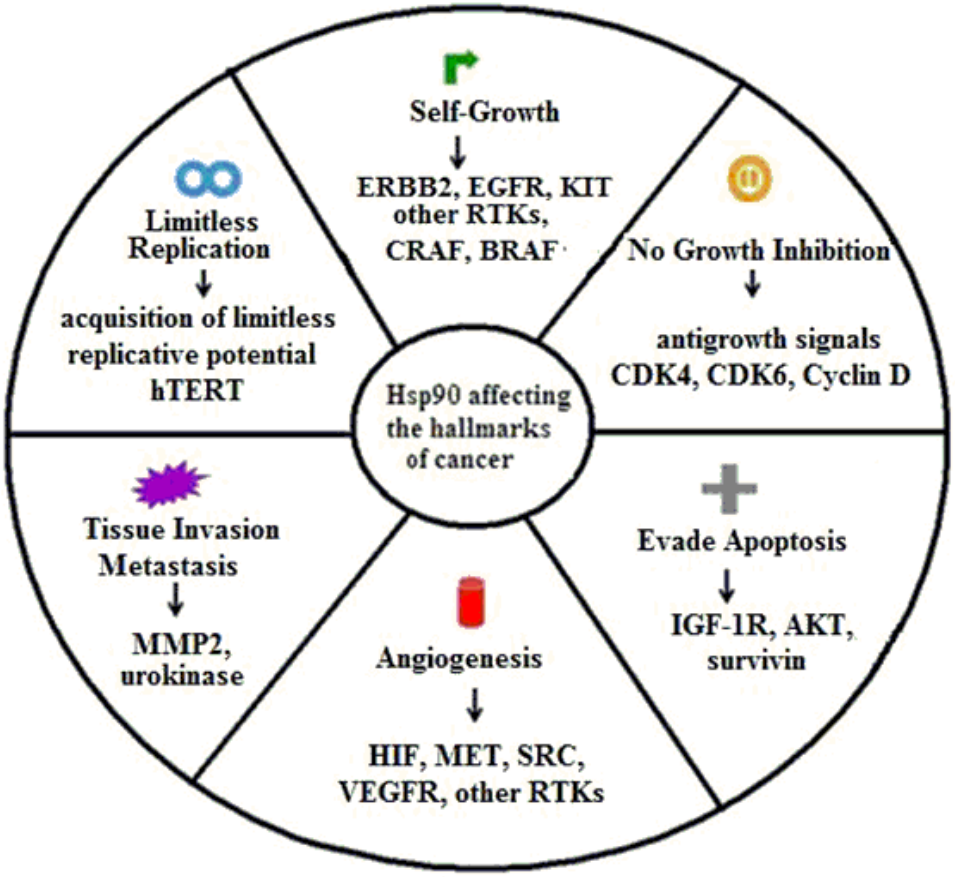

Figure 1.4 Diagramatic representation of how all the six hallmarks of cancer can be affected by the multiple Hsp90 client proteins (adapted from Xu and Neckers, 2007).

1.3 Telomerase activity and its downstream effects (*in vivo* studies of telomerase)

In addition to telomere maintenance, recent observations have indicated other complex roles of telomerase in cell proliferation, differentiation and DNA damage response (Calado and Chen, 2006). Suppression of telomerase activity in animal models has provided some useful data and clues. One such study showed that suppressing telomerase in the mouse model system reduced tumour invasion (Bagheri *et al*., 2006). Another study conducted in

mouse embryonic stem cells suggested that telomerase confers cellular resistance against apoptosis by antagonizing the p53 pathway (Lee *et al*., 2005). *In vivo* studies have highlighted a few unidentified roles of telomerase such as, a decrease in telomerase activity leads to an increased expression of tyrosinase, a key enzyme in melanin biosynthesis, the inhibition of telomerase activity results in down regulation of glycolytic pathway genes, which correlates with decreased glucose consumption and lactate production (Bagheri *et al*., 2006; Kondo *et al*., 1998). These studies have opened up new roles for telomerase in altering the energy state of the cells, thereby providing a model for explaining the mechanism by which an increase in telomerase activity can promote tumour invasion and metastasis (Bagheri *et al*., 2006; Kondo *et al*., 1998).

Studies of animal models provides an excellent depiction of processes that take place inside the organism, this data increases the confidence level with respect to the processes taking place *in vivo*. However, research shows that many of the results obtained with animal cells are not transferable to human systems due to the high diversity in biochemical characteristics among the different species (Guilleret and Benhattar, 2003). Thus, it is essential to be able to study the protein levels in primary cultures to mirror the changes taking place in human cells.

1.4 Proteomic studies of telomerase

Though mRNA studies are informative they do not necessarily reveal the true picture of the condition of the cell because mRNA levels do not necessarily correlate with the cellular protein content. Proteins are often subjected to proteolytic cleavage, alternative splicing or

post-translational modifications, such as phosphorylation or glycosylation (Walsh *et al*., 2005). The proteome is the cell-specific protein complement from the genome and encompasses all proteins that are expressed in a cell in a particular condition. An estimation of over 1.5 million proteins have been predicted to be a part of cancer proteome due to the various post translation and epigenetic changes (Khalil and Madhamshetty, 2006; Alaoui-Jamali and Xu, 2006; Sun *et al*., 2007). In contrast to the genome, the proteome is dynamic and is in constant flux (Srinivas *et al*., 2002). Genomic studies alone will not be able to fully identify the fate of telomerase and hence the outcomes of these studies need to be complemented with proteomic data. Therefore, it is important to use proteomic methods which will generate a circuit of information on the various regulatory and downstream effects of telomerase that take place within the cancer proteome (Thakkar and Shervington, 2008).

Very few proteomic based studies have been undertaken so far that target telomerase. A few significant proteomic studies on telomerase after the ectopic expression of hTERT have been summarised. Recombinant hTERT retrovirus transduction of human bone marrow mesenchymal stem cells (hMSCs) prolonged the life span of these cells and changed the cellular protein level (Huang *et al*., 2008). Proteomic analysis was carried out using two-dimensional gel electrophoresis and peptide mass fingerprinting by matrix-assisted laser desorption/ionization time-of-flight (MALDI-TOF) mass spectrophotometry. Comparing the expression of these transduced cells with primary hMSCs, 20 differentially expressed proteins have been identified which highlights various non-catalytic functions of telomerase. These proteins are part of several biological processes that are related to proliferation and transformation of cells. Annexin A1 and Reticulocalbin 1, in particular,

are both calcium dependent proteins and have a direct effect on cell proliferation (Huang *et al*., 2008). One of the important observations made was the significant down regulation of glutathione S-transferase P1 (GSTP1) in the transduced cells, suggesting that telomerase modified cells suffer less oxidative stress. The results of Annexin A1, Reticulocalbin 1 and GSTP1 (all downregulated) in primary and transduced cells did not correlate with the mRNA levels highlighting the importance of proteomics in identifying the post transcriptional and translational changes. The hTERT–hMSCs cells did not show tumourogenecity and this was also evident in the proteomic profile of the protein prohibitin, which remained unaffected in the treated as well as control cells (sustaining a consistent level of prohibitin causes a concomitant sustained level of p53 expression and prohibitin and p53 keep hTERT–hMSCs in a non-transforming status) (Huang *et al*., 2008).

The over expression of hTERT in human umbilical vein endothelial cells (HUVECs) resulted in their immortalization compared to their normal and senescent counterparts; however, no tumourgenic transformation was observed. Phenotypically, these transformed cells are similar to their normal counterparts. However, their protein expression profile assessed by two-dimensional differential in-gel electrophoresis (DIGE) technology followed by mass spectrophotometry analysis was different. Moreover, a number of valued proteins such as GSTP1, inter-cellular adhesion molecule 1 and carbohydrate sulfotransferase 3 were found to play a role in atherosclerosis which could be attributed to the presence of the senescent and hTERT immortalized endothelial cells in the atherosclerotic lesions (Changa *et al*., 2005). These findings shed light on a few downstream pathways influenced by telomerase and reveal the importance of performing a

proteomic study in order to trace the downstream effect of telomerase on various biological functions as well as disease formation processes (Changa *et al*., 2005).

Mazzucchelli and colleagues extensively studied the effect of the hTERT transfection on the proteome of human fibroblast cells (WI38) (Mazzucchelli *et al*., 2008). Cytosolic and nuclear fractions of WI38 cells were subjected to a 2D-DIGE followed by MALDI-TOF-TOF. This study confirms the correlation of Hsp90 with hTERT, playing an important role in the regulation of telomerase and tumour cell transformation (Mazzucchelli *et al*., 2008). The over expression of Hsp90α reported in this study was consistent with the genomic data mentioned earlier which showed that Hsp90 is one of the major regulators of telomerase. Proteomic studies help to provide an additional dimension and conformation of existing genomic data. An interesting observation from this study was the upregulation of the cajal bodies (CBs) associated factors, which provide evidence that hTR localizes in CBs that could act as storage sites and deliver components of the telomerase complex when needed. This may shed light on the possible mechanism of the formation and transport of this holoenzyme.

In addition to these regulatory proteins, it also identified a few proteins that are a part of the downstream pathways of telomerase (Mazzucchelli *et al*., 2008). For example, it supports the hypothesis that hTERT transfection enhances natural endoplasmic reticulum (ER) capacity and modulates Calcium cell signaling pathways potentially resulting in an over protection mechanism against endogeneous and exogeneous disorders. These results are in accordance with the identified down-regulation effect of the apoptotic effectors Galectin-1 and Annexin 5 (Mazzucchelli *et al*., 2008).

Thus, it is clear that hTERT proteomic studies have provided further evidence of the involvement of telomerase in other physiological processes besides telomere elongation, such as apoptosis, cell cycle regulation and ER homeostasis (Changa *et al*., 2005; Huang *et al*., 2008; Mazzucchelli *et al*., 2008). It is also apparent that hTERT induced cells are stress resistant and exhibit enhanced natural cell repair mechanisms. The significance of proteomic based studies on telomerase can therefore

i) Underpin the regulation of this complex enzyme itself, as evident by the cajal bodies,

ii) Highlight the post-translational changes which may not be detected by genomic studies as in the case of GSTP1,

iii) Reinforce the hypothesis put forward by genomic studies as evident with Hsp90, annexin 1 and others,

iv) Shed light on the downstream effect of telomerase in the various biological processes.

These studies have provided us with a model for proteomic investigations aimed at deciphering telomerase regulation and evaluating anti-telomerase drugs that induce proteome alterations.

Thus, it is evident that besides the canonical functions of telomerase, it is also involved in various other proinvasive and prometastatic pathways. Although the importance of telomerase for tumour proliferation is well documented, very little is known about the downstream effect of telomerase on the various physiological and signaling pathways. Silencing telomerase at the genetic level highlights the changes caused in the cancer

proteome and may identify the potential downstream pathways controlled by telomerase in tumour progression and maintenance (Fig 1.5)

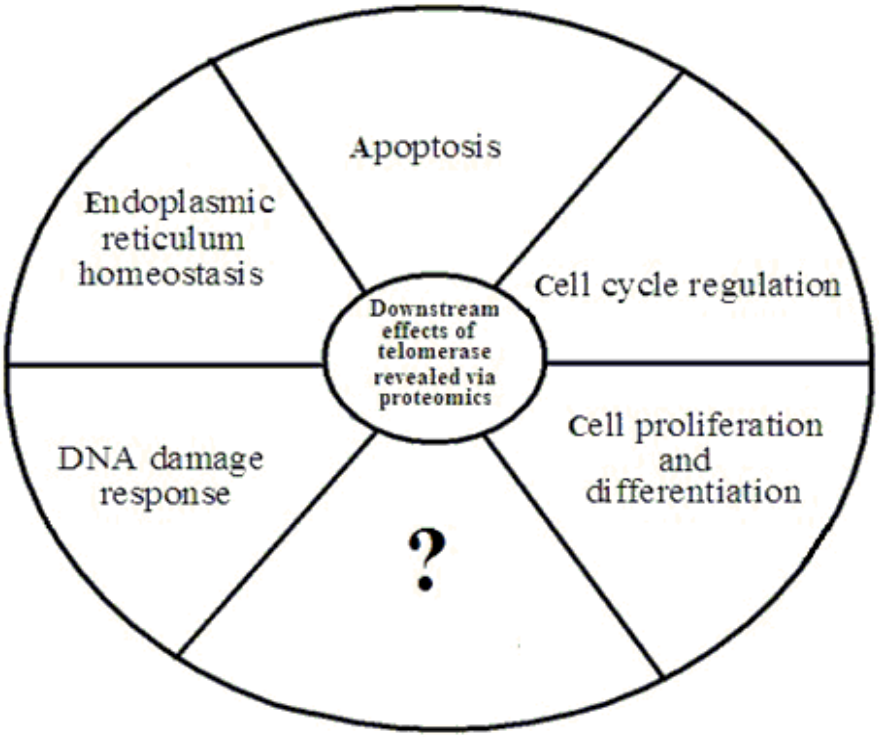

Figure 1.5 Non catalytic functions of telomerase as reported by various proteomic studies.

1.5 Telomerase a future prognostic and diagnostic marker for cancer

Telomerase activity is detected in almost all cancers, to include breast, head, neck, lung and skin and is found to be activated in the early stages of these cancers. However, in colon, pancreas and thyroid it is activated in late pathogenesis (Shay and Gazdar, 1997, Hiyama and Hiyama, 2003). It is possible to predict survival rates in patients with β-cell

chronic lymphocytic leukaemia by measuring telomerase expression (Terrin *et al*., 2007). In patient with Wilms' tumour, a correlation between high *hTERT* mRNA levels and tumour reoccurrence has been established (Dome *et al*., 1999).

Neuroblastoma studies have shown poor outcomes in the late-stages of the disease associated with high telomerase activity. Though the activation of telomerase is not concomitant with carcinogenesis in human tumours, the overall prevalence of telomerase activity in 85% of human tumour samples involving more than 3000 samples tested using the telomeric repeat amplification protocol (TRAP) assay, makes telomerase activity the most universal marker for human cancers (Shay and Gazdar, 1997, Hiyama and Hiyama, 2003). Telomerase inhibition enhances chemosensitivity towards drugs such as cisplatin and can be used as an adjuvant therapy (Elenitoba-Johnson, 2001; Kiyozuka *et al*., 2000), hence telomerase can be advocated as a potential prognostic or diagnostic marker of the future.

1.6 Telomerase and glioma

Of all the benign and malignant brain and central nervous system (CNS) tumours, gliomas are the most common, accounting for approximately 45-50% of all those diagnosed (Phatak and Burger, 2007). Glioma refers to tumours that arise in glial cells; these tumours are typically the most aggressive primary tumours in the central nervous system (CNS) (Morii *et al*., 1997). Based on their histology gliomas are classified into four grades according to the World Health Organization (WHO). Grades I and II are indicated as low-grade glioma, and Grade III is referred to as anaplastic astrocytoma,

while Grade IV is referred to as glioblastoma multiforme (GBM), both of which are malignant gliomas (Morii *et al*., 1997; Phatak and Burger, 2007).

Malignant gliomas are among the most lethal and intractable of all human tumours due to its aggressive and invasive nature (Pillai *et al*., 2004). While less than 20-30% malignant gliomas respond to chemotherapy, surgery presents constraints due to the diffused nature and close proximity of tumours to vital anatomy (Pouratian *et al*., 2007). GBM has a median survival rate of 9 to 12 months (Pouratian *et al*., 2007). Gliomas account for 1.6% of all cancers in England and Wales. Of all the cancers, glioma is the 12^{th} most common cancer in males, and the 15^{th} most common in females with a survival rate of 12–13% for males, and 15% for females. Survival rates depends on the grade of glioma with low grade glioma having the highest survival rates (Pulkkanen and Yla-Herttuala, 2005; Ohgaki and Kleihues, 2005). Malignant gliomas are usually refractory to therapy and despite multidisciplinary approach the prognosis of glioma and the clinical outcome remains very poor. Efforts are being focused on developing new treatments that could simultaneously affect multiple signaling pathways in glioma.

It has been demonstrated that chemosensitivity of gliomas is related to telomerase activity. Langford *et al*. first reported the presence of telomerase activity in glioma in 1995 where he established a correlation between telomerase activity and rate of malignancy. Other reports also show that the incidence of telomerase expression closely correlates with the grade of malignancy in glioma (Komata *et al*., 2002). In malignant gliomas, telomerase is positive in 10-100% of anaplastic astrocytomas and 26-100% of GBM; in contrast to the telomerase activity of 0% and 0 to 33% in Grade I and II of glioma, respectively (Langford *et al*., 2005; Mattei *et al*., 2005; Harada *et al*., 2000). It

is also reported that the level of telomerase activity and *hTERT* expression is significantly higher in secondary glioblastomas than in primary (Harada *et al*., 2000; Chen *et al*., 2006). In particular, malignant gliomas are one of the best candidates for telomerase targeted therapy. The fact that malignant glioma are predominantly telomerase positive whereas normal brain tissues do not express telomerase makes telomerase a very attractive target and an extremely useful prognostic and diagnostic marker of glioma (Yin *et al*., 2007).

Studies in our laboratory have show that *hsp90α* is expressed in both glioma tissue and cell lines whereas it was absent in normal brain tissues and cell lines, making it an important target in glioma cells. Predesigned siRNAs were used to inhibit *hsp90α at* the post transcriptional level. siRNA oligo 3 directed towards exon 9 was reported as the most efficient oligo for silencing *hsp90α* after 24 hr in glioma cell lines (Cruickshanks *et al*., 2010).

1.7 Current project

The activity of telomerase can be regulated at multiple levels. One such aspect is the regulation of telomerase by various telomerase and/or telomere associated proteins which either mediate or regulate the association of telomerase with the telomere. Previous results from our laboratory have shown that siRNA directed towards *hsp90α* not only completely silences *hsp90α* but also results in almost 80% silencing of *hTERT*. Hence in this study, two different approaches regulating telomerase activity was used in order to inhibit telomerase activity and to study the downstream effect of this inhibition. Direct silencing

of the catalytic subunit hTERT, by siRNA was used as the first regulatory mechanism to inhibit telomerase activity. The second approach involved an indirect mechanism of telomerase regulation by silencing the hsp90α chaperone. In order to characterize the changes caused due to the inhibition of telomerase by the two approaches, a differential proteomic analysis was performed to compare wild type U87-MG cells, U87-MG cells after silencing *hTERT* (U87-MG-si*hTERT*) and U87-MG cells after silencing *hsp90α* (U87-MG-si*hsp90α*).

The approach of studying the changes induced at the cellular protein after silencing the *hTERT* gene has never been attempted before. This study, for the first time, elucidates relationships between the direct and indirect effect of silencing two telomerase regulatory mechanisms. Although the importance of telomerase for tumour proliferation is well documented, very little is known about the downstream effect of telomerase on the various physiological and signaling pathways. Silencing telomerase at the genetic level with a view to identify the potential downstream pathways controlled by telomerase in glioma is novel.

The aims of this thesis were to:

1) Establish the best siRNA oligo treatment for the inhibition of telomerase activity by targeting two different regulatory mechanism of telomerase.
2) Perform a differential proteomic ananlysis with a view to study the downstream effect of silencing two different, telomerase regulatory mechanisms on the cancer proteome.

CHAPTER 2

MATERIALS AND METHODS

2.1 Cell culture

2.1.1 Cell Lines

In this study, three glioma cell lines were primarily used, namely grade I astrocytoma, which expressed a mutant p53 (1321N1), grade II/III astrocytoma/ oligodendroglioma (GOS-3), grade IV glioblastoma (U87-MG). The cell lines were purchased from the European Collection of Cell Cultures (ECACC) and the American Type Culture Collection (ATCC) and were from human origin. There was no evidence for the presence of any infectious viruses or toxic products (routine mycoplasma testing was performed on the cell line). Cells were received in 1 ml plastic cryotubes as frozen ampoules and were present in an appropriate freezing medium with 10% (v/v) dimethylsulphoxide (DMSO). The cell lines were handled as recommended by the Advisory Committee on Dangerous Pathogens (ACDP) for Category 2 containment.

2.1.2 Media and reagents

Complete medium for cell growth was aseptically prepared by the addition of supplement as recommended by ECACC/ATCC. For U87-MG cell line, Eagle's Minimum Essential Medium (EMEM) was used as the cell culture medium with a formula consisting of 2.2 g/l sodium bicarbonate, 1 g/l glucose Earle’s salt and 0.0053 g/l phenol red. EMEM was supplemented with 10% Fetal Bovine Serum (FBS), 2 mM L-glutamine and 1% Non essential amino acids. Dulbecco's-Modified Eagle's Medium (DMEM) was used as a cell culture medium for 1321N1 and GOS-3. It was composed of 25mM Hepes 1.0 g/l glucose 1.0 mM sodium bicarbonate 0.011 g/l phenol red. DMEM was supplemented with 10%

FBS, 2 mM L-glutamine. The completed medium was pre-incubated overnight before cells resuscitation.

To calculate the volumes of supplements added to the medium the following formula was used

$$v = \frac{b \times c}{a}$$

Where a = stock concentration

b= required final concentration

c= final reaction volume

v= required volume

After the addition of the supplements the medium was mixed and labelled with the date of preparation. This was stored at 4°C for a maximum of two weeks. Composition of supplements and reagents used for cell culture are detailed in Table 2.1.

Table 2.1 Reagents and chemicals used in cell culture

Reagents	Supplier	Components
Foetal bovine serum	Gibco BRL	Heat inactivated foetal bovine serum
Non essential amino acid	Sigma	100 x Non essential amino acid
L-glutamine	Sigma	200 mM L-glutamine
Phosphate buffer saline 0.1M	Sigma	8 g/l Sodium chloride 0.2 g/l Potassium chloride
DMSO	Sigma	Dimethyl sulfoxide 99.5%
Trypan blue (0.4%)	Sigma	0.81% Sodium chloride 0.06% Potassium phosphate dibasic

2.1.3 Resuscitation of frozen cells

Each medium was pre-warmed in a water bath at 37°C before the frozen ampoules (containing the cells) were thawed. The following protocol was used, as suggested by ECACC:

1. Cell line was thawed at 37°C in a water bath for 1-2 min.
2. Thawed cells were immediately re-suspended into 2 ml of growth medium to remove the freezing medium and centrifuged at 150 x g for 5 min.
3. The supernatant was discarded and the pellet was resuspended in 2-3 ml of medium and was aliquoted into two flasks of 25 cm^2.

4. Appropriate medium (5 ml) was added into each flask then mixed manually by rocking the flask backward and forward.
5. The flasks were labelled with the name of the cell line, passage number and date.
6. These flasks were then incubated at 37°C with 5% CO_2 in filtered air.

2.1.4 Subculture and cell library maintenance

The cells were observed under the light microscope following overnight incubation. When a mono-layer growth of 70-80% confluence was obtained, the cells were scraped and subcultured. However, for slow growing cells the medium was changed every 48 hours of incubation in order to maintain enough nutrients for the cells.

The cells were scrapped and subcultured as follows:

1. The culture medium was removed and the cells were washed with 1 x phosphate buffer saline (PBS) pH 7.4 to remove any excess medium.
2. Cells were gently scraped using a disposable scraper.
3. To ensure that all the cells were detached and floating, they were examined using a phase contrast microscope.
4. The cells were then re-suspended in 8 ml of media and were transferred to a 15 ml centrifuge tube and were centrifuged at 1000 rpm for 5 min. A suspension of 20 µl of cells was collected in an eppendorf tube for cell quantification.
5. For passaging, the cell pellet was resuspended in 8 ml of growth medium and an appropriate aliquot (approximately 2 x 10^4 cells/cm^2) was transferred to a new 75cm^2 flask containing 10 ml of growth medium. The flask was suitably labelled

with the name of the cell line, passage number and date and then incubated under ordinary culture conditions.

6. Alternatively, for cryopreservation, 1 x 10^6 cells were re-suspended in a cell freezing medium (complete culture medium with 10% DMSO) in 1 ml cryoprotective ampoules, labelled with the cell line name, passage number and date.
7. The ampoules were placed into a Mr Frosty passive freezer (Nalgene, UK) filled with isopropanol and placed at -80°C overnight.
8. Following overnight storage, the ampoules were then transferred into -195°C liquid nitrogen container.
9. A data entry log book was maintained which had a record of the position of storage in liquid nitrogen, to make it easy to be traced at a later date for further use.
10. For mRNA isolation 2×10^6 cells were frozen. These cells were stored as pellets at -80°C without the freezing medium. Cells required for immunofluorescence were cultured in chamber slides, and fixed with paraformaldehyde. Cells required for luminescent cell viability assay were seeded in 96 well opaque-walled multiwell plates.

2.1.5 Quantification of cells and cell viability

Cells were quantified as follows:

1. Cell aliquots (20 µl) (section 3.1.4) were diluted 1:1 with trypan blue (Freshney, 1987) to identify the number of viable cells.
2. A haemocytometer was prepared by attaching the cover slip with a slight pressure to create Newton's refraction rings.
3. Both sides of haemocytometer chamber were filled with the stained cell suspension and the cells were counted under a light microscope using x 20 magnification. Viable cells were observed as glowing cells, whereas non viable cells were stained blue.
4. Cell viability was calculated as a percentage using the following equation:

Total number of cells counted/ml = total viable cells + total dead cells x 10^4.

$$\text{Percentage of non viable cells} = \frac{\text{Non viable cells}}{\text{Total number cell}} \times 100$$

2.1.6 Tumour specimens

Tissue specimens, which included three control and fifteen tumour tissue specimens, were provided by courtesy of Royal Preston Hospital, United Kingdom. All the work on tissues was performed after obtaining ethical approval from the North Manchester Research Ethics Committee under REC Ref: 06/Q1406/104 as well as the Ethics Committee at the University of Central Lancashire. Written consent was also obtained from the donors. Control tissues were obtained from patients who required resection of normal brain for

purposes other than primary glioma treatment whereas the tumour specimens were acquired from glioma cancer patients.

For each patient, the sample was surgically dissected and frozen immediately in liquid nitrogen until required for assay. Biopsy tissues were fixed in 10% Formol Saline for 24 hours and processed through an automated processor (carried out by neurosurgeons and the Pathology Department at the Royal Preston Hospital).

2.2. mRNA isolation

The mRNA was isolated using the mRNA isolation kit (Roche-Diagnostics, UK) which isolates mRNA without preparing total RNA. It is a safe method as no aggressive organic reagents are used and the mRNA isolated from this kit was of the highest purity.

The principle of this kit is that, the $(A)^+$ tail of mRNA hybridizes to a biotin-labelled oligo$(dT)_{20}$ probe. These biotinylated hybrids are in turn captured by streptavidin-coated magnetic particles. A magnetic separator is then used to capture these magnetic particles. Excess fluid is then removed by washing with PBS buffer and finally the mRNA is eluted from the particles by incubating with redistilled water (Roche-Diagnostics, Germany).

The mRNA was isolated following the manufacturer's protocols as shown in the schematic diagram (Fig 3.1). The composition of all reagents and buffers used are shown in Table 2.2.

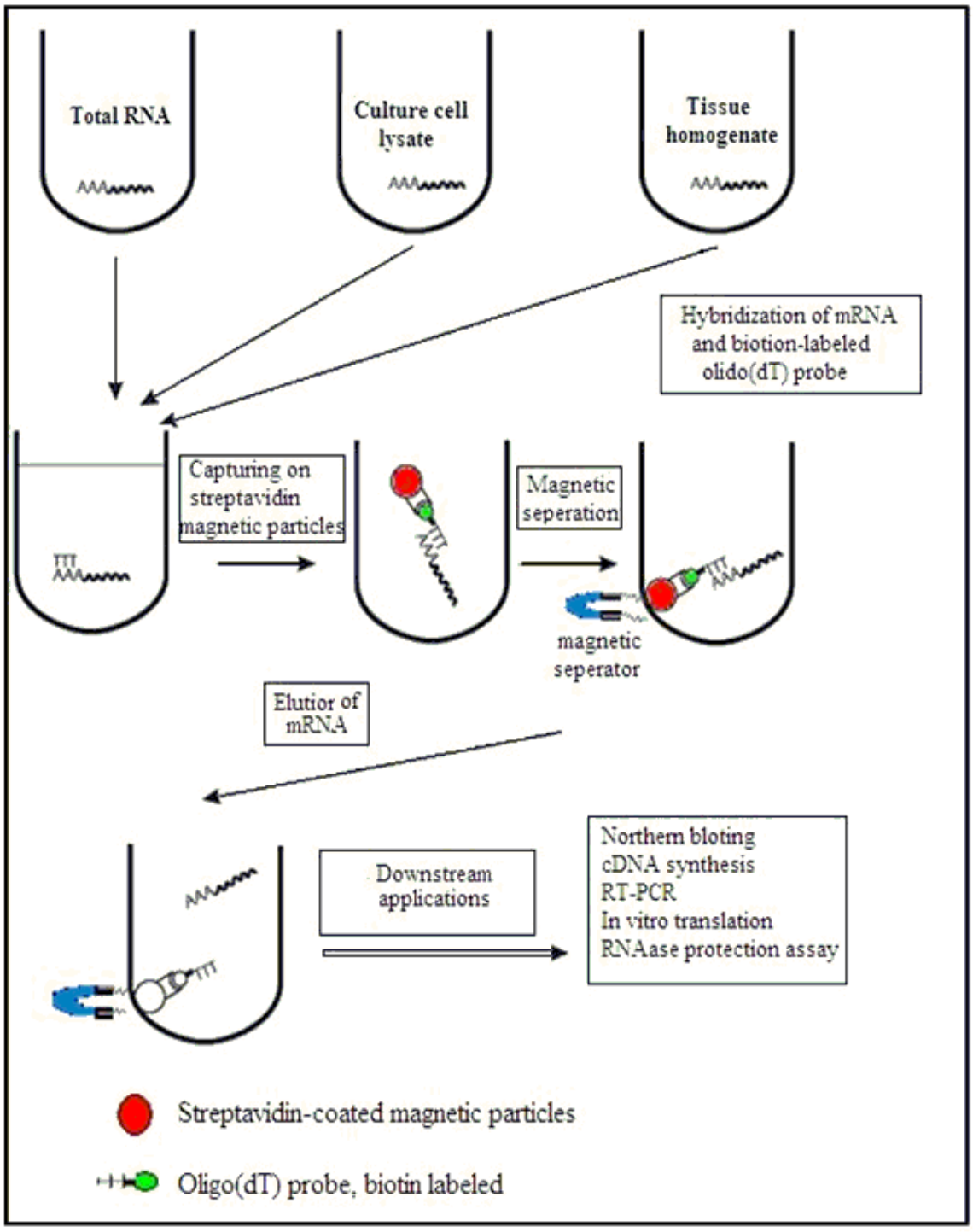

Figure 2.1 Schematic diagram showing the principle of mRNA isolation (Roche diagnostic, UK).

Table 2.2 Materials and reagents provided in mRNA isolation kit.

Reagents	Components
Lysing Buffer	0.1 M buffer, 0.1 M LiCi, 10 mM EDTA, 1% lithium dodecylsulfate and 5mM DTT (dithiothreitol) at pH 7.5
Streptavidin magnetic particles	(10 mg/ml) in 50 mM Hepes, 0.1% bovine serum albumin, 0.1% chloracetamide and 0.01% methylisothiazolone at pH 7.4
Oligo$(dT)_{20}$ probe, biotin labelled	100 pmol biotin labelled oligo $(dT)_{20}$ per µl redistilled water
Washing buffer	10 nM Tris buffer, 0.2 M LiCi and 1 mM EDTA at pH 7.5
Redistilled water	RNAse free
Storage buffer	10 mM Tris buffer, 0.01% methylisothiazolone, pH 7.5

The isolation procedure was followed according to the number of cells and the manufacturer's recommendation. In this study 2 $x10^6$ cells were used to isolate mRNA following the recommended highlighted protocol in Table 2.3.

Table 2.3 Materials and reagents adjusted for the number of cells for mRNA isolation.

Reagents	1 x 10^8	2 x 10^7	1 x 10^7	2 x 10^6	2 x 10^5
Lysing buffer	15 ml	3 ml	1.5 ml	0.5 ml	0.1 ml
Streptavidin magnetic Particles	1.5 ml (15 mg)	300 µl (3 mg)	150 µl (1.5 mg)	50 µl (0.5 mg)	50 µl (0.5 mg)
Lysing buffer for preparation of streptavidin magnetic particles	2.5 ml	500 µl	250 µl	70 µl	70 µl
Oligo $(dT)_{20}$ biotin labelled	15 µl 1.5 nmol	3 µl 0.3 nmol	1.5 µl 150 pmol	0.5 µl 50 pmol	0.5 µl 50 pmol
Washing Buffer	3 x 2.5 ml	3 x 500 µl	3 x 250 µl	3 x 200 µl	3 x 200 µl
Redistilled water	250 µl	50 µl	25 µl	10 µl	5 µl

The volume of reagents used in this study is highlighted in the shaded column.

Procedure:

1. Cells were washed three times using ice cold PBS to remove excess medium as this could interfere with UV spectrophotometric analysis.
2. Appropriate volume of lysing buffer was then added to the cell pellet as shown in Table 3.3 and cells were mechanically sheared six times using 21G needle.
3. 0.5 µl of biotin-labelled oligo $(dT)_{20}$ probe was added to the lysate and allowed to hybridise with mRNA 37°C for 5 min.
4. Simultaneously, 50 µl of streptavidin magnetic particles was aliquoted into a sterile eppendorf tube. Streptavidin magnetic particles were separated from the storage buffer using the magnetic separator. These particles were then washed once in 75 µl of lysing buffer to remove any excess storage buffer.
5. Following magnetic separation and disposal of the supernatant, the prepared particles were resuspended in the dT-mRNA hybrid mixture and were incubated at 37°C for 5 min to achieve immobilisation.
6. The hybrid-linked particles were magnetically separated from the fluid and the supernatant was discarded.
7. Magnetic particles were then resuspended thrice in washing buffer (3 × 200 µl) which quantitatively removed all contaminants.
8. After the final wash the supernatant was discarded and the mRNA was eluted from the magnetic particles by the addition of 10 µl redistilled water followed by incubation at 65°C for 2 min.
9. mRNA was separated from the magnetic beads using the magnetic separator
10. The supernatant containing the mRNA was stored at –20°C in RNAse free eppendorf tube.

2.2.1 Quantification of nucleic acid by UV spectrophotometry

Optical density (OD) was applied at wavelengths of 260 nm and 280 nm to quantify the isolated mRNA using gamma thermo Helios spectrophotometer (Thermospectronics, UK). mRNA was diluted with of 1x TAE buffer (400 mM Tris, 0.01 M EDTA; pH 8.3) at a ratio of 1:199. The OD of diluted sample was measured and the concentration of the mRNA was calculated using the readings at 260 nm. The standard formula used was:

An emission of 1 OD = 40 μg/ml for single-stranded (ss) RNA.

The purity of isolated nucleic acids was determined using the ratio of 260/280 nm. A ratio of 1.9 - 2.1 indicated the presence of pure (ss) RNA.

The concentration of the isolated mRNA samples were calculated as follows:

A_{260} reading × 250 (dilution factor) × 40 (ssRNA) = Concentration (μg/ml)

2.2.2 Analysis of nucleic acid by alkaline gel electrophoresis

Alkaline gel was used to analyse the isolated mRNA which helped to determine whether the isolated mRNA was degraded or intact.

Procedure:

1. A gel of 2% concentration was prepared by dissolving 0.6 g of agarose powder in 30 ml distilled water
2. The gel solution was heated in a domestic microwave at maximum power (100%) for 1-2 minutes until a transparent molten solution was formed.

3. The solution was cooled to 50°C before the addition of NaOH and EDTA (from the stock 10 N NaOH and 0.5 M EDTA) to achieve a final concentration of 50 mM and 1 mM, respectively.
4. The solution was mixed and poured into the prepared electrophoresis tank set with the comb in place and allowed to solidify for 30-45 min.
5. Upon solidification, the running buffer with a final concentration of 50 mM NaOH and 1 mM EDTA in distilled H_2O was added in the gel tank.
6. The comb was removed from the gel and the samples containing loading dye in 1: 4 dilution were loaded onto the gel.
7. The gel was electrophoresed at 50 V for 1-2 h.
8. A stock solution of ethidium bromide was prepared by dissolving 10 mg ethidium bromide tablet in 10 ml of distilled H_2O to obtain a final concentration of 1 mg/ml.
9. After the electrophoresis was complete the gel was stained in fresh 0.4 µg/ml ethidium bromide for approximately 10 min and then destained in distilled H_2O.
10. GENE GENIUS bioimaging system (Syngene, UK), a fully automated gel documentation and analysis system was used to analyse the gel.

The Syngene gel analyser or GENE GENIUS (Syngene, UK) with the software Genesnap (Syngene, Cambridge UK) is a comprehensive and fully automated system for all UV and white light fluorescence applications.

Safety precautions were adopted while handling ethidium bromide since it is mutagenic and is suspected carcinogen.

Table 2.4 Materials and reagents used for gel electrophoresis.

Reagent	Supplier	Preparation	Working concentration
Ultrapure agarose	Gibco BRL	0.6 g/2 gAgarose 30/100 ml 1x TBE. Solubilized by boiling in a microwave for 3-4 minutes	2% w/v
10x TBE (Ultrapure 10x Tris borate EDTA electrophoresis buffer)	Sigma	1 M Trizma base 0.9 M 1 Boric acid 0.01 M EDTA Diluted to 1x concentration with distilled water	1x
Gel loading dye	Sigma	0.25% w/v Bromphenol blue 0.25% w/v Xylene cyanole 40% w/v Sucrose Supplied ready for use 4x concentration	1:4 sample:dye
Ethidium bromide 10 mg/ tablet	Amresco	10 ml Distilled water. Diluted to 0.5 µg/ml with distilled water	1:20
Molecular marker (100bp)	Sigma	100 µg supplied ready for use	1 µg/ml

2.3 Complementary DNA Synthesis (cDNA)

mRNA was reverse transcribed using the First strand cDNA synthesis kit which harnesses AMV Reverse Transcriptase enzymes isolated from Avian Myeloblastosis Virus (Roche Diagnostic, UK). The cDNA strand was synthesised by the AMV Reverse Transcriptase at the 3'-end of the poly (A) – mRNA. Oligo dT was used as a primer. Since cDNA was used for the analysis of various genes, universal oligo $(dT)_{15}$ primer rather than gene specific primers was used.

RNAse inhibitor and AMV reverse transcriptase were thawed on ice; all other solutions were thawed at room temperature and kept on ice after thawing. All reagents were vortexed and briefly centrifuged before starting the procedure.

A master mixture was prepared to achieve consistency between samples. The amount of mRNA added depended on the concentration of the mRNA isolated. The recommended 100 ng of poly $(A)^+$ RNA was used.

The composition of the reagents provided in the kit and the volume of reagents used are shown in Table 2.5 and Table 2.6, respectively.

Table 2.5 Reagents provided with the kit for cDNA synthesis.

Reagent	Formula
Reaction Buffer (10 x)	100 mM Tris, 500 mM KCl; pH 8.3
$MgCl_2$	25 mM
Deoxynucleotide mixture	dATP, dCTP, dTTP,dGTP; 10 mM each
Gelatin	0.5 mg/ml (0.05% [w/v])
Oligo-$p(dT)_{15}$ Primer	0.02 A260 units/µl (0.8 µg/µl)
Random Primer $p(dN)_6$	0.04 A260 units/µl (2 µg/µl)
RNase inhibitor	50 units/µl
AMV Reverse Transcriptase	≥ 25 units/ µl
Control Neo pa RNA	0.2 µg/µl; 1.0 kb in length with 19-base 3'-Poly(A) tail
Sterile Water	

Table 2.6 Volumes of reagents and their final concentration.

Reagent	Volume	Final concentration
10x Reaction Buffer	2.0 µl	1 mM
25 mM $MgCl_2$	4.0 µl	5 mM
Deoxynucleotide Mix	2.0 µl	1 mM
Primer Oligo-p$(dT)_{15}$	2.0 µl	**0.04 A260 units (1.6 µg)**
RNAse inhibitor	1.0 µl	50 units
AMV reverse transcriptase	0.8 µl	≥20 units
Sterile water variable	(depend on the amount of mRNA added)	
RNA sample variable (depend on the concentration of isolated mRNA 100 ng mRNA was added)		
Final volume for one sample =	**20.0 µl**	

Procedure:

1. The master mixture was briefly vortexed and centrifuged and 11.8 µl of the master mixture was aliquotted into sterile microfuge tube.
2. Appropriate amount of mRNA was added to achieve a final concentration of 100 ng.
3. Sterile water was added to make the final volume of 20 µl.

4. The mixture was briefly vortexed, centrifuged and incubated at 25°C for 10 min which allowed mRNA and primer annealing.
5. The mixture was further incubated at 42°C for 60 min where the mRNA template was reverse transcribed into single-stranded cDNA.
6. As the final step, the mixture was then incubated at 99°C for 5 min which denatured the AMV Reverse Transcriptase.
7. The sample was then cooled to 4°C for 5 min and was stored at -20°C until required.

2.4. Use of Bioinformatics to establish gene information and primers

Bioinformatics is defined as a technique of conceptualising biology in terms of molecules (in the sense of physical chemistry) and applying "informatics techniques" derived from disciplines such as applied mathematics, computer science and statistics to understand and organise the information associated with these molecules, on a large scale (Oxford English Dictionary). In short, bioinformatics is management information systems for molecular biology and has many practical applications.

Bioinformatics encompasses a wide range of subject areas from structural biology, genomics to gene expression studies and stores, organizes data and provides specialized tools to view and analyze the data generated by biological scientists throughout the world (Kim, 2007). The ultimate goal of the field is to enable the discovery of new biological insights as well as to create a global perspective from which unifying

principles in biology can be discerned. The World Wide Web has become an essential feature to the world of bioinformatics, as it makes DNA, RNA and protein data available to users throughout the world through databases such as National Centre for Biotechnology Information (NCBI), GenBank (USA), European molecular biology laboratory (EMBL) (Europe) (Fenstermacher, 2005). The present accomplishments of bioinformatics hold substantial promise to revolutionize the medical world.

Various bioinformatics softwares have been used in this study, each of which have been listed and described below.

2.4.1 Gene location and gene mRNA sequence using National Centre for Biotechnology Information (NCBI)

The location of each of the genes used in this study was found using public databases which are held by GeneCards and from NCBI. NCBI provides the GenBank DNA sequence database. In addition to GenBank, it also provides tools such as online mendelian inheritance, molecular modeling database for 3D protein structures, database of Single Nucleotide Polymorphisms (dbSNP), gene map of the human genome, human gene sequence collection and taxonomy browsers.

GeneCards is an integrated database of human genes which provides a concise integrated summary on various genes, extracted from major public and proprietary databases. With Genecards it is possible to attain a gene annotation from over 40 mined resources (Shmueli *et al*., 2003).

The nucleotide sequence of the genes of interest was established using the public databases (GenBank, EMBL, SwissPort) held by the NCBI. Gene location data

obtained from Genecards, along with the diagrammatic representation of each gene locus obtained from NCBI was generated for *hTERT, hsp90α, vimentin* and *GAPDH* (Figures 2.2-2.5).

These websites can be accessed at:

GeneCards = http://genome-www.stanford.edu/genecards/index.shtml

NCBI

http://www.ncbi.nlm.nih.gov/entrez/query.fcgi?db=nucleotide&cmd=search&term

2.4.2 Primer design using Primer 3

Sequences obtained from the NCBI database were used to design primers using the primer 3 software. These primers were then used in the polymerase chain reaction (PCR) to amplify the gene of interest. For designing primers which would give yields of the specific amplicon in question the following parameters are generally followed:

a) The primer should be approximately 20 nucleotides in length. Although long primers are more specific, they have higher annealing temperatures but are less efficient, because thermodynamically the annealing takes longer.

b) It should have a G/C and A/T content similar to or higher than that of the sequence to be amplified. For example, a primer, which is 20 nucleotides long, normally corresponds to 45-55% GC content. It should have a melting temperature between 55 and 65^{o}C (Dieffenbach *et al*., 1993).

Primers with melting temperatures above 65 ^{o}C have a tendency for secondary annealing. Within a primer pair, the GC content and T_m should be well matched. Poorly

matched primer pairs can be less efficient and specific because loss of specificity arises with a lower melting temperature (T_m). Thus, PCR primers should maintain a reasonable GC content. Oligonucleotides 20 bases long with a 50% G + C content generally have a melting T_m values in the range of 52-58 ^oC. This provides a sufficient thermal window for efficient annealing (Dieffenbach *et al*., 1993).

Primer 3, can be accessed at:

http://frodo.wi.mit.edu/cgibin/primer3/primer3_www.cgi

The output from gene locations and primer designs for *hTERT*, *hsp90α*, *Glyceraldehyde-3-phosphate dehydrogenase* (*GAPDH*) and *vimentin* can be found in Fig 2.2, 2.3, 2.4, and 2.5 respectively.

A.

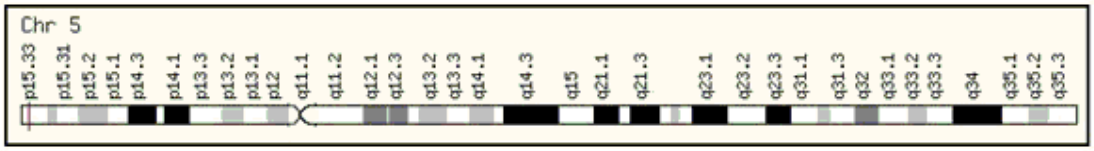

B.

***hTERT* Primer3 Output**

```
Using 1-based sequence positions
OLIGO         start len  tm     gc%    any    3'   Primer sequence
LEFT PRIMER   857   20   60.05  55.00  2.00   1.00 cgtggtttctgtgtggtgtc
RIGHT PRIMER 1070   20   60.01  60.00  5.00   1.00 ccttgtcgcctgaggagtag
SEQUENCE SIZE: 3979
INCLUDED REGION SIZE: 3979

PRODUCT SIZE: 214, PAIR ANY COMPL: 2.00, PAIR 3' COMPL: 1.00

cgtggtttctgtgtggtgtcacctgccagacccgccgaagaagccacctctttggagggtgcgctct
>>>>>>>>>>>>>>>>>>>>

ctggcacgcgccactcccacccatccgtgggccgccagcaccacgcgggccccccatccacatcgcg


gccaccacgtccctgggacacgccttgtcccccggtgtacgccgagaccaagcacttcctctactcc
                                                                <<<<<<<

tcaggcgacaagg
<<<<<<<<<<<<<
```

Key:

>>>>>> - Left / (sense) forward primer binding site

<<<<<< - Right / (anti-sense) reverse primer binding site

Figure 2.2 Bioinformatic data generated for *hTERT*

A) The gene location for *hTERT* on its respective human chromosome denoted by the red bar (taken from GeneCards database). B) Primer 3 output for *hTERT* showing annealing temperature, GC %, primer sequence and amplicon size (adapted from Primer 3).

A.

B.

***hsp90α* Primer3 Output**

```
Using 1-based sequence positions
OLIGO          start   len    tm      gc%     any     3'   Primer sequence
LEFT PRIMER    2742    20    60.05    55.00   8.00   0.00 tctggaagatccccagacac
RIGHT PRIMER   2930    20    59.94    55.00   5.00   3.00 agtcatccctcagccagaga
SEQUENCE SIZE: 3887
INCLUDED REGION SIZE: 3887

PRODUCT SIZE: 189, PAIR ANY COMPL: 5.00, PAIR 3' COMPL: 0.00


tctggaagatccccagacacatgctaacaggatctacaggatgatcaaacttggtctgggtattgatgaaga
>>>>>>>>>>>>>>>>>>>>

tgaccctactgctgatgataccagtgctgctgtaactgaagaaatgccacccccttgaaggagatgacgacac


atcacgcatggaagaagtagactaatctctggctgagggatgact
                        <<<<<<<<<<<<<<<<<<<<<
```

Key:

>>>>>> - Left / (sense) forward primer binding site

<<<<<< - Right / (anti-sense) reverse primer binding site

Figure 2.3 Bioinformatic data generated for *hsp90α*

A) The gene location for *hsp90α* on its respective human chromosome denoted by the red bar (taken from GeneCards database) or the blue bar (taken from ensemble database). B) Primer 3 output for *hsp90α* showing annealing temperature, GC %, primer sequence and amplicon size (adapted from Primer 3).

A.

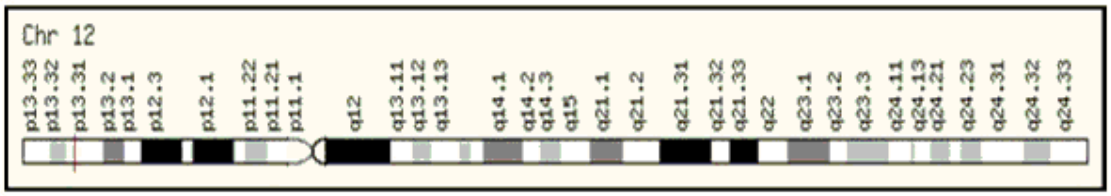

B.

***GAPDH* Primer3 Output**

```
No mispriming library specified
Using 1-based sequence positions

OLIGO         start len  tm    gc%    any   3'  Primer sequence
LEFT PRIMER   122   20   59.97 50.00 3.00  0.00 gagtcaacggatttggtcgt
RIGHT PRIMER 359   20   60.01 45.00 4.00  2.00 ttgattttggagggatctcg
SEQUENCE SIZE: 1310
INCLUDED REGION SIZE: 1310

PRODUCT SIZE: 238, PAIR ANY COMPL: 4.00, PAIR 3' COMPL: 1.00

gagtcaacggatttggtcgtattgggcgcctggtcaccagggctgcttttaactctggtaaagtgg
>>>>>>>>>>>>>>>>>>>>

atattgttgccatcaatgacccccttcattgacctcaactacatggtttacatgttccaatatgatt


ccacccatggcaaattccatggcaccgtcaaggctgagaacgggaagcttgtcatcaatggaaatc


ccatcaccatcttccaggagcgagatccctccaaaatcaa
                    <<<<<<<<<<<<<<<<<<<
```

Key:

>>>>>> - Left / (sense) forward primer binding site

<<<<<< - Right / (anti-sense) reverse primer binding site

Figure 2.4 Bioinformatic data generated for *GAPDH*

A) The gene location for *GAPDH* on its respective human chromosome denoted by the red bar (taken from GeneCards database). B) Primer 3 outputs for *GAPDH* showing annealing temperature, GC %, primer sequence and amplicon size (adapted from Primer 3).

A.

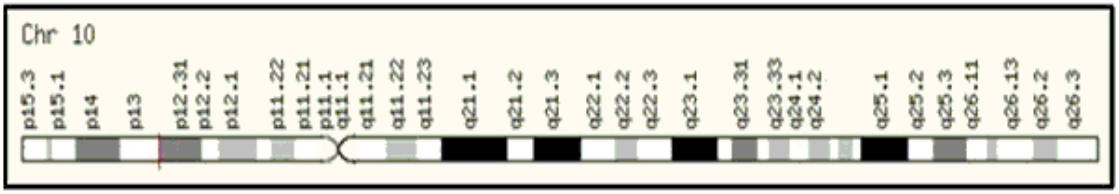

B.

***Vimentin* Primer3 Output**

```
Using 1-based sequence positions


OLIGO         start len   tm     gc%     any   3'   Primer sequence
LEFT PRIMER   1458   20    60.00    50.00  3.00  2.00 gagaactttgccgttgaagc
RIGHT PRIMER  1627   20    60.01    55.00  5.00  2.00 tccagcagcttcctgtaggt
SEQUENCE SIZE: 2136
INCLUDED REGION SIZE: 2136

PRODUCT SIZE: 170, PAIR ANY COMPL: 5.00, PAIR 3' COMPL: 1.00


gagaactttgccgttgaagctgctaactaccaagacactattggccgcctgcaggatgagattcagaatatga
>>>>>>>>>>>>>>>>>>>>

aggaggaaatggctcgtcaccttcgtgaataccaagacctgctcaatgttaagatggcccttgacattgagat


tgccacctacaggaagctgctgga
    <<<<<<<<<<<<<<<<<<<<
```

Key:

>>>>>> - Left / (sense) forward primer binding site

<<<<<< - Right / (anti-sense) reverse primer binding site

Figure 2.5 Bioinformatic data generated for *vimentin*

A) The gene location for *vimentin* on its respective human chromosome denoted by the red bar (taken from GeneCards database). B) Primer 3 outputs for *vimentin* showing annealing temperature, GC %, primer sequence and amplicon size (adapted from Primer 3).

2.5 Real time quantitative reverse transcriptase polymerase chain reaction (qRT-PCR)

Polymerase Chain Reaction (PCR) is a process which allows logarithmic amplification of short DNA sequences (usually 100-400 bases) within a longer double stranded DNA/cDNA molecule. qRT-PCR allows low copy mRNA to be amplified.

The level of *GAPDH*, *hTERT* and *hsp90α* expressions was calculated by qRT-PCR using the LightCycler 2.0 system. (Roche Diagnostics, UK) and LightCycler® FastStart DNA Master^{PLUS} SYBR Green I kit following the manufacturer's instructions. A master mix was prepared using the reagents from the kit.

Table 2.7 The composition and quantity of each reagent provided within the LightCycler® FastStart DNA Master^{PLUS} SYBR Green I kit.

Reagent	Reagent Composition	Quantity
LightCycler® FastStart Enzyme (1a)	FastStart Taq DNA Polymerase	1 vial
LightCycler® FastStart Reaction Mix SYBR Green (1b)	Reaction buffer, dNTP mix (with dUTP instead of dTTP), SYBR Green I dye and 10 mM $MgCl_2$	3 vials
H_2O, PCR-grade	RNase-free H_2O	2 ml

Table 2.8 The quantities of reagents required for each RT-PCR reaction using those provided within the LightCycler® FastStart DNA Master^{PLUS} SYBR Green I kit.

Reagent	Quantity
Molecular biology-grade H_2O	12 µl
PCR primer mix	2 µl
Enzyme Master Mix	4 µl
Single-stranded cDNA template	2 µl

Procedure:

1. The samples and reagents were kept on ice throughout the experiment.
2. Each capillary had a 20 µl total reaction volume comprising 12 µl molecular biology-grade H_2O, 2 µl of 10 µM PCR primer mix, 4 µl of Master Mix and 2 µl single-stranded cDNA template.
3. Negative control was prepared by using template-free reaction mixture (20 µl) (molecular biology-grade H_2O substituted for cDNA).

The PCR protocol is as follows:

1. The PCR enzyme reaction mix was prepared by transferring 14 µl of LightCycler® FastStart Enzyme (1a) into the LightCycler® FastStart Reaction Mix SYBR Green vial (1b)

2. This experiment involves a hot-start induction, wherein FastStart *Taq* DNA polymerase enzyme is activated by pre-incubating the reaction mixture at 95°C for 10 min. This was carried out to avoid non specific elongation.

3. The single-strand cDNA template was then subjected to 35 amplification cycles composed of the following parameters:

- Denaturation of 95°C for 15 sec.
- Annealing at the primer dependent temperature for 15 sec
- Extension at 72°C for 25bp/sec (amplicon dependent)

4. At the end of each cycle, the emitted fluorescence was measured in a single step to acquire quantification analysis data. A slope of 20°C/s was maintained for heating and cooling purposes.

5. On completion of the 35^{th} cycle, the produced amplicon was prepared for melting curve analysis, and hence, it was heated to 95°C (denaturation) slope of 0.1°C/s and the emitted fluorescence was constantly measured. It was then rapidly cooled to the previously used annealing temperature (+10°C) for 40 s.

6. The generated amplicon was cooled to 40°C for 30 sec and stored at -20°C until required.

Hot start induction is crucial in this method to prevent non specific elongations and thus increases PCR specificity, sensitivity and yield (Dang and Jayasena, 1996). The specificity of the amplified PCR product could be assessed via the melting curve which discriminates between primer-dimers and specific product. The default qRT-PCR conditions used in this study are shown in Table 2.9 and the primer

sequence, annealing temperatures and amplicon size for the various genes used in this study are listed in Table 2.10.

Table 2.9 qRT-PCR conditions used as default conditions for all amplifications.

Analysis Mode	Cycles	Segment	Target Temperature (^{o}C)	Hold Time (min)
-	Pre-Incubation	-	-	-
None	1	-	95	10
-	Amplification	-	-	-
Quantification	35	Denaturation	95	1
-	-	Annealing	variable	2
-	-	Extension	72	1
-	-	-	72	7
-	Cooling	-	-	-
None	1	-	4	∞

Table 2.10 Primer sequence, annealing temperatures and amplicon size for *hTERT, hsp90α, GAPDH and vimentin* primers utilised in qRT-PCR [designed using Primer3 software and commercially synthesised by TIB MOLBIOL syntheselabor (Germany)].

Gene	Primer Sequences	Annealing Temperature (^{o}C)	Expected amplicon size (bp)
hTERT	Sense: 5' -CGTGGTTTCTGTGTGGTGTC- 3' Antisense: 5' -CCTTGTCGCCTGAGGAGTAG- 3'	67	214
hsp90α	Sense: 5' -TCTGGAAGATCCCCAGACAC- 3' Antisense: 5' -AGTCATCCCTCAGCCAGAGA- 3'	63	189
GAPDH	Sense: 5' –GAGTCAACGGATTTGGTCGT- 3' Antisense: 5' -TTGATTTTGGAGGGATCTCG- 3'	56	238
vimentin	Sense: 5' -GAGAACTTTGCCGTTGAAGC- 3' Antisense: 5' -TCCAGCAGCTTCCTGTAGGT- 3'	56	170

2.5.1 Analysis of qRT-PCR product by agarose gel electrophoresis

The amplicons from the qRT-PCR reaction were run on a 2% (w/v) agarose gel (section 3.4.1). Aliquots (10 µl) of each amplicon were mixed with 2 µl of loading dye and were loaded onto the gel. A 100 bp molecular weight marker (2 µl) mixed with 5 µl loading dye was loaded. The gel was electrophoresed at 70 V. The banding patterns were visualised using a GENE GENIUS Bioimaging system and Gensnap software.

2.5.2 Quantification analysis of qRT-PCR

Copy numbers were used to express the absolute quantification of the target amplicon. In real time PCR, a positive reaction is detected by accumulation of a fluorescent signal. The number of cycles required for the fluorescent signal to cross the threshold is give by the Ct (cycle threshold) value. Genomic DNA can be used as an external standard, showing that 1 µg corresponds to 3.4×10^5 copies of a single gene (Wittwer *et al.*, 2004). Previously in our laboratory (Shervington *et al*., 2007; Mohammed and Shervington, 2007) genomic DNA of known concentration was used as a standard to amplify *GAPDH* gene using the LightCycler instrument. The Ct which serves as a tool for calculating the starting template amount was used to plot a standard curve to aid with the calculation of copy numbers in unknown samples. A standard curve was generated from five concentrations of Genomic DNA in duplicate: 0.005, 0.05, 0.5, 5 and 50 ng and their corresponding average Ct's (Table 2.11 and Fig 2.6) were used to generate the copy number verses concentration.

Table 2.11 Genomic DNA corresponded to its average Ct values and equivalent copy number.

Concentration of Genomic DNA (ng)	Average Ct	Copy number
0.005	30.15	1.7
0.05	29.10	17
0.5	26.42	170
5	22.60	1700
50	18.30	17000

A.

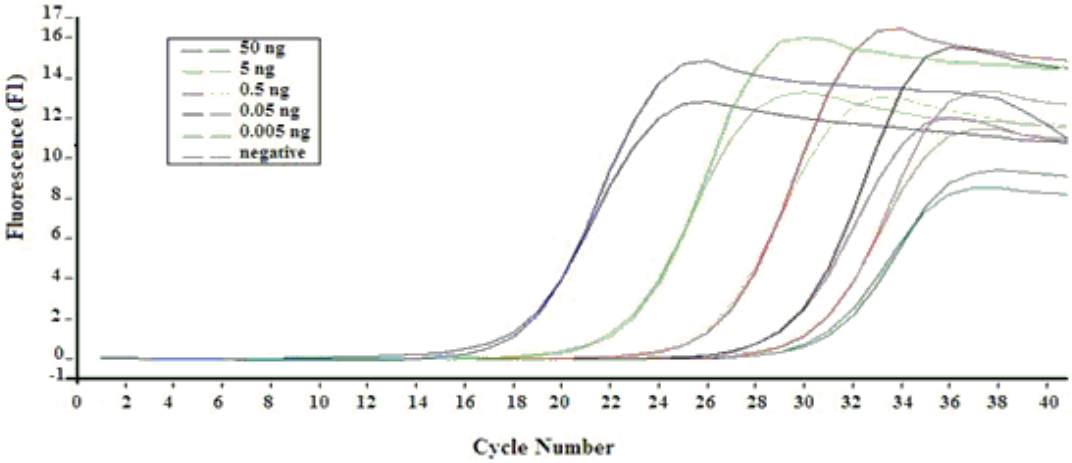

B.

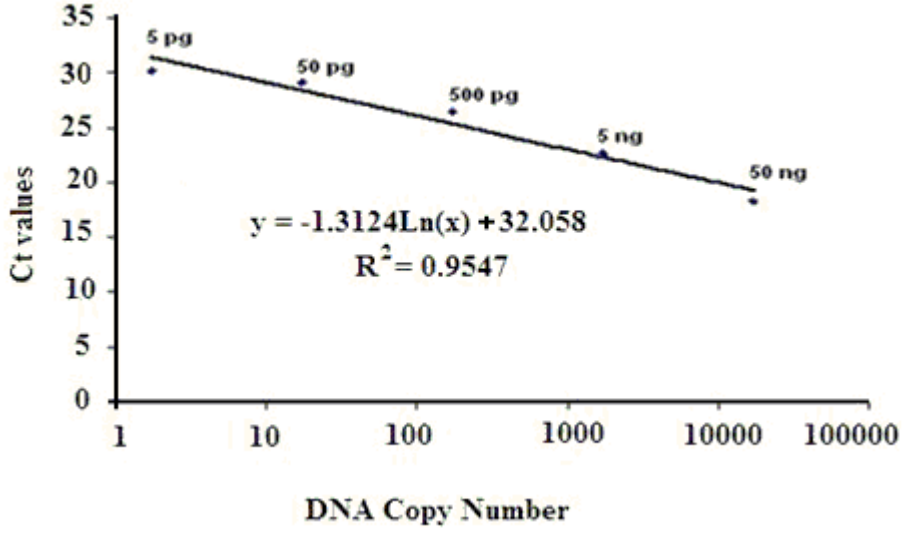

Figure 2.6 Standards used to generate the copy numbers for each gene.

A) LightCycler quantification curve generated when known concentration of genomic DNA were amplified, which shows that the higher the concentration of DNA the lower the Ct value i.e. earlier the acquisition of florescence. The negative control shows no florescence acquisition until after 30 Ct (straight line). B) The standard generated from the crossing points shows the relationship between Ct values and the copy numbers of the amplified genomic DNA using *GAPDH* reference gene (adapted from Mohammed, 2007).

The equation generated (y = -1.3124Ln(x) + 32.058) from this standard graph was rearranged to (=EXP ((Ct value-32.058)/-1.3124)) and used to determine copy numbers of the mRNA expression of all the genes used throughout this project.

2.6 Immunofluorescence

Procedure:

1. The cells were washed three times with warm PBS (0.1 M) with gentle aspiration.
2. They were then fixed using freshly made 4% Paraformaldehyde and incubated for 10 min on a shaker.
3. The paraformaldehyde was then removed and permeablized using 0.3% Triton X-100 at room temperature for 7 min.
4. Bovine Serum Albumin (BSA) blocking solution was then added to prevent any non-specific binding and incubated for 30 min at room temperature.
5. BSA was removed and primary monoclonal Hsp90α antibody (Cambridge Biosciences, UK) and/or telomerase antibody (Abcam, UK) (diluted in 1% BSA in PBS to achieve working dilution of 1:50 and 1:2000) was added to each chamber and incubated for 1 h at room temperature.
6. Primary antibody was removed by washing three times with Triton X-100.
7. Later, the cells were incubated with secondary antibody for 1 hour at room temperature. The secondary antibodies were diluted in 1% BSA in PBS to achieve a working dilution of 1:128. The secondary antibodies were light sensitive and were conjugated either with Fluorescein Isothiocyanate (FITC)

or Texas red. The primary Hsp90α antibody was detected with IgG FITC (Sigma,UK). The primary telomerase antibody was detected with IgM FITC (Sigma,UK). For co-localization experiments telomerase was detected with IgM Texas Red (Abcam, UK).

8. Secondary antibody was removed by washing three times with Triton X-100.
9. Nucleus was counterstained by incubation with 1.5 µg/ml VECTASHIELD mounting medium with PI (Vector, USA) for 10 min.
10. The cells were visualised and scanned using an Axiovert 200 LSM 510 laser scanning confocal microscope (Carl Zeiss, UK) (Long *et al*., 2005).
11. Negative control cells from each sample received identical preparations for immunofluorescence staining, except that the primary antibodies were omitted and for quantification purposes 500 cells were analysed per sample.

2.7 Small Interfering RNA

2.7.1 Preperation of siRNA

Three sets of pre-designed *hTERT* siRNA duplexes were designed by Ambion (UK). *Hsp90 α* siRNA, control *GAPDH* siRNA and negative control siRNA were also included in this study. All the siRNA comprised of 21-nt sense and antisense strands. Oligonucleotides sequences for all the siRNA used are listed in the Table 2.12.

Table 2.12 Oligonucleotides sequences and targeted exons for all the siRNA.

siRNA oligo	Exon targeted		Sequence
hTERT Oligo1	11	sense	5'GCACGGCUUUUGUUCAGAUtt3'
		antisense	5'AUCUGAACAAAAGCCGUGCca3'
hTERT Oligo2	4	sense	5'GGCCGAUUGUGAACAUGGAtt3'
		antisense	5'UCCAUGUUCACAAUCGGCCgc3'
hTERT Oligo3	3	sense	5'CGGAGACCACGUUUCAAAAtt3'
		antisense	5'UUUUGAAACGUGGUCUCCGtg3'
hsp90α Oligo3	3	sense	5'GCGAUGAUGAGGCUGAAGAtt3'
		antisense	5'UCUUCAGCCUCAUCAUCGCtt3'
GAPDH Oligo3	3	sense	5'GGUCAUCCAUGACAACUUUdTdT3'
		antisense	5'AAAGUUGUCAUGGAUGACCdTdT3'

The *hsp90α* siRNA used in this study was previously optimised in our laboratory and was chosen as the best oligo amongst a set of three pre-designed *hsp90α* siRNAs (Cruickshanks *et al*., 2010). The control *GAPDH* siRNA, negative control siRNA and a Cy3 labelled control siRNA were part of the siPORT^{TM} siRNA electroporation kit (Applied Biosystems, UK). The negative control siRNA is a scrambled siRNA which has limited similarity to the human genome. All the siRNA were supplied in a freeze-dried powdered form and were resuspended in nuclease-free water to achieve a stock concentration of 100 μM. This was further diluted in the nuclease-free water to achieve a working concentration of 50 μM. Cy3 labelled control siRNA was also resuspended in nuclease free water prior to its use. The quantity and composition of each reagent provided within the kit is detailed in Table 2.13.

Table 2.13 Quantity of reagents provided within the siPORT™ siRNA Electroporation Kit.

Reagent	Quantity
siRNA electroporation buffer	3 × 1.5 ml
50 µM GAPDH siRNA	75 µl
50 µM negative control siRNA	38 µl
Cy3 labelled control siRNA (requires re-suspension in 42 µl nuclease free water)	2.1 nmol
Nuclease-free water	1.75 ml

2.7.2 Optimisation of siRNA transfection

Cells were efficiently transfected with siRNA using electroporation. In electroporation an electric field is used to induce the trans-membrane voltage. This leads to pore formation via a structural rearrangement of the membrane thereby increasing the membrane permeability (Chen *et al*., 2007).

Conditions of electroporation vary according to the cell types. Various other factors can also affect electroporation efficiency, these include: pulse length, number of pulses, and concentration of siRNA. The electroporation conditions supplied by Ambion were verified by transfecting U87-MG cells with Cy3 labelled control siRNA. The siRNA was delivered to the cells using the siPORT™ siRNA Electroporation Kit according to the manufacturer's instructions (Ambion, UK). Bio-Rad gene pulser Xcell was used for electroporation.

The reaction parameters used in this study was:

3 pulses (square wave type pulse) at 400 V for 100 µS with 0.1 sec intervals between the pulses.

Procedure:

1. U87-MG cells were cultured in 75 cm^2 tissue culture-treated polystyrene flasks as described in section 2.1.4.
2. After scraping the cells, 75 × 10^4 cells per electroporation sample were centrifuged at 200 x g for 7 min at room temperature.
3. The medium was removed and the cells were resuspended in 75 µl of siRNA electroporation buffer.
4. The cell suspension was transferred to a 1 mm electroporation cuvette and prior to electroporation 2.25 µl of Cy3 labelled control siRNA was added to the cuvette and mixed gently.
5. These cells were then electroporated using the conditions mentioned above.
6. The sample cuvette was incubated for 10 min at 37°C after which the cells were transferred to chamber slides containing an appropriate volume of medium.
7. The chamber slides were incubated for 24 hrs under normal cell culture conditions.
8. The integration of Cy3 in the cell (Fig 2.7) was visualised using the Axiovert 200 LSM 510 laser scanning confocal microscope (Carl Zeiss, UK) which showed that the siRNA was efficiently delivered to the cells.

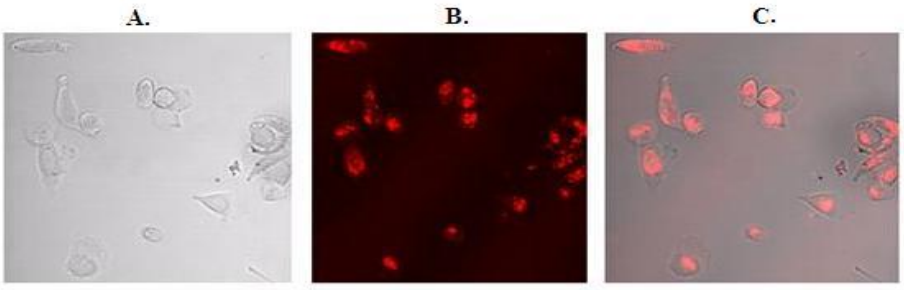

Figure 2.7 Uptake of Cy3 labelled siRNA in U87-MG cells.
A) phase contrast image B) Cy3 fluorescence (550 nm, Em 570 nm) C) Overlay of A and B to confirm Cy3 uptake.

2.7.3 siRNA treatment

Procedure:

1. Similar to the optimization procedure, U87-MG cells were cultured in 75 cm^2 tissue culture-treated polystyrene flasks and after scraping 75 × 10^4 cells per electroporation sample were centrifuged at 200 x g for 7 min at room temperature.
2. The medium was removed and the cells were resuspended in 75 µl of siRNA electroporation buffer and the cells were transferred to a 1 mm electroporation cuvette.
3. Prior to electroporation, 1.5 µg of diluted experimental *hTERT* siRNA oligos 1-3, *hsp90α* siRNA oligos 1-3, *GAPDH* siRNA or negative control siRNA was added to the cuvette and mixed gently.
4. The cells were electroporated using the above mentioned parameters.
5. After the electroporation, the sample cuvette was incubated for 10 min at 37°C
6. Cells were transferred either to a 25 cm^2 tissue culture-treated polystyrene flasks (qRT-PCR), or chamber slides (section 3.5) containing an appropriate volume of prewarmed medium.
7. These cells were either incubated for 24 or 48 hr, after which the cells were harvested for mRNA isolation (Chi *et al*., 2003) to measure *hTERT* and *hsp90α* expressions.
8. PCR products were analysed using gel electrophoresis, stained and visualised using the gel analyser (SynGene, UK) as previously explained in section 3.4.1.
9. Chamber slides were fixed with 4% paraformaldehyde for subsequent detection of telomerase or Hsp90α protein.

2.8 Proteomics

2.8.1 Protein extraction

Procedure:

1. The cell pellets were freshly collected and washed three times with Washing Buffer (10 mM Tris-HCl, 5 mM magnesium acetate, pH 8.0) to remove culture medium.
2. For 10 mg of cultured cell pellet, 200 µl of 2-D cell lysis buffer (400 mM Tris, 0.01 M EDTA; pH 8.3) was added.
3. The mixture was sonicated at 4°C followed by shaking for 30 min at room temperature.
4. The samples were then centrifuged for 30 min at 14,000 rpm and the supernatant was collected.
5. Protein concentration was measured using Bio-Rad protein assay method.

2.8.2 Protein quantification

The Bio-Rad Protein Assay is based on the Bradford method of protein quantification. It is a dye-binding assay which produces differential color change in response to various concentrations of protein (Bradford, 1976). The dye reagent concentrate was purchased in a kit with BSA (Biorad, UK) which was used as a standard.

Procedure:

1. Lyophilized BSA standards were reconstituted by adding 20 ml of deionized water and were mixed thoroughly until dissolved.

2. The standard was aliquoted and stored at -20°C when not used.
3. The dye reagent was prepared by diluting 1 part Dye Reagent Concentrate with 4 parts of distilled deionized water and this was then filtered through Whatman #1 filter.
4. Protein solution to be tested was prepared by pipetting 100 µl of each standard and sample solution into a clean and dry test tube.
5. Diluted dye reagent (5 ml) was added to each tube.
6. The tubes were vortexed and incubated at room temperature for at least 5 min.
7. Absorbance was measured at 595 nm using gamma thermo Helios spectrophotometer (Thermospectronics, UK).
8. A standard curve was plotted and the value of the unknown protein was extrapolated.
9. Each protein was assayed at least 2-3 times.

In this thesis 2D-DIGE was used for protein separation and MALDI-TOF was used for protein identification. Gel separation (section 2.8.3 –section 2.8.7) and Protein ID (section 2.8.8 – section 2.8.9) were performed by Applied Biomics, Inc (Hayward, CA).

2.8.3 2D-DIGE

2D-DIGE involves tagging the protein solutions with different fluorescent dyes (Cy2, Cy3 or Cy5) prior to performing the 2D gel electrophoresis wherein the samples are separated based on their isoelectric point and molecular weight. Computer software such as the DeCyder allows comparison of these protein mixtures and, by using a

pooled standard labelled with the third dye, the software can reliably compare differences in protein levels across multiple gels (Srinivas *et al*., 2002). Table 2.14 shows the composition of each reagent used for 2D-DIGE.

Table 2.14. Composition of reagents used for 2D-DIGE.

Reagent	Composition
Washing Buffer	10 mM Tris-HCl, 5 mM magnesium acetate, pH 8.0
2-D cell lysis buffer	30 mM Tris-HCl, pH 8.8, containing 7 M urea, 2 M thiourea and 4% CHAPS
2-D Sample buffer	8 M urea, 4% CHAPS, 20 mg/ml DTT, 2% pharmalytes and trace amount of bromophenol blue
Rehydration buffer	7 M urea, 2 M thiourea, 4% CHAPS, 20 mg/ml DTT, 1% pharmalytes and a trace amount of bromophenol blue
Equilibration buffer-1	50 mM Tris-HCl, pH 8.8, containing 6 M urea, 30% glycerol, 2% SDS, trace amount of bromophenol blue and 10 mg/ml DTT
Equilibration buffer-2	50 mM Tris-HCl, pH 8.8, containing 6 M urea, 30% glycerol, 2% SDS, trace amount of bromophenol blue and 45 mg/ml Iodacetamide
SDS-gel running buffer	0.1% w/v SDS, 25 mM Tris, 198 mM Glycine
Matrix solution	0.01g α-cyano-4-hydroxycinnamic acid, 5 mg/ml in 50% acetonitrile, 0.1% trifluoroacetic acid, 25 mM ammonium bicarbonate

2.8.4 CyDye labelling

Procedure:

1. For each sample, 30 µg of protein was mixed with 1.0 µl of diluted CyDye, and kept in the dark on ice for 30 min.
2. Cells treated with *hTERT* siRNA and *hsp90α* siRNA were labelled with Cy2 and Cy5, respectively. Control sample was labelled with Cy3.
3. The labelling reaction was stopped by adding 1.0 µl of 10 mM lysine to each sample, and incubating in the dark on ice for an additional 15 min.
4. The labelled samples were then mixed together.
5. The 2-D Sample buffer, 100 ul destreak solution and Rehydration buffer were added to the labelled mix to give the total volume of 250 µl.
6. The samples were vortexed before loading them into the strip holder for 2D electrophoresis.

2.8.5 Isoelectric Focusing (IEF) and Sodium Dodecyl Sulphate Polyacrylamide Gel Electrophoresis (SDS-PAGE)

The DIGE gel is a low fluorescent 12 % polyacrylamide gel and is precast in a glass cassette with a buffer for increasing its shelf-life. IEF was performed using the protocol developed by Amersham Biosciences (USA).

Procedure:

1. Labelled samples were loaded onto a pH 3-10 linear IPG strips (GE healthcare)
2. IEF was performed using the following parameters
    - Rehydration at 20°C for 12 hours

- Step 1: 500 V for 1000 VHr
- Step 2: 1000 V for 2000 VHr
- Step 3: 8000 V for 24000 VHr

3. Upon completing the IEF, the IPG strips were incubated in the freshly made equilibration buffer-1 for 15 min with gentle shaking.
4. This was followed by rinsing the strips in the freshly made equilibration buffer-2 for 10 min with gentle shaking.
5. The IPG strips were then rinsed in the SDS-gel running buffer and immediately transferred into a 12% SDS-gels (18 cm x 16 cm).
6. The gel was then sealed with 0.5% agarose (Bio-Rad, USA) in SDS-PAGE running buffer.
7. The SDS-gels were run at 15°C at 200 V until the dye front ran off the gels.

2.8.6 Image scan and data analysis

Gel images were scanned immediately following the SDS-PAGE using Typhoon TRIO (Amersham BioSciences, USA). The scanned images were analyzed by Image Quant software (version 6.0, Amersham BioSciences, USA), followed by in-gel analysis using DeCyder software version 6.0 (Amersham BioSciences, USA). The fold change of the protein expression levels was obtained from in-gel DeCyder analysis.

2.8.7 Spot picking and trypsin digestion

1. The spots of interest were picked up by Ettan Spot Picker (Amersham BioSciences, USA) based on the in-gel analysis and spot picking design by DeCyder software.

2. The gel spots were washed a few times with 100% acetonitrile and were digested in-gel with modified porcine trypsin protease (Trypsin Gold, Promega, USA).
3. The digested tryptic peptides were desalted by Zip-tip C18 (Millipore, USA). (Zip-tips are pipette tips with small amount of chromatography media bedded at the end which helps in eluting peptides after desalting it).
4. Peptides were eluted from the Zip-tip with 0.5 µl of matrix and spotted on the MALDI plate (model ABI 01-192-6-AB).

2.8.8 MALDI-TOF

MALDI-TOF MS and TOF/TOF tandem MS/MS were performed on an ABI 4700 mass spectrometer (Applied Biosystems, USA). MALDI-TOF mass spectra were acquired in reflectron positive ion mode, averaging 4000 laser shots per spectrum. TOF/TOF tandem MS fragmentation spectra were acquired for each sample, averaging 4000 laser shots per fragmentation spectrum on each of the 10 most abundant ions present in each sample (excluding trypsin autolytic peptides and other known background ions).

2.8.9 Database search

Both of the resulting peptide mass and the associated fragmentation spectra were submitted to GPS Explorer workstation equipped with MASCOT search engine (Matrix science, US) to search the database of the National Center for Biotechnology Information non-redundant (NCBInr). Searches were performed without constraining protein molecular weights or isoelectric points, with variable carbamidomethylation of cysteine and oxidation of methionine residues, and with one missed cleavage also allowed in the search parameters. Candidates with either protein score C.I.% or Ion C.I.% greater than 95 were considered significant.

2.8.10 Ingenuity Pathway Analysis (IPA)

Data mining and knowledge base software like IPA (Ingenuity® Systems) was used to identify molecular functions and pathways which correlate with the dataset generated by the proteomic analysis.

The Ingenuity pathway analysis program uses a knowledgebase derived from the literature to relate gene products with each other based on their interaction and function. IPA helps to gain insights into experimental data by quickly identifying relationships, mechanisms, interaction networks, functions, and global pathways. This software allows profiling data to be analyzed in a systematic way using known protein–protein interactions published in the literature (Jimenez-Marin *et al*., 2009). IPA provides a platform which enables one to access information on genes and proteins implicated in cancer-related processes and pathways, generate testable hypotheses and discover new cancer targets.

In IPA biofunctions are grouped into three categories i) disease and disorders ii) molecular and cellular functions and iii) physiological system development and functions, whereas canonical pathways are grouped in metabolic pathways and signaling pathways. Functional pathways and networks most significant to the data set are identified from the IPA library of canonical pathways. The identified proteins are mapped to networks available in the Ingenuity database and ranked by score. The scores take into account the number of focus proteins and the size of the network to approximate the relevance of the network to the original list of focus proteins. The results generated by IPA are shown in Figure 4.5. and 4.6 and Table 4.5.

CHAPTER 3

siRNA DOWNREGULATION OF *hTERT* AND *hsp90α* GENES IN GLIOMA

3.1 Introduction

Ribonucleic acid interference (RNAi) is a process that along with sequencing specifically destroys mRNA, resulting in hypomorphic phenotypes (Elbashir *et al.*, 2001). It is a gene silencing process whose role is vital for development as well as preservation of the genome (Tomari and Zamore 2005). RNA interference uses short double-stranded RNA to selectively prevent gene expression of complementary RNA nucleotide sequences after transcription but before translation (Pellish *et al*., 2008). RNAi offers an effective technology base, on which gene expression as well as gene functions researches can be carried out. RNAi makes it easy for researchers to partly or fully suppress the expression of specific genes thereby resulting in targeted gene knockout and gene knockdown (Martinez, 2010). Due to the potent and specific RNAi triggering activity, the development of siRNA-based therapeutics has advanced rapidly (Zhou and Rossi, 2010).

RNAi mechanisms results either in the degradation of target RNA, (e.g. short interfering RNA), or translation arrest of the target RNA, (e.g. in the case of micro RNA). There are two types of RNAi-based therapies i) DNA-based RNAi in which plasmid DNA encodes for a short hairpin RNA (shRNA) and ii) RNA-based RNAi in which a siRNA duplex is chemically synthesized without a DNA intermediate (Pardridge, 2007).

Small interfering RNAs (siRNA) are short RNA molecules with a length of twenty to twenty five nucleotides (Elbashir *et al*., 2001). RNAi technology harnesses a straightforward mechanism of interrelating complementary RNA sequences. Initially the RNase enzyme, processes the long dsRNA segments (Dicer), into small dsRNA duplexes of 21–23 nucleotides; called as siRNA. The small interfering RNAs are then

integrated into an RNA-induced silencing complex (RISC) and then unwound into single-stranded small interfering RNA (Koller 2006). One strand is discarded by the RISC which leaves a 'processed' strand of siRNA that is integrated in the protein complex. For the recognition of target mRNA this 'processed' strand of siRNA functions as a guiding sequence. Complementary mRNAs are degraded by endonuclease argonaute, which is the catalytic component of RISC (Tuschl *et al*., 1999). This results in post-transcriptional gene silencing (Tuschl *et al*., 1999; Pellish *et al*., 2008). Figure 3.1 shows a basic working model of siRNA mechanism.

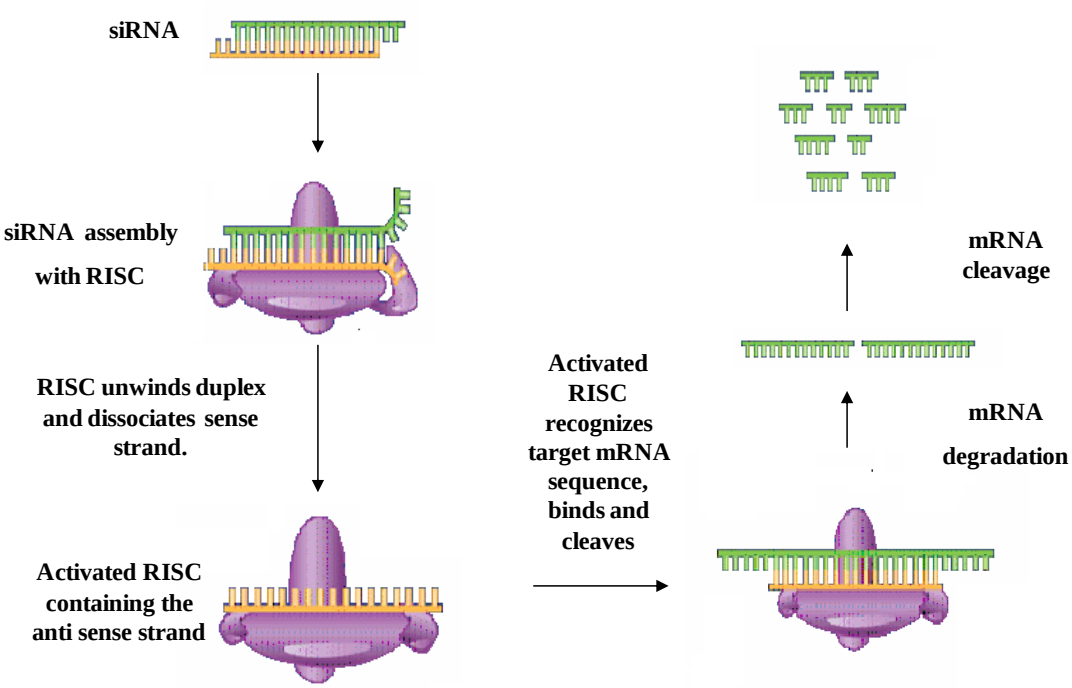

Figure 3.1 Diagrammatic representation of siRNA at working mechanism (adapted in part from - Sigma, 2006 and Ambion Technotes 2004).

The role of RNAi as a therapy in cancer is to knockout the cell cycle gene expression and/or the anti-apoptotic gene in the cancer cells thereby stopping the tumor growth and terminating cancer. RNAi technology and the use of siRNAs has been used at length in target validation experiments (Behlke, 2006; Novobrantseva *et al*., 2008). Of

late many siRNAs have been assessed in clinical trials with encouraging proposals for enhancing its efficacy and safety profiles (de Fougerolles *et a*l., 2007). Till date, only one antisense drug, Vitravene, has managed to receive FDA approval. Vitravene, which is a DNA antisense drug from Isis Pharmaceuticals in Carlsbad, California, is used to treat cytomegalovirus infections in the eye for patients with HIV. The powerful and precise suppression of gene expression by siRNA is presently being evaluated as a promising functional method for advancing gene-silencing therapies for cancer (Robinson, 2004).

RNA interference (RNAi) has been instrumental for specific inhibition of telomerase. Reports have shown that RNAi against *hTERT* could effectively restrain telomerase activity in many cancer cell lines. Successful attempts have been made to silence telomerase by direct transfection via lipofection and also by plasmid transfection via pZeoSV2-hTR construct in colon carcinoma cells (Kosciolek *et al*., 2003). Also studies in human colon carcinoma cells, HCT-15, involving siRNA targeted towards *hTR* as well as *hTERT* have shown to suppress telomerase activity in a dose-dependent manner. The transfection of HeLa cells utilizing a plasmid consisting the hTR gene have resulted in decreased telomerase RNA content, telomerase activity and telomeric DNA (Kosciolek *et al*., 2003). Attempts have been made to use siRNA targeted telomerase as an effective anti-cancer agent, especially in adjuvant therapies. siRNA based strategy have been used to enhance the effect of ionizing radiation and chemotherapy (Nakamura *et al*., 2005).

RNAi technology has also been successfully used in cancer cells to inhibit telomerase activity and to increase cell death through suppression of the *hTERT* expression in cancer cells with no side effect on normal cells (Chen *et al*., 2007). RNA interference

was harnessed in this study as it offers a new mode for efficient and selective inhibition of specific gene expressions in cancer with few side effects. Also, inhibiting telomerase activity in glioma cell lines, using siRNA, targeted towards two different telomerase regulatory mechanisms is novel.

3.2 Results

3.2.1 Optimization

In order to ensure that optimum conditions were used throughout the project, validation experiments were performed to verify the efficiency of the protocol used for mRNA isolation, cDNA conversion as well as siRNA transfection.

3.2.1 Spectrophotometry for the cell lines extracted mRNA

After the extraction of mRNA from the cell lines, they were checked for purity using spectrophotometry. The absorbance was measured at 260 and 280 nm and the concentration of RNA present in each cell line was calculated. These isolated mRNA samples were further run on a denaturing alkaline agarose gel (Figure 3.2). An example of the spectrophotometry results obtained for 1321NI, U87-MG and GOS-3 were represented Table 3.1.

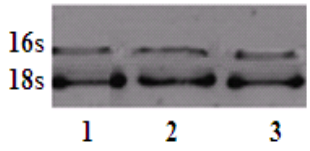

Figure 3.2 Agarose gel electrophoresis showing mRNA extracted from different grades of glioma cell lines.
Lanes 1-3 represent 2µl of mRNA isolated from 1321N1, U87-MG, GOS-3, respectively, run on a denaturing alkaline agarose gel (2 %).

Table 3.1 An example of the determined spectrophotometric readings for mRNA extracted from untreated 1321N1, GOS-3 and U87-MG cell lines.

Cell line	A_{260} reading	A_{280} reading	A_{260} / A_{280} ratio
1321N1	0.013	0.006	2.1
U87- MG	0.008	0.004	2.0
GOS-3	0.062	0.032	1.9

The mRNA band obtained was intact showing no running streak, which suggests that there was no degradation of the extracted mRNA. The purity of all the mRNA samples used in this study was found to be within the range of 1.9 and 2.1. A ratio of 1.9 - 2.1 indicates the presence of pure single-stranded (ss) RNA suggesting that the mRNA used in this study was of an optimum quality ((Roche diagnostic, UK).

3.2.2 Expression of *hTERT, hsp90α* and *GAPDH* genes

RT-PCR was carried out using the optimum annealing temperature (section 2.1.2) for *hTERT, hsp90α* and *GAPDH* in each of the three cell lines. This study was aimed at silencing the mRNA transcripts of *hTERT* and *hsp90α* as a mean of directly and indirectly shutting down the telomerase regulatory mechanisms with a view of studying its effect on the cancer proteomes. Hence, it was extremely important to check the expression levels of *hTERT* and *hsp90α* in different grades of glioma cell lines.

In order to ensure that the mRNA level was a true reflection of the expression of the gene studied, qRT-PCR was carried out for *GAPDH* in each of the three cell lines. *GAPDH* is a known endogenous reference gene used in several studies (Herms *et al*.,

2005). *GAPDH* expression was consistent throughout the results. Copy numbers of the gene was calculated as described earlier (section 2.5.2) and the results have been summarized in Fig. 3.3 and Table 3.2.

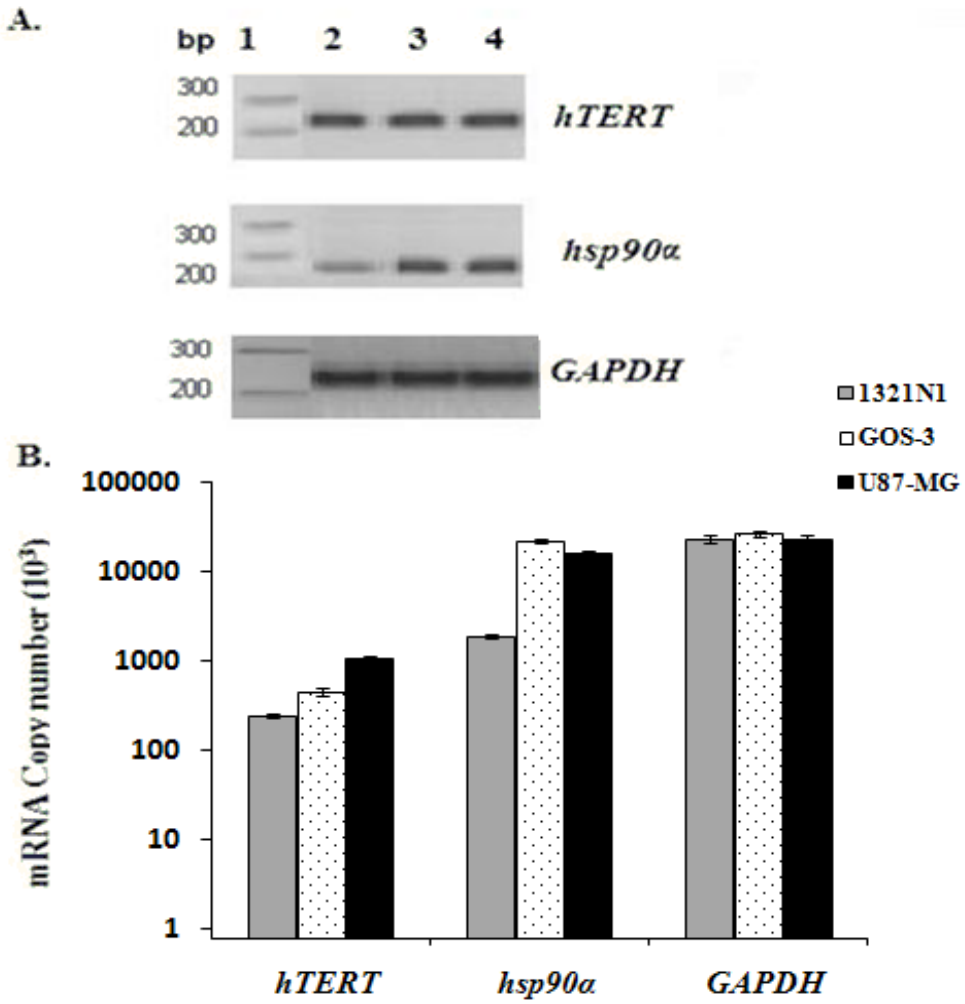

Figure 3.3 Expression levels of *hTERT, hsp90α* and *GAPDH* in cell lines.

Assessed by: (A) Agarose gel electrophoresis: Lane 1 represents a 100 bp molecular weight marker, Lanes 2, 3 and 4 represent the qRT-PCR amplicons from 1321N1, GOS-3, U87-MG cell lines respectively, (B) Graph showing copy number of *hTERT*, *hsp90α* and *GAPDH* in 1321N1, GOS-3 and U87-MG (data values are mean ± standard deviation of three independent experiments).

Table 3.2 *hTERT, hsp90α* and *GAPDH* transcription level.

Quantification of *hTERT, hsp90α* and *GAPDH* mRNA copy numbers in 1321N1, GOS-3 and U87-MG cell lines using qRT-PCR.

Cell line	mRNA/100 ηg cells extract (1×10^6 cells)		
	hTERT	***hsp90α***	***GAPDH***
1321N1	264.02	1914.38	21629.37
GOS-3	464.00	21106.39	25059.31
U87-MG	1075.18	15209.66	22106.36

The observed transcription of *hTERT* was consistent with the literature where the expression of *hTERT* is related to the grade of glioma; with U87-MG showing the maximum level of *hTERT* expression while 1321N1 showed the least. The expression levels *hsp90α* was also very high in all three cell lines. These results were in agreement with various reports suggesting *hsp90α* playing a crucial role in glioma as well as telomerase regulation. *GAPDH* was expressed in all three cell lines in approximately equal amounts.

Since the endogenous control was unaffected and stable in all the cell lines, it was confirmed that the methods used for the acquisition of the cDNA correctly followed and they did not induce any foreign alterations in the cellular gene expression and thus, results generated from these samples were a true reflection of the gene expression after the amplification protocol.

3.2.3 siRNA downregulation

Quantitative Real Time PCR was used to measure the mRNA levels of *hTERT* and *hsp90α* in 1321N1, GOS-3 and U87-MG glioma cells treated with experimental *hTERT* and *hsp90α* siRNAs, *GAPDH* siRNA and negative control siRNA (scrambled RNA).

3.2.3.1 Silencing *hsp90α*

hsp90α was silenced using siRNA oligo optimised previously in our laboratory. siRNA oligo 3 directed towards exon 9 was reported as the most efficient oligo for silencing *hsp90α* after 24 hr (Cruickshanks *et al*., 2010). It was also shown that silencing *hsp90α* resulted over 80% silencing of *hTERT* (unpublished). The experiment was repeated for confirmation (Table 3.3 and Figure 3.4).

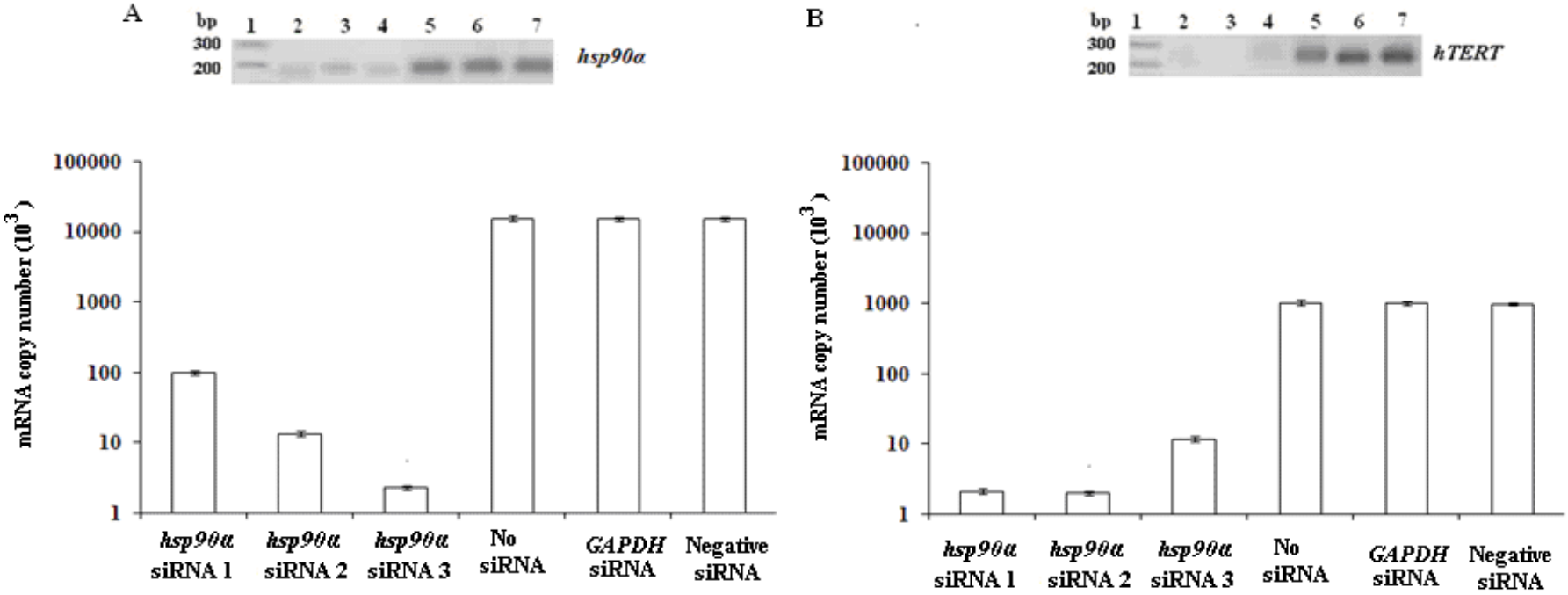

Figure 3.4 Expression levels of *hsp90α* and *hTERT* in U87-MG assessed after treatment with si*hsp90α* oligos 1-3 assessed after 24 hr using qRT-PCR.

Agarose gel electrophoresis and copy numbers of gene expression (data values are mean ± standard error, n = 3). hours: lane 1 represents molecular marker, lanes 2-4 represent *hsp90α* siRNAs 1-3, respectively; lane 5 control untreated cells; lane 6 represents *GAPDH* siRNA and lane 7 negative control siRNA .

Table 3.3 Expression levels of *hsp90α* and *hTERT in* U87-MG MG after treatment with si*hsp90α* oligos 1-3 assessed after 24 hr using qRT-PCR.

	mRNA/100 ηg cells extract (1×10^6 cells)					
	hsp90α **siRNA 1**	***hsp90α*** **siRNA 2**	***hsp90α*** **siRNA 3**	***No siRNA***	***GAPDH*** **siRNA**	**Negative siRNA**
hsp90α	98.05	13.01	2.23	15068	15191	15189
hTERT	11.30	2.23	1.04	987	1003	970

The results obtained were consistent with the previous work carried out in the laboratory where in siRNA oligo 3 directed towards exon 9 is the most efficient oligo for silencing *hsp90α* after 24 hr. Also treating the cell lines siRNA directed towards *hsp90α* resulted in decrease in the the expression of *hTERT*.

Immunofluorescence was also used to confirm the detected decrease in the Hsp90α and telomerase proteins after silencing the cells under the same conditions as qRT-PCR using siRNA 3 targeted against *hsp90α.* Using confocal microscopy, Hsp90α and telomerase protein levels were simultaneously checked in the cells using co-localization technique. Protein levels were quantified as a percentage of Hsp90α and telomerase positive expressing cells per tissue sample (a total of 250 cells were counted per sample). An example of co-localization of Hsp90α and telomerase proteins in U87-MG cells with and without siRNA are shown in Fig 3.5and summarized in Table 3.4.

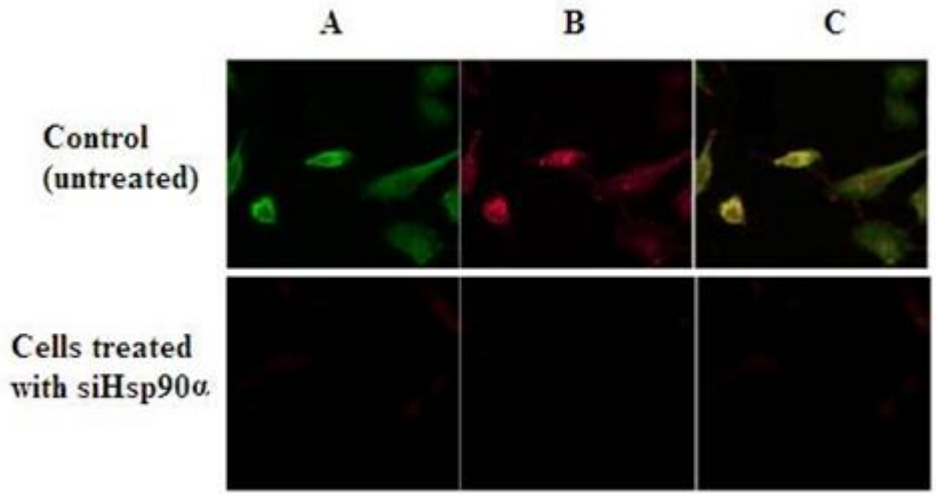

Figure 3.5 Example of Hsp90α and telomerase protein levels assessed using immunofluorescence in siRNA-treated and untreated U87-MG cells.

(A) Cells stained with FITC conjugate secondary antibody bound to Hsp90α (green) fantigens the (B) Cells stained with texas red conjugate secondary antibody bound to hTERT (red) antigens the (C) Overlay of A and B showing co-localization of Hsp90α and telomerase proteins.

Table 3.4 Protein levels of Hsp90α and telomerase.

Quantification of protein levels in U87-MG cell lines after 24 hr of siRNA treatment using oligo 3 targetted towards *hsp90α*.

	% Cell expressing Hsp90α	% Cell expressing telomerase	% of co-localized cells
Control	86	64	77
sihsp90α	3	0	0

Co-localization experiments confirmed that silencing hsp90 results in a decrease of telomerase expression only at the transcriptional level but also at the protein level. As a

result silencing *hsp90α* was used as the indirect regulatory mechanisms for inhibiting telomerase activity.

3.2.3.2 Silencing *hTERT*

Predesigned siRNAs were used to inhibit *hTERT* and *hsp90α at* the post transcriptional level. Three different oligos of siRNA targeted towards *hTERT* were designed by Ambion (UK) targeting exon 11; exon 4 and exon 3, respectively. qRT-PCR was used to examine mRNA levels of *hTERT* after siRNA treatment in all three cell lines after 24 and 48 hr incubation.

siRNA oligo 1 was unable to completely silence telomerase in all three cell lines after 24 hr though it did show silencing in U87-MG cells. However, after 48 hr it was very effective. The results showed that treatment with oligo 2 significantly reduced the expression of *hTERT* in the all three cell lines after 24 as well as 48 hr. siRNA oligo 3 was unable to downregulate *hTERT* expression after 24 hr and only showed silencing in U87-MG cell line after 48hr. Thus, siRNA oligo 2 was selected as the most effective siRNA against *hTERT*. U87-MG cell line showed silencing of *hTERT* expression by all the three oligos and was selected as the most suitable cell line (Fig 3.6 and Table 3.5)

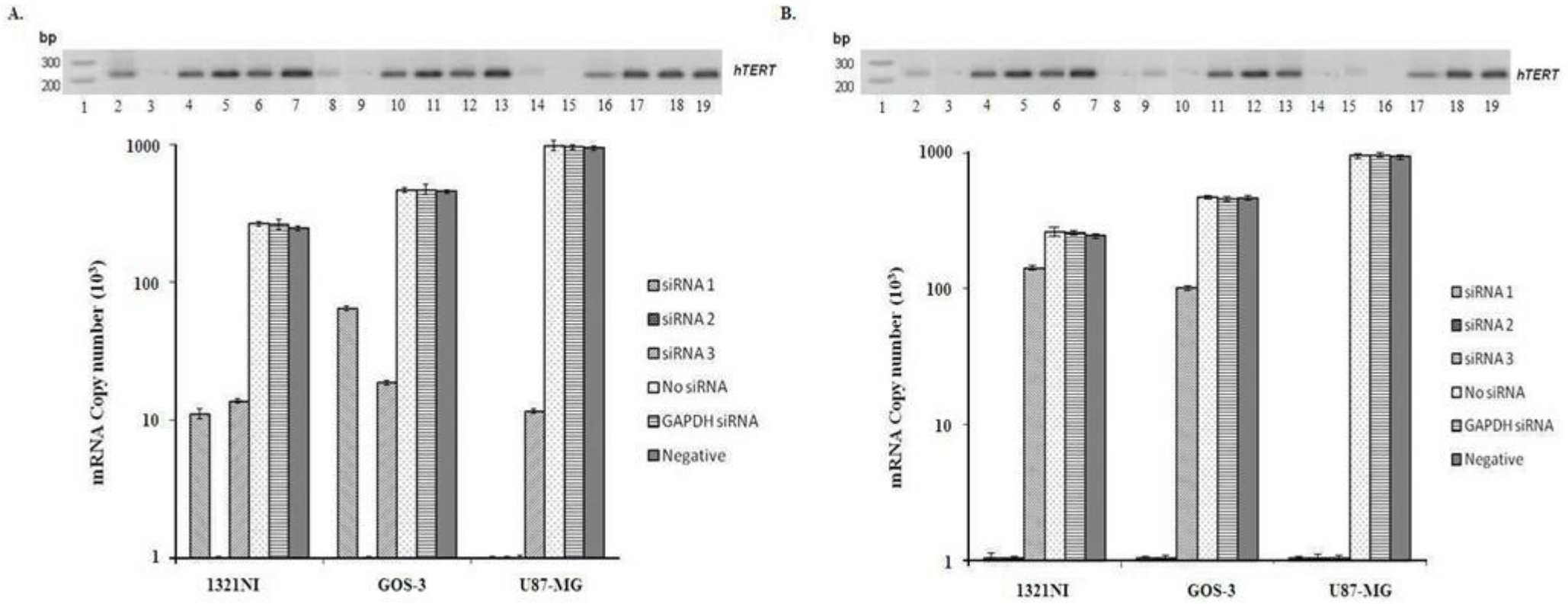

Figure 3.6 Expression levels of *hTERT* in 1321N1, GOS-3 and U87-MG siRNA treated cells assessed after 24 and 48 hours. Agarose gel electrophoresis and copy numbers of gene expression (data values are mean ± standard error, n = 3). (A) after 24 hr (B) after 48 hours: lane 1 represents molecular marker, lanes 2-4 represent *hTERT* siRNAs 1-3, respectively; lane 5 control untreated cells; lane 6 represents *GAPDH* siRNA and lane 7 negative control siRNA in 1321N1 cell lines. Similarly lanes 8-10 represent *hTERT* siRNAs 1-3, respectively; lane 11 control untreated cells; lane 12 represents *GAPDH* siRNA and lane 13 negative control siRNA in GOS-3 cell lines, lanes 14-16 represent *hTERT* siRNAs 1-3, respectively; lane 17 control untreated cells; lane 18 represents *GAPDH* siRNA and lane 19 negative control siRNA in U87-MG cell lines.

Table 3.5 *Expression* levels of *hTERT* in 1321N1, GOS-3 and U87-MG siRNA treated cells along with untreated *GAPDH* siRNA and negative control siRNA assessed after 24 and 48 hr using qRT-PCR.

Cell line	mRNA/100 ηg cells extract (1×10^6 cells)					
	hTERT **siRNA 1**	***hTERT*** **siRNA 2**	***hTERT*** **siRNA 3**	***No siRNA***	***GAPDH*** **siRNA**	**Negative siRNA**
After 24 hr						
1321NI	10.98	1.04	13.52	264	260	245
GOS-3	64.47	1.04	18.69	464	467	460
U87-MG	1.04	1.04	11.52	942	966	970
After 48 hr						
1321NI	1.04	1.04	141.04	260	257	248
GOS-3	1.04	1.04	101.08	472	457	466
U87-MG	1.04	1.04	1.04	962	957	944

Immunofluorescence was performed in order to correlate transcription to protein levels after silencing *hTERT* in U87-MG cell line. Telomerase protein levels were quantified as a percentage of telomerase positive expressing cells per tissue sample (a total of 250 cells were counted per sample). Only 3 % and 15% cells were positive for telomerase with oligos 1 and 3 respectively. siRNA oligo 2 completely downregulated telomerase protein. No telomerase protein was detected after 48 hr of siRNA treatment with all three oligos (Fig. 3.7 and Table 3.6).

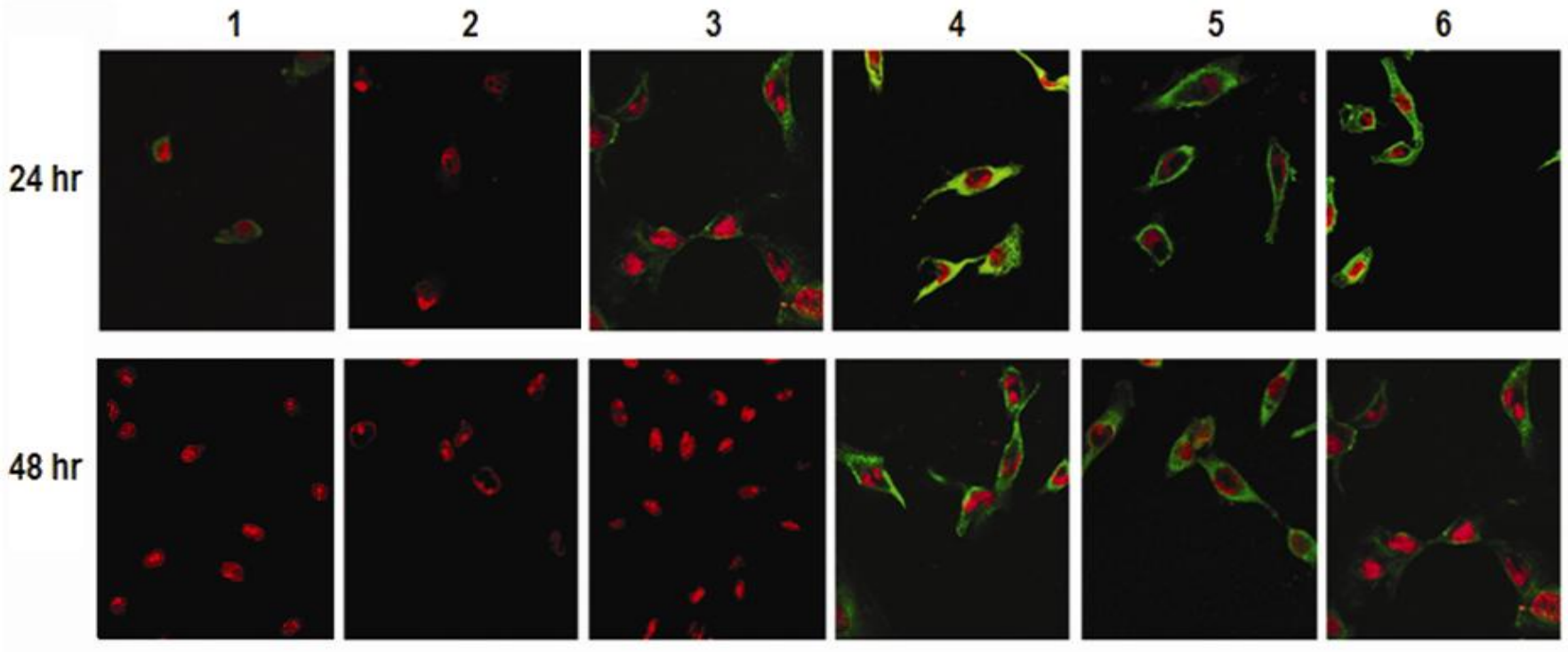

Figure 3.7 Telomerase protein levels assessed using immunofluorescence in U87-MG cells treated siRNA

Image 1–6 represent siRNA 1-3 targeted towards *hTERT*, GAPDH siRNA, negative siRNA, and control cells, respectively, after 24 and 48 hr of treatment. Cells are stained with FITC conjugate secondary antibody, bound to telomerase (green) antigens and the nuclei is labelled with propidium iodide (red) × 40 objective magnifications.

Table 3.6 Telomerase protein level levels assessed using immunofluorescence in U87-MG cells .

Quantification of protein levels in the U87-MG cell line after 24 and 48 hr of siRNA treatment with *hTERT* siRNA and *GAPDH* siRNA.

Treatment	% Cell expressing telomerase	
	24 hr	48 hr
siRNA 1	3	0
siRNA 2	0	0
siRNA 3	15	0
No siRNA	60	63
GAPDH siRNA	54	54
Negative	58	53

3.2.4 Effect of cytotoxic drug cisplatin and a green tea derivative epigallocatechin-3-gallate (ECGC) in combination with siRNA on cell viability.

To study the effect of combination treatment in inhibiting telomerase activity together with the chemotherapeutic drug cisplatin or the natural product ECGC (Shervington *et al*., 2009), cells were first treated with siRNA targeted towards either *hTERT* or *hsp90α*. The treated and untreated cells were further treated with 100 µM ECGC and

20 μM of cisplatin. These concentrations were previously optimised as the IC_{50} values for cisplatin and ECGC in our laboratory (Shervington *et al*., 2009).

Treatment with cisplatin or ECGC in the absence of siRNA demonstrated approximately 40 % decrease in cell viability. However, treating the cells with siRNA targeted towards either *hTERT* or *hsp90α* achieved over 50 % reduction in cell viability in comparison to using the chemotherapeutic drug cisplatin or the natural product ECGC. siRNA treatment in combination with either cisplatin or ECGC showed the best results reducing cell viability of over 60% (Fig. 3.8).

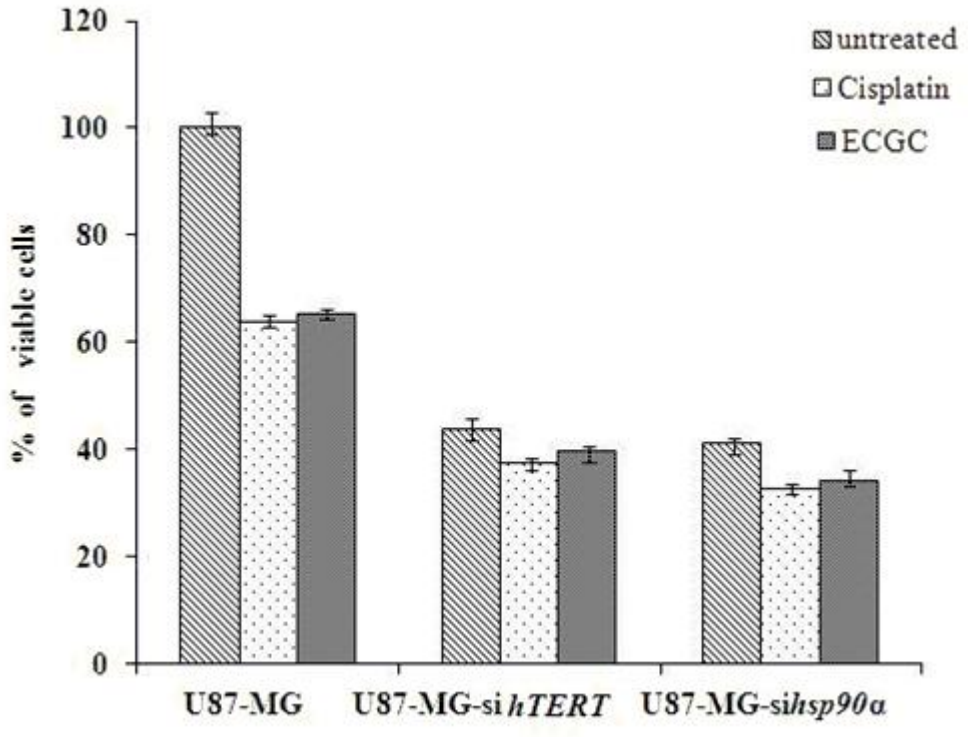

Figure 3.8 Cell viability U87-MG glioma cell line treated with IC_{50} Cisplatin or ECGC for 24 hr with and without siRNA (Data Values are Mean, n =3).

3.3 Discussion

Preliminary experiments undertaken for optimization of the experimental conditions confirmed that *hTERT* and *hsp90α* were upregulated in the different grades of glioma cell lines and hence are effective targets against glioma. Previous studies in our laboratory showed that, targeting *hsp90α* via siRNA also leads to a reduction in the *hTERT* expression (unpublished). *hsp90α* was silenced using siRNA oligo 3 targeting exon 9, which was previously optimized in our laboratory and reported as the most suitable oligo for silencing *hsp90α* after 24 hr (Cruickshanks *et al*., 2010). The experiment was repeated and similar results were obtained wherein treating U87-MG cell line with siRNA oligo 3 directed towards *hsp90α* for 24 hr resulted in decrease in the expression of *hTERT* along with *hsp90α*. Also, co-localization experiments using confocal microscopy was undertaken to visualize the simultaneous redetection of both the proteins (telomerase as well as Hsp90α) in the cell after inhibiting the expression of *hsp90α*. Co-localization experiments confirmed that along with the reduction of Hsp90α proteins, the levels of telomerase also decreased when treated with siRNA targeted towards *hsp90α*. Hence, *hsp90α* was used as an effective indirect regulatory mechanism for silencing telomerase.

Thus, telomerase activity was inhibited using two different approaches that play an important role in the regulation of telomerase. The first approach involved direct silencing of *hTERT* by using siRNA. For the second approach, *hsp90α* was silenced using siRNA targeted towards it. RNA interference is an ancient defence mechanism that guards against foreign dsRNA. Introduced foreign dsRNA is diced into siRNA that binds to RNA induced silencing complex (RISC) leading to the degradation of targeted mRNA (Agarway *et al*., 2003). The manufactures of the siRNA provided a set three

different siRNAs oligos which targets different locations of the same gene. The company guarantees that atleast two oligos, from the set of three provided, would result in at least 70% reduction of the gene expression (Ambion, UK).

For *hTERT* silencing, the three siRNA oligos used, were directed towards exon 11, 4 and 3, respectively. siRNA oligo 2 showed a successful downregulation of *hTERT* after 24 as well as 48 hr in 1321NI, GOS-3 and U87-MG cell lines. siRNA 1 did not completely silence *hTERT* after 24 hr in 1321N1 and GOS-3, however, the expression was dramatically reduced after 48 hr in all the three cell lines. siRNA oligo 3 was only effective in the U87-MG cell line. The expression of *hTERT* was unaffected by either the negative control or *GAPDH* siRNAs. siRNA 2 directed towards exon 4 was selected as the most efficient oligo for siRNA treatment. The U87-MG cell line showed maximum reduction in *hTERT* expression with all the three siRNA oligos after 24 as well as 48 hr. The U87-MG cell line, which is a grade IV glioblastoma cell line with the highest expression levels of *hTERT,* was used for the proteomic study. The result from this study showed that after 24 hr of siRNA treatment with oligo 2, *hTERT* expression significantly decreases in the U87-MG cell lines.

A cell viability assay was performed on glioma cell lines combining si*hTERT* and si*hsp90α*, along with cisplatin or ECGC. It was observed that by inhibiting telomerase by either si*hTERT* or si*hsp90α* alone resulted in more than a 50% decrease in cell viability. This was comparable to the cell death caused by chemotherapeutic agent cisplatin alone. Moreover, combining RNAi treatment with ECGC, decreased cell viability by over 60%. Hence, these results support our hypothesis, that siRNA targeted towards telomerase along with the natural product ECGC or chemotherapeutic agent cisplatin, helps to sensitize glioma cells. Both ECGC and RNAi treatment have no

known toxic effect to the cells and thus, could possibly be used to replace certain harmful chemotherapeutic agents which are toxic.

This study authenticates that the antisense oligodeoxynucleotides directed against *hsp90α* can inhibit *hsp90α* directly and *hTERT* mRNA expression indirectly in U87-MG cell lines, ultimately leading to reduced telomerase protein levels and activity. Combination treatments with siRNA and natural products like ECGC would potentially be the most effective therapy regime as it produces results comparable to those of chemotherapeutic agents like ciplatin with no known side effects. Multi drug resistance is one of the leading causes for the failure of chemotherapy in glioma (Ohgaki and Kleihues, 2005; Komata *et al.,* 2000). Using a non toxic approach such as RNAi treatment targeted against telomerase and natural products like ECGC can be very useful in solving the problems of drug resistace in chemotherapy.

CHAPTER 4

PROTEOMICS ANALYSIS TO STUDY THE DOWNSTREAM EFFECT OF TELOMERASE INHIBITION

4.1. Introduction

The term proteomics describes the study and characterization of complete set of proteins present in a cell, organ, or organism at a given time (Wilkins *et al*., 1995). The human genome harbors 26000–31000 protein encoding genes (Baltimore *et al*., 2001); whereas the total number of human protein products, including splice variants and essential post-translational modifications, has been estimated to be close to one million (Zimmermann and Brown, 2001). Contrary to the single protein analysis by techniques like western blotting or immunohistochemistry, proteomics display patterns of hundreds of thousands of proteins being differentially regulated at one time point being dynamically modified by different treatments (Whiteley G, 2006). Proteomic analysis includes a combination of complex and sophisticated analytical techniques such as 2D Gel electrophoresis for protein separation, image analysis, mass spectrophotometry and bioinformatics tools for quantification and characterization of the complex proteins. Proteomic studies have its applications in proteome profiling, comparative protein expression analysis under different conditions, monitoring post-translational modifications, in addition to studying protein–protein interactions. There is a wide range of proteomic approaches ranging from the gel based polyacrylamide gel electrophoresis (2DE and 2D-DIGE), to gel free technologies like the multidimensional protein identification technology MudPIT (Florens and Washburn *et al*., 2006), isotope-coded affinity tag ICAT (Gygi *et al*., 1999), stable isotope labelling with amino acids in cell culture (SILAC) (Ong *et al*., 2002)*;* isobaric tagging for relative and absolute quantitation (iTRAQ) (Ross *et al*., 2004). Table 4.1 gives a brief overview of these techniques.

Table 4.1 Comparisions of the wide range of proteomic approaches available (Chandramouli and Quian, 2009).

Technology	Application	Strengths	Limitations
2D	Protein separation Protein expression profiling	Relative quantification Detects post translation modification	Poor separation of hydrophobic, acidic, basis, and low abundant proteins
DIGE	Protein separation Protein expression profiling	Relative quantification Detects post translation modification High sensitivity Reduces intergel variability	Proteins without lysine cannot be labelled. Requires special equipment for visualization and fluorophores Very expensive
ICAT	Chemical isotope labelling for quantitative proteomics	Sensitive and reproducible Detect peptides with low expression levels.	Proteins without cysteine residues and acidic proteins are not detected
iTRAQ	Isobaric tagging of peptides	Relative quantification Sample multiplexing	Increases sample complexity Require fractionation of peptides before MS
MUDPIT	Identification of protein-protein interactions Deconvolve complex sets of proteins	High degree of separation Identifies large protein complexes	Not quantitative Difficulty in analyzing huge data set Isoforms cannot be identidied easily

Thus, a wide range of techniques are available for proteomic analysis. Each technique has its own pros and cons. Proteomic analysis of this study was performed by Applied Biomics (Hayward, CA). Fig 4.1 shows an overview of different proteomic statergies and their workflow has been summarised. Also the proteomic methodologies used in this study have been highlighted.

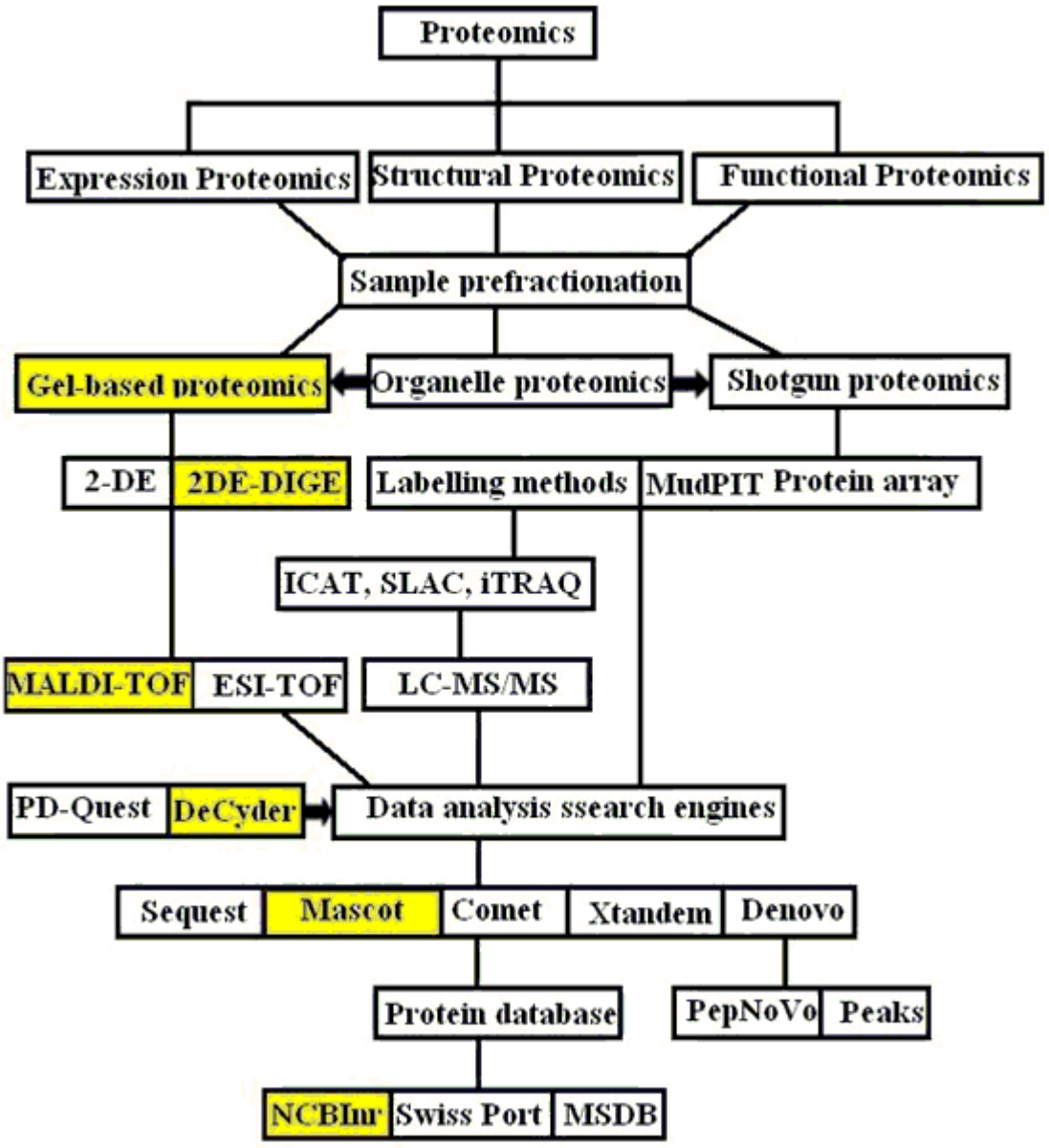

Figure 4.1 A summary of the methods used from of the wide range of proteomic strategies available (adapted from Chandramouli and Quian, 2009). Methods used in this project are highlighted.

4.1.1 Two-Dimensional Polyacrylamide Gel Electrophoresis (2D-PAGE)

Two-dimensional polyacrylamide gel electrophoresis (2D-PAGE) has been the workhorse of proteomics for many decades. This technique used for protein separation under denaturing conditions was introduced by the Italian biochemist, O'Farrell in 1975 and is based on the principle, first acknowledged in 1956 by Smithies and Poulik, that a combination of two orthogonal electrophoretic processes on a gel yields a greater degree of resolution than obtained by a single process. These two electrophoretic processes are molecular size and isoelectric focusing (IEF). The proteins are separated according to their iso-electric point (pI) in the first dimension and apparent molecular weight in the second dimension (O' Farrell, 1975; Klose, 1975). Each spot resulting on the two dimensional array corresponds to a single protein species in the sample.

Following separation the gels are stained to visualize separated protein spots using various dyes like dyes such as colloidal Coomassie brilliant blue G, silver stain and fluorescent stain SYPRO Ruby (Gygi *et al*., 2000). The different staining methods available have their own advantages and vary in limit of detection, dynamic range, and compatibility with analysis by masss spectrometry and have been summarized in Table 4.2.

Table 4.2 Different staining methods available for protein detection in gel-based proteomics (adapted from Cristea *et al*., 2004).

Visualization method	Limit of detection (ng)	Dynamic range	Comments
Colloidal Coomassie blue	8-10	20 fold	This method, results in esterification of aspartic and glutamic side chain carboxyl groups which complicates the interpretation of the mass spectra.
Silver	2-10	8 to 10 fold	Staining times and reaction temperatures are critical for reproducibility.
Cy3, Cy5	5-10	1000 fold	Intragel as well as intergel relative quantification of protein spots can be achieved.
SYPRO Ruby	1-8	1000 fold	It is a rapid method wherein the staining time is not critical and can be varied between experiments

2D-PAGE proteomics have certain shortcomings such as reproducibility, inability to resolve proteins that are too basic or too acidic, too large or too small. However, this problem has now been resolved by the introduction of, immobilized pH gradients strips (IPGs) which have replaced the traditional capillary tubes with pH gradients generated by carrier ampholytes. This has significantly enhanced the resolution of 2D gels and it is now possible to resolve basic proteins using IPGs in the pH range of 4–12 (Essader *et al*., 2005). The problems of reproducibility and quantitation have been solved to a great extent by the introduction of 2D-DIGE.

4.1.2 2D Fluorescence Difference gel electrophoresis (2D-DIGE)

The 2D-DIGE technique was first described by Jon Minden's laboratory in 1997 (Unlu *et al*., 1997). Samples are labelled with one of three spectrally different succinimidyl esters of the fluorescent cyanide (Cy) dyes: Cy2, Cy 3 or Cy 5 before the first dimension IEF separation. These fluorophores are similar in their charge and molecular weight however they have distinct fluorescent properties which allows them to be discriminated when scanned using appropriate optical filters (Marouga *et al*., 2005; Timms and Cramer, 2008; Minden, 2007). There are currently two forms of CyDye labelling chemistries available: CyDye™ DIGE Fluor (GE Healthcare, Uppsala, Sweden) minimal dye and CyDye DIGE Fluor saturation dye. The minimal dye causes a minimuml change in the electrophoretic mobility of the protein because it labels only a small percentage of available lysine residues. The saturation dye is more sensitive because it labels all available cystein residues however it causes electrophoretic mobility shift of labelled proteins (Kondo and Hirohashi, 2007; Shaw *et al*., 2003; Wheeler *et al*., 2003). The CyDye™ DIGE Fluor minimal dye chemistry is the most established. In this chemistry CyDye DIGE Fluors react with primary amino groups, typically the terminal amino group of lysine side chains (Tonge *et al*., 2001; Alban *et al*., 2003).

In a 2D-DIGE experiment, three different samples are covalently labelled, with a different Cy dye. One of the samples is a control sample which can either be an untreated sample or a mixture of all samples pooled together thus forming a control. The samples are migration matched, so that the same protein labelled with any of the dyes will migrate to the same position on the gel. This control sample serves as an internal standard which is used for normalization and spot matching (Minden, 2007;

Loeffler-Ragg *et al*., 2008) and enables inter as well as intra gel analysis. The gel is scanned using a fluorescence imager at specific wavelengths for Cy2 (488 nm), Cy3 (532 nm) and Cy5 (633 nm), and a gel image for each of the different samples is obtained. The images are then merged and analyzed using imaging software to check the differential regulation amongst the proteins (Minden, 2007).

By using 2D-DIGE three different samples can be separated within the same 2D gel. As a result more samples can be compared within the same gel considerably enhancing the accuracy by totally avoiding gel to gel variation. The use of an internal control in DIGE eliminates any error related to gel misalignment and ensures accurate quantitation (Bergh and Arckens, 2005). Other advantages of the DIGE technology include easy comparison and accurate imaging (since a single gel plate is used) and compatiblility with MS.

Visualization is followed by proteolytic digestion and spot excision which can be done directly on the gel itself. Trypsin is the most commonly used proteolytic enzyme which cleaves the proteolytic digestion (Olsen, 2004).

To capitalize on the increasing accuracy of DIGE and its ability to multiplex samples, fully automated software such as DeCyder which are specifically designed for 2D-DIGE analysis (Marouga *et al*., 2005). DeCyder, is the only software to contain proprietary algorithms to perform co-detection of differently labelled samples within the same gel. DeCyder permits automated detection, background subtraction, quantitation, normalization and inter-gel matching and spot picking. This results in high throughput, minimum introduction of human error and greatly increases the

reproducibility. A typical workflow of 2D-DIGE using DeCyder software is shown in Fig 4.2.

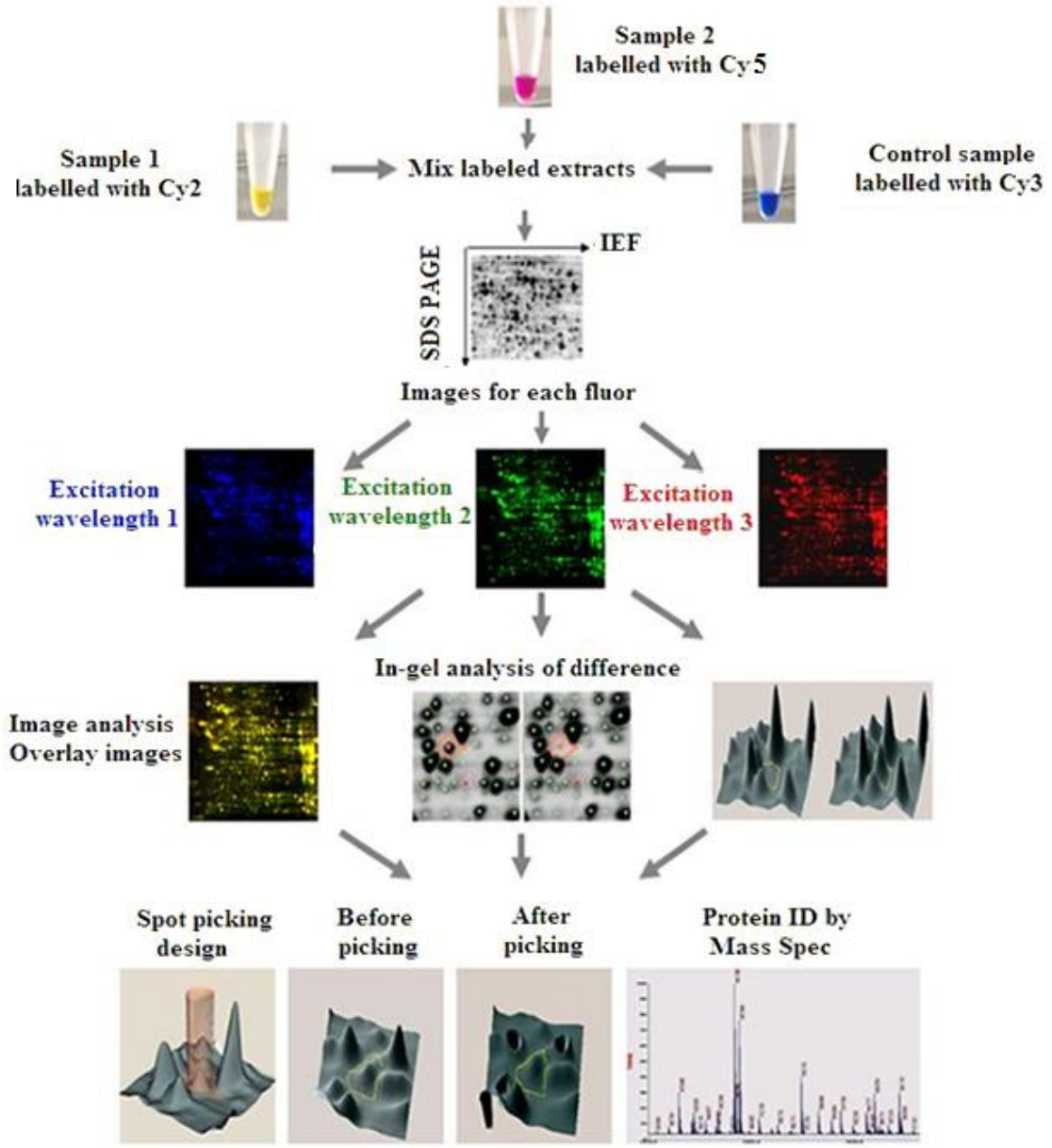

Figure 4.2 Typical workflow of 2D-DIGE via DeCyder (adapted from Ettan DIGE User Manual, 2002).

4.1.3 Mass spectrometry analysis

Irrespective of the method used for protein separation, protein identification is primarily achieved by mass spectrophotometry. Mass spectrophotometry consists mainly of three fundamental units a) an ion source where protein ionization takes place and gas-phase ions are generated, b) a mass analyzer which separates ions according to their mass to charge ratio on the basis of their motion in a vacuum under the influence of electric or magnetic fields, and c) an ion detection system (Domon and Aebersold, 2006). Fig 4.3 shows a typical workflow of a mass spectrometer analysis.

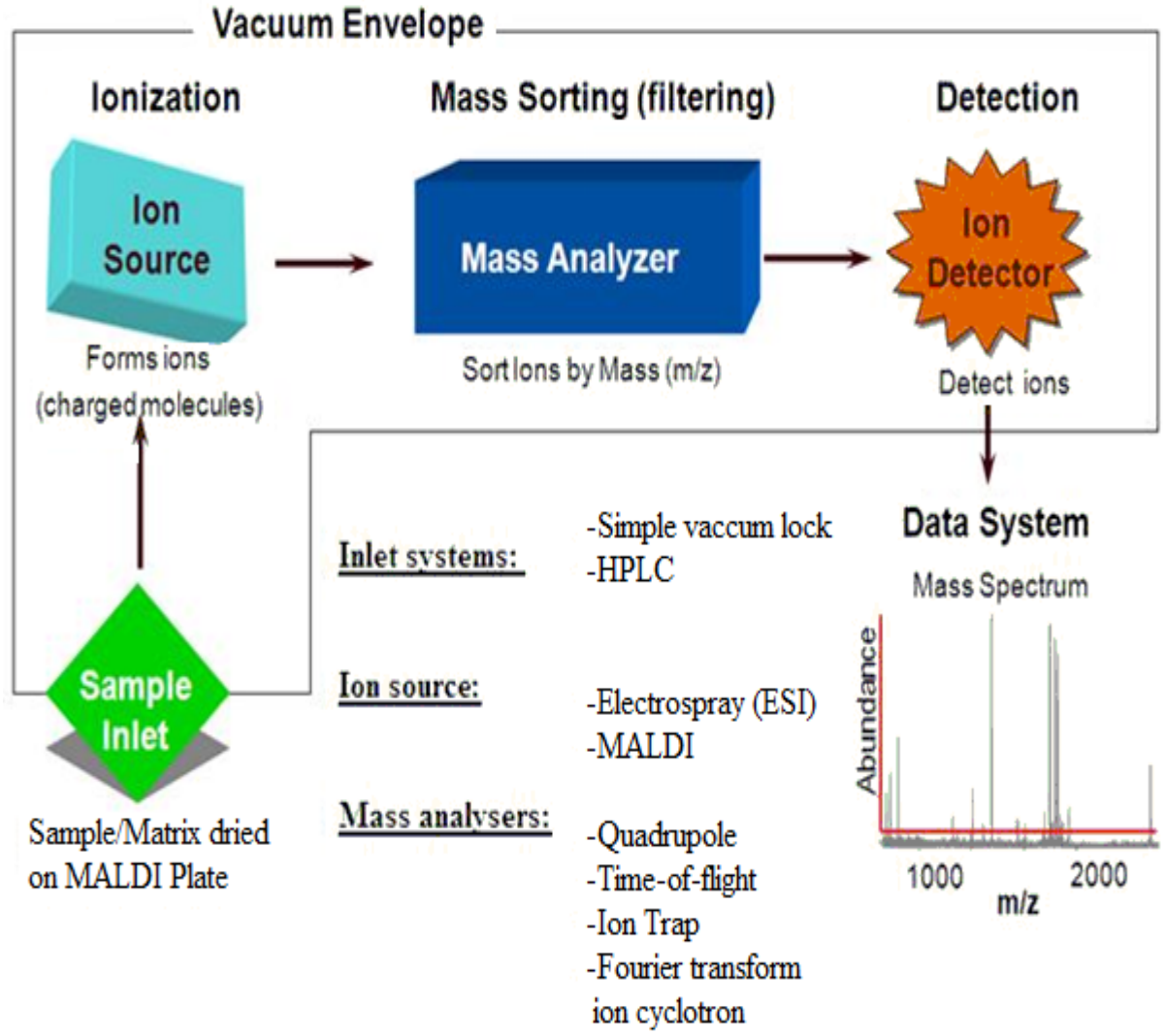

Figure 4.3 Typical workflow of a mass spectrometer analysis.

There are two main types of ion source first, the matrix assisted laser desorption/ionization (MALDI) and second, the electrospray ionization (ESI). Mass analysers can be characterised by four major types which include time-of-flight (TOF), ion trap, quadrupole, and fourier transform ion cyclotron (FTIC). A TOF analyzer employs a long tube with the inlet from the ion source at one end and a detector at the other. The ions generated in the source are exposed to an electrical field which transfers kinetic energy to the ions. The ions are then allowed to fly through a field-free tube of known length. Since the length of the TOF tube and the voltage applied are known and the actual flight time can be determined and it is possible to resolve mass over charge (Mann *et al*., 2001; Mann and Pandey, 2001).

Simple mass spectrometers such as MALDI-TOF are used for only measurements of mass, whereas tandem mass spectrometers are used for amino acid sequence determination. In tandem mass spectrophotometry techniques, one mass spectrometer isolates a peptide of a particular m/z while a second mass spectrometer is used to catalogue fragment ions resulting after induced or spontaneous fragmentation (Dubey and Grover, 2001).

In MALDI-TOF-MS the sample of interest is crystallized with a chemical matrix like alpha-cyano-4-hydroxy cinnamic acid, which is mixed with the analyte and spotted on the MALDI plate reader. Hydrophobic and hydrophilic molecules dissolve in their respective solvents. The solvents vaporize to leave a spreaded analyte in the recrystallized matrix. The sample is ionized by bombarding the sample with laser light. A nitrogen laser beam is usually used to trigger the ionization process. Light wavelength matches that of absorbance maximum of matrix so that the matrix transfers

some of its energy to the analyte which are then released into the gas phase. MALDI measures the mass of peptides derived from a trypsinized parent protein and generates a list of experimental peptide masses, often referred to as "mass fingerprints" (Vestling and Fenselau, 1994; Medzihradszky *et al*., 2000). The TOF measurement is a procedure where instead of operating continuously, the pulsed laser takes individual shots (Duncan and Hunsucker, 2008).

In ESI, the analyte is ionized from a solution and transferred into the gas phase by generating a fine spray from a high voltage needle which results in multiple charging of the analyte and generation of multiple consecutive ions (Chalmers and Gaskell, 2000; Yates *et al*., 1999; Yates *et al*., 1997).

4.1.4 Database search

The peptide masses derived from the mass spectrometer analysis is correlated with peptide fingerprints of known proteins in a protein sequence database using search engines like Sequest, MASCOT, Comet, X!tandem, MOWSE , PeptIdent-2 and Profound (Pappin. 1993, Mann, 1993; Yates, 1993; Colinge, 2003; Geer, 2004). Results are scored based to a scheme which is specific to each search engine which also depends on the database searched (Domon, 2006). The various search engines do not yield identical results as different algorithms and scoring functions are used (Carr *et al*., 2004; Bradshaw *et al*., 2005). Typically, these search engines provide a list of the best matching peptide sequences for an individual tandem mass spectrum. In addition, they provide scores that are related to the confidence level in the match. In this project MASCOT search engine developed by Matric science was used.

High resolution proteomic methods such as the 2D-DIGE and MALDI-TOF were used to study the downstream effect of targeting two different regulatory mechanisms of telomerase. Proteomics has the inherent advantage of the identified proteins themselves being the endpoint of various biological processes. Furthermore, very few proteomic based studies have been undertaken so far that target telomerase with no studies being reported in glioma. Hence, this thesis aimed to collate the genomic and proteomic data in order to bridge the gap between telomerase regulation and its crucial role in carcinogenesis.

4.2 Result

4.2.1 2D-DIGE and MALDI-TOF

A comprehensive proteomic study was performed on untreated U87-MG (as control) and treated U87-MG-si*hTERT* and U87-MG-si*hsp90α* cells using 2D-DIGE and MALDI-TOF. 2D-DIGE revealed 54 spots that were found to be differentially expressed across the three samples tested. The gel images have circled and numbered spots which represent a change in the volume ratio, by 1.5 fold or greater, in at least one of the pair of comparisons (Fig. 4.4). These spots were selected by the software and confirmed visually. A few spots that shifted between samples were circled and numbered and may be differentially modified between the 3 treated groups. Slight shifts in molecular weights between spots can be attributed to modifications such as glycosylation.

Mass spectrophotometry analysis was performed using MALDI-TOF. For protein identification, a subset 26 spots which showed over 2 fold change from a total of 54

spots were selected. Protein identification was based on peptide fingerprint mass mapping (using MS data) and peptide fragmentation mapping (using MS/MS data). MASCOT search engine was used to identify proteins from primary sequence databases. 20 of 26 spots were confidently identified as human proteins. “Protein ID” numbers correspond to the assigned numbers on the overlay gel images and are summarized in Table 4.3. Protein identification identified more than one spots as the same protein. This could either be because of the presence of different isoforms of the same proteins due to post-translational modifications such as phosphorylation or methylation that change the protein's pI and/or molecular weight, causing the spots to shift in addition to protein fragmentation. Publically available database Human protein research database (HPRD) was used to analyse the biological significance of these proteins and are summarized in Table 4.4.

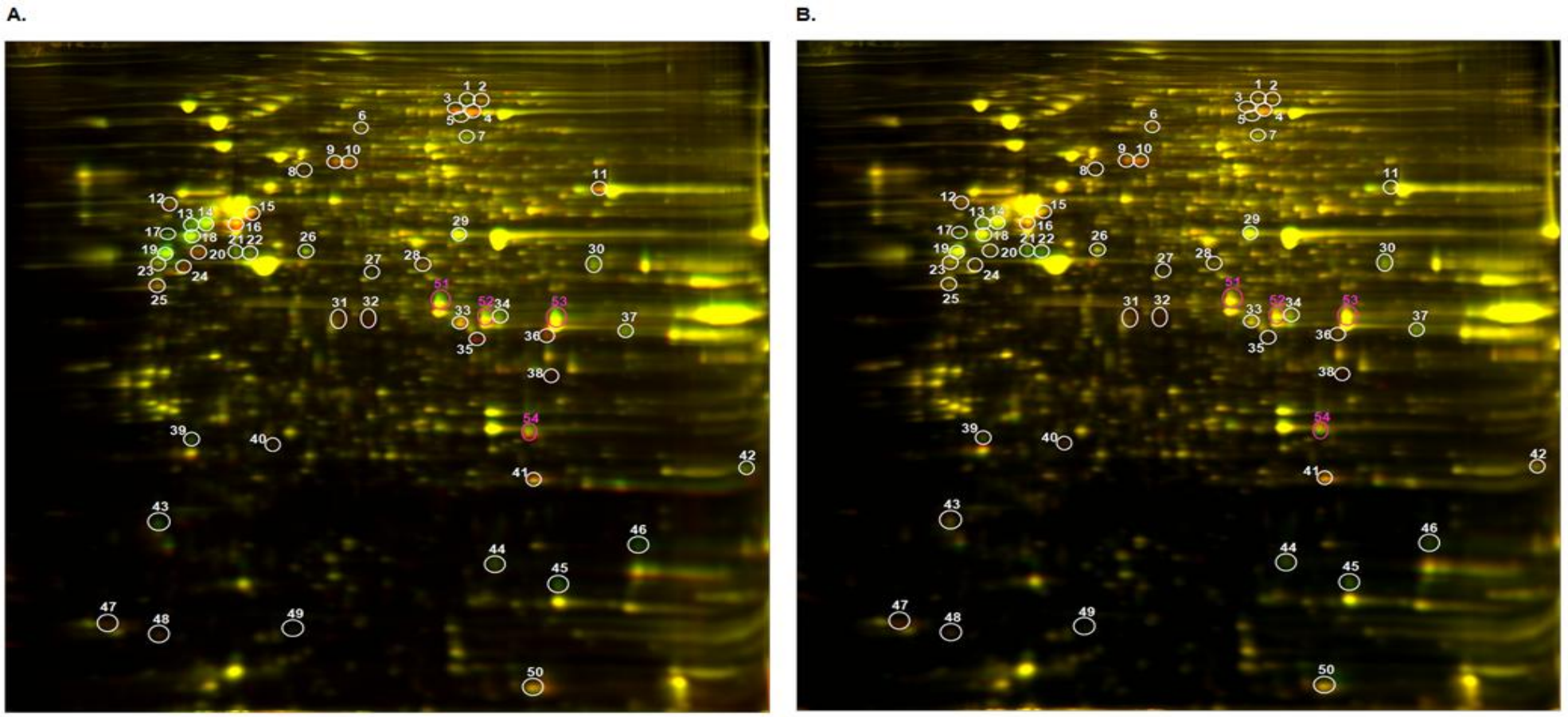

Figure 4.4 2D-DIGE protein profile obtained by overlaying untreated cells with A) U87-MG-si*hTERT* and B) U87-MG-si*hsp90α*.

Spots with Vol Ratio ≥ 1.5 were picked automatically by Ettan Spot Picker.

Table 4.3 Proteins identified by Mass spectrophotometry analysis along with their differential expression after 2D-DIGE seperation.

Identified peptides of over 1.5-fold over-and under expressed were searched against the Mascot database. Proteins were categorized according to the change in its expression after siRNA treatment. Protein name, NCBI GI number, protein molecular weight, ion charge, peptide count, protein score protein score C. I. %, total ion score and total ion C.I. % score and fold change as generated by MASCOT are summarized.

Top Ranked Protein Name(Species)	Accession No.	Protein MW	Protein PI	Peptide Count	Protein Score	Protein Score C. I. %	Total Ion Score	Total Ion C. I. %	Fold change	
									U87-MG-si*hTERT*/ U87-MG	U87-MG-si *Hsp90α*/ U87-MG
Proteins upregulated by inhibition of telomerase by siRNA targeted towards *hTERT* and *hsp90α*										
eukaryotic translation elongation factor 2	gi|4503483	95277	6.41	24	289	100	111	100	2.83	1.61
eukaryotic translation elongation factor 2	gi|4503483	95277	6.41	34	566	100	280	100	2.81	2
albumin	gi|763431	52047.8	5.69	7	78	99.7	56	99.8	2.1	2.34
vimentin variant 3	gi|167887751	49623.1	5.19	35	709	100	277	100	4.25	1.81
67 kda laminin receptor	gi|250127	32746.4	4.83	11	322	100	207	100	2.87	1.13
ribosomal protein P0 variant	gi|62896495	34279.8	5.71	14	267	100	156	100	2.01	1.83
ribosomal protein P0	gi|4506667	34251.8	5.71	14	329	100	181	100	2.54	2.14
annexin I	gi|4502101	38690	6.57	25	383	100	101	100	5.26	1.17
glyceraldehyde-3-phosphate dehydrogenase	gi|31645	36031.4	8.26	18	296	100	99	100	3.1	1.78

Table 4.3 (contd)

Top Ranked Protein Name(Species)	Accession No.	Protein MW	Protein PI	Peptide Count	Protein Score	Protein Score C. I. %	Total Ion Score	Total Ion C. I. %	Fold change	
									U87-MG-si*hTERT*/ U87-MG	U87-MG-si*Hsp90α*/ U87-MG
Proteins differentially regulated on treatment with si*hTERT* and si*hsp90α*										
myosin regulatory light chain MRCL3 variant	gi|62896697	19780.5	4.72	8	246	100	159	100	-3.22	1.31
RAN, member RAS oncogene family	gi|48734884	24437.6	7.01	18	467	100	264	100	2.09	-2.44
Proteins downregulated by inhibition of telomerase using siRNA targeted towards *hTERT* and *hsp90α*										
RNH1 protein	gi|15029922	48336.4	4.83	26	547	100	270	100	-2.45	-1.65
vimentin	gi|340219	53681.1	5.03	31	526	100	176	100	-2.85	-1.89
vimentin	gi|340219	53681.1	5.03	35	704	100	306	100	-2.35	-1.6
vimentin	gi|340219	53681.1	5.03	31	662	100	309	100	-2.29	-1.57
vimentin	gi|340219	53681.1	5.03	35	723	100	296	100	-3.1	-1.71
beta actin variant	gi|62897409	41695.7	5.29	15	156	100	49	99.4	-1.92	-2.64
ACTB protein	gi|15277503	40194.1	5.55	15	283	100	168	100	-1.5	-2.52
Chain A, Cyclophilin A complexed with dipeptide Gly-Pro	gi|1633054	17869.8	7.82	4	125	100	93	100	-1.78	-2.14
cofilin 1 (non-muscle)	gi|5031635	18490.7	8.22	10	149	100	48	98.9	-2.35	-2.2

Table 4.4 Molecular function, biological process and location of proteins identified by mass spectrophotometry using Human Protein Research Database.

Protein	Molecular function	Biological process	Location
Proteins upregulated by inhibition of telomerase by siRNA targeted towards *hTERT* and *hsp90α*			
eukaryotic translation elongation factor 2	Translation regulator activity	Protein metabolism ; Translation	Cytoplasm
albumin	Transporter activity	Transport	Extracellular
vimentin variant 3	Structural constituent of cytoskeleton	Cell growth and/or maintenance	Intermediate filament
67 kda laminin receptor	Cell adhesion molecule activity	Cell communication ; Signal transduction ; Cell adhesion	Cytoplasm
ribosomal protein P0	Structural constituent of ribosome	Protein metabolism	Ribosome
annexin I	Calcium ion binding	Cell communication ; Signal transduction	Plasma membrane
glyceraldehyde-3-phosphate dehydrogenase	Catalytic activity	Metabolism ; Energy pathways	Cytoplasm

Table 4.4 (contd)

Proteins differentially regulated on treatment with si*hTERT* and si*hsp90α*			
myosin regulatory light chain MRCL3	Cytoskeletal protein binding	Cell growth and/or maintenance	Cytoplasm
RAN, member RAS oncogene family	GTPase activity	Cell communication ; Signal transduction	Nucleus
Proteins downregulated by inhibition of telomerase using siRNA targeted towards *hTERT* and *hsp90α*			
RNH1 protein	Translation regulator activity	Regulation of nucleobase, and nucleic acid metabolism	Cytoplasm
vimentin	Structural constituent of cytoskeleton	Cell growth and/or maintenance	Intermediate filament
ACTB protein	Structural constituent of cytoskeleton	Cell growth and/or maintenance	Cytoplasm
Chain A, Cyclophilin A complexed with dipeptide Gly-Pro	Isomerase activity	Protein folding ; Peptide metabolism	Cytoplasm
cofilin 1	Cytoskeletal protein binding	Cell growth and/or maintenance	Cytoplasm

4.2.2 Ingenuity Pathways Analysis

Data mining and knowledgebase softwares like Ingenuity Pathways Analysis (IPA) (Ingenuity® Systems) were used to identify molecular functions and pathways which correlate with the proteins identified by mass spectrophotometry after the direct and indirect inhibition of telomerase. Two parameters were taken into consideration for the identification of the most significant pathways. Firstly, the ratio of the number of proteins that map to the pathway divided by the total number of proteins that map to the canonical pathway; secondly, Fisher's exact test is used to calculate a p-value determining the probability that the association between the protein in the dataset and the canonical pathway be explained by chance alone. Each of these networks was ranked by a score based on negative log of p-value. These scores ranked different networks based on its statistical significance.

Top five i) disease and disorders ii) molecular and cellular functions and iii) Physiological System Development and Function and iv) canonical pathways are shown (Fig 4.5).

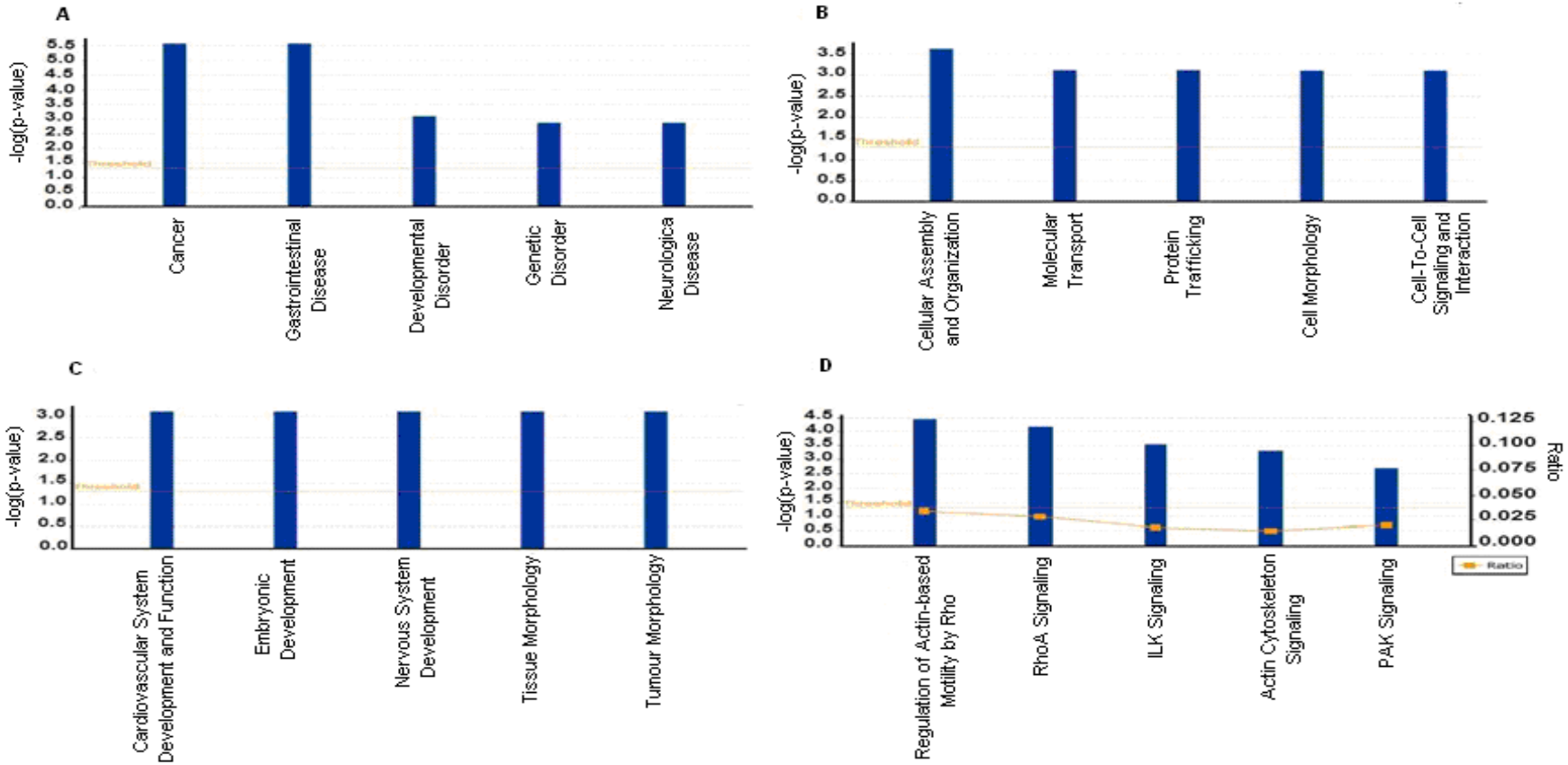

Figure-4.5-Functional-network-analysis-by-IPA.

Top 5 A) diseases and disorders; B) molecular and cellular functions and C) Physiological System Development and Function and D) pathways selected from total 96 canonical pathways relevant to the dataset defined by Ingenuity Pathway Analysis program.

Each of these networks are ranked by a score based on negative log of p-value computed using a right tailed Fisher's exact test and has been summarized in Table 4.5

Table 4.5 Top biofunction as generated by IPA.

Values are based on negative log of p-value computed using a right tailed Fisher's exact test.

Top Bio Functions		
Diseases and Disorders		**p-value**
1	Cancer	2.58×10^{-6} - 4.94×10^{-2}
2	Gastrointestinal Disease	2.58×10^{-6} - 2.58×10^{-6}
3	Developmental Disorder	7.90×10^{-4} - 7.90×10^{-4}
4	Genetic Disorder	1.37×10^{-3} - 3.67×10^{-2}
5	Neurological Disease	1.01×10^{-3} - 4.55×10^{-2}
Molecular and Cellular Functions		
1	Cellular Assembly and Organization	2.47×10^{-4} - 4.57×10^{-2}
2	Molecular Transport	7.65×10^{-4} - 2.50×10^{-2}
3	Protein Trafficking	7.65×10^{-4} - 2.50×10^{-2}
4	Cell Morphology	7.90×10^{-4} - 4.57×10^{-2}
5	Cell-To-Cell Signaling and Interaction	7.90×10^{-4} - 4.34×10^{-2}
Physiological System Development and Function		
1	Cardiovascular System Development and Function	7.90×10^{-4} - 1.26×10^{-2}
2	Embryonic Development	7.90×10^{-4} - 4.11×10^{-2}
3	Nervous System Development	7.90×10^{-4} - 8.66×10^{-3}
4	Tissue Morphology	7.90×10^{-4} - 3.50×10^{-2}
5	Tumour Morphology	7.90×10^{-4} - 3.04×10^{-2}
Top Cannonical Pathways		
1	Regulation of Actin-based Motility by Rho	3.38×10^{-5}
2	RhoA Signaling	6.58×10^{-5}
3	ILK Signaling	2.84×10^{-4}
4	Actin Cytoskeleton Signaling	4.62×10^{-4}
5	PAK Signaling	1.96×10^{-3}

The ingenuity analysis did not generate any pathways from among the proteins identified in our database. A possible reason for this could have been attributed to the small number of proteins identified by mass spectrophotometery. IPA generated a network of cellular assembly and organization with a score of 42. Applying filters for human species and only cancer relationships, a network of 7 proteins from our database was obtained. This network was then overlayed with the ingenuity knowledgebase biomarkers with a view of identifying potential biomarkers in our database; the results reiterated the importance of targeting hTERT as well as Hsp90α as biomarkers in various cancers. Besides these vimentin was recognised as a potential biomarker from-our-database-(Fig-4.6).

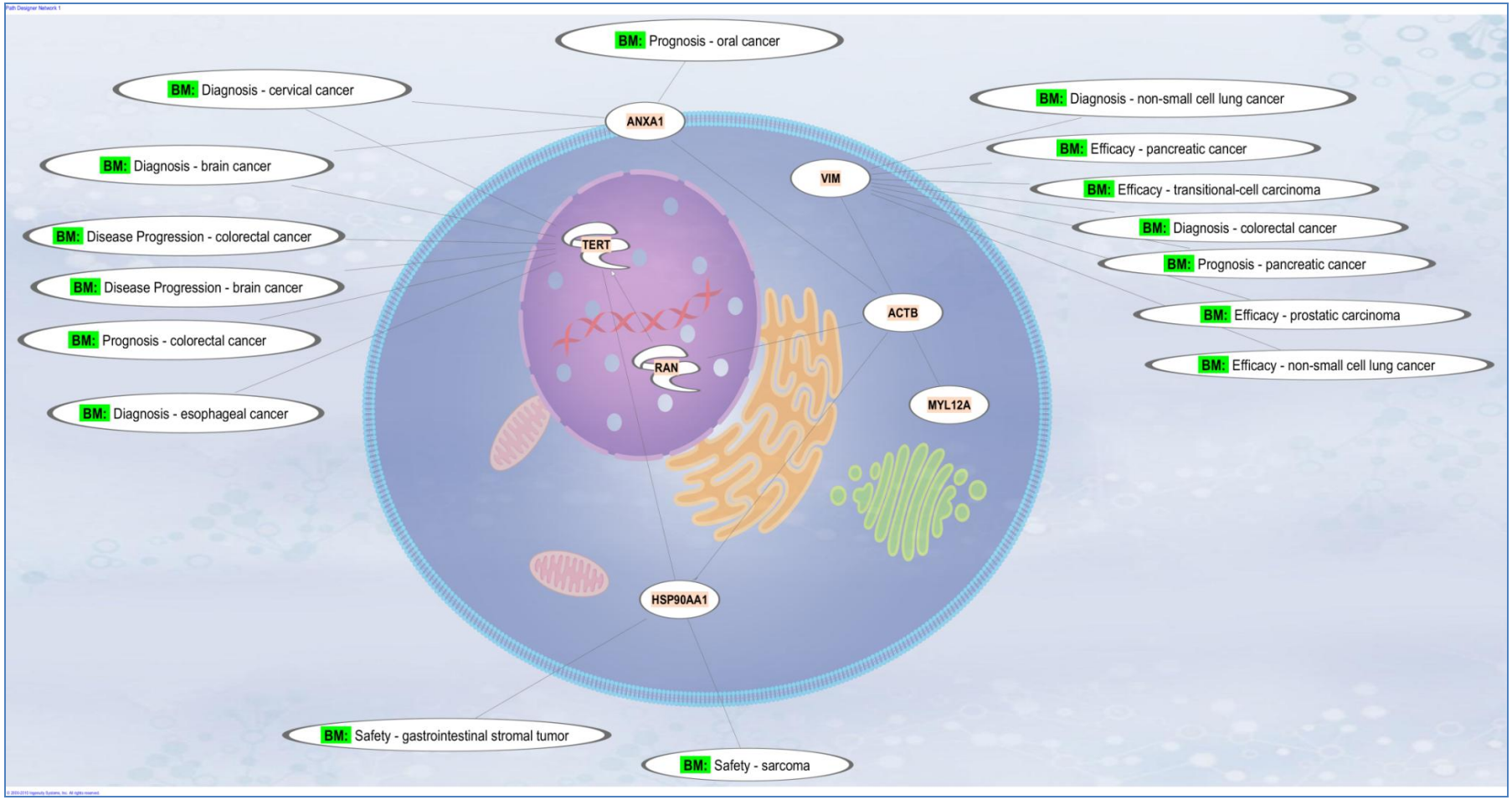

Figure 4.6 Overlay of Cellular assembly and organization network with cancer biomarkers database generated by IPA path designer.

Cellular assembly and organization network was generated using the proteomic data obtained by MALDI-TOF analysis whereas the cancer biomarkers dataset was obtained from ingenuity knowledge database. BM= Biomarker. Filters were used to select onlt those molecules which were of and human origin and were specific for cancer

4.2.3 Vimentin transcription levels in glioma tissues and cell lines

The proteomic analysis revealed that 5 diffrent spots as vimentin all of which were downregulated. To verify whether the expression of vimentin was affected by telomerase inhibition, its expression level was studied in different grades of glioma cell lines before and after treatment with siRNA directed towards *hTERT*. The cell lines used included 1321N1 (Grade 1), GOS-3 (Grade II/III) and U87-MG (Grade IV).

The expression of vimentin was related to the grade of glioma, with the U87-MG cell line showing maximum expression. It was also found that silencing *hTERT* significantly reduced the expression of *vimentin* in a grade specific manner (Fig. 4.9).

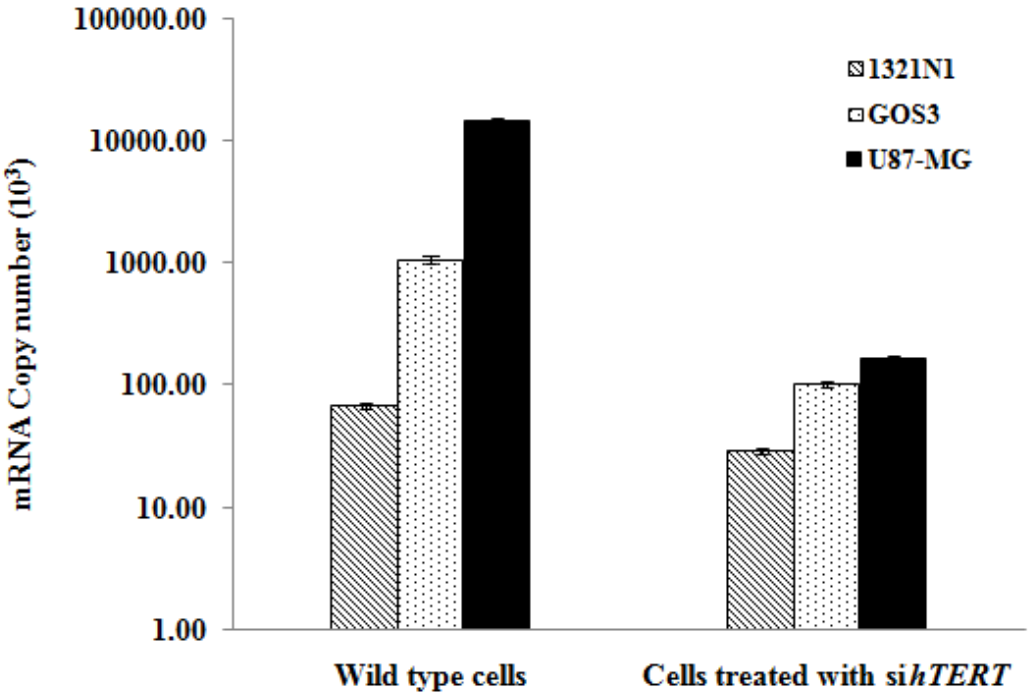

Figure 4.7 Transcription level of vimentin in different grades of glioma cell lines before and after treatment with si*hTERT* .

The expression of vimentin was further evaluated in 15 different glioma tissues and 3 normal brain tissues. *Vimentin* was found to be significantly expressed in 9 of 12 glioblastoma tissues. The expression of vimentin was not detected in the normal tissue samples and the low grade glioma cell lines (Fig. 4.10 A). The high grade glioblastoma tissues showed that *vimentin* transcription level was 10^4 fold higher than the lower grade glioma and the normal brain tissues (Fig. 4.9 B). However, unlinke the cell lines, the expression level of vimemtin didnot correlate with the grade of the tissue specimens used.

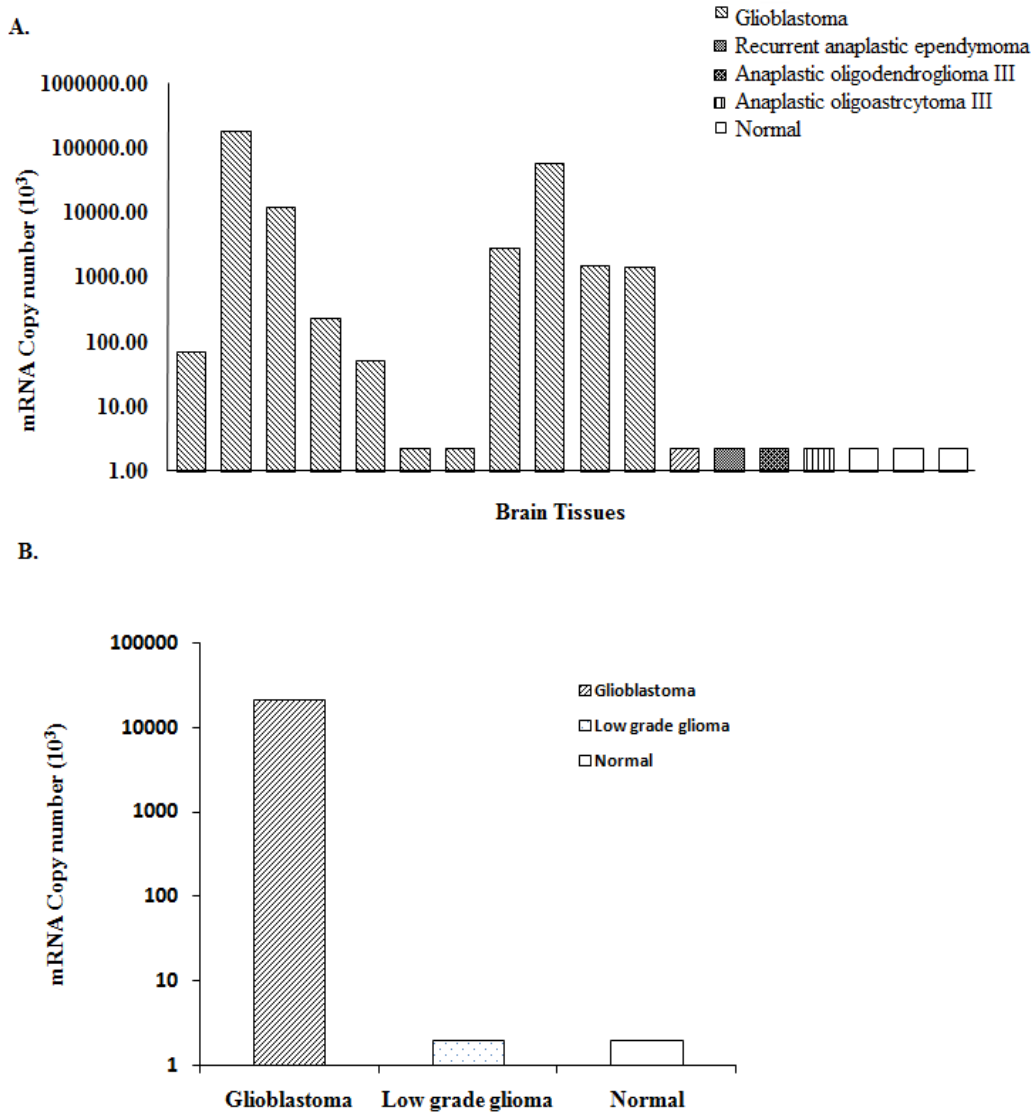

Figure 4.8 Transcription level of vimentin in tissue samples.
A) Transcription levels of vimemtin in tissue samples B) Average expression of vimentin in glioblastoma, lower grade glioma and normal tissues.

4.3 Discussion

The standard protocol for proteomics includes extraction of cell proteins from samples, digestion with proteases for example trypsin, separation of the resulting mixture by two-dimensional (2D) electrophoresis or liquid chromatography (LC) digestion and excision of the gel spots followed by mass spectrophotometry for protein identification and/or quantification. In this thesis, 2D-DIGE was used for protein separation and MALDI-TOF was used for protein identification.

To characterize the changes caused at the cellular protein levels by inhibition of telomerase, a differential proteomic analysis was performed to compare wild type U87-MG cells, U87-MG cells after silencing *hTERT* gene (U87-MG-si*hTERT*) and U87-MG cells after silencing *hsp90α* gene (U87-MG-si*hsp90α*). 2D-DIGE was used for protein separation and MALDI-TOF was used for protein identification. 2D-DIGE was used in order to minimize inter-gel variation,. 2D-DIGE allows comparison of over two samples on the same gel as three different fluorescent dyes, Cy2, Cy3 and Cy5 can be used on the same gel. Only those spots which showed over 2 fold change when compared in either U87-MG, U87-MG-si*hTERT* or U87-MG-si*hsp90α* were selected for protein identification. This study, from a unique angle, elucidates relationships between the direct and indirect effect of silencing different telomerase regulatory mechanisms.

2D-DIGE revealed 54 spots that were found to be differentially expressed across the gels. Due to financial constraints only a subset of the spots which showed over 2 fold changes were selected for further analysis. Out of the 54 spots, 26 spots showed over 2 fold change across the samples and were selected for protein ID using MALDI-TOF. 20 spots could be successfully identified with a high confidence level of over 95%.

The IPA software identified dynamically regulated biological networks, global canonical pathways and global functions which correlated with cellular responses to telomerase inhibition. The top networks significantly modulated by the inhibition of telomerase providing a score of 42 were categorized by IPA as those involving cancer and cellular assembly and organization. The top diseases and disorders modulated in response telomerase inhibition were cancer, genetic disorders and neurological diseases. IPA analysis thus, added confirmation that alteration in the *hTERT* levels significantly alters the cancer proteome including brain disorders. IPA also showed that alteration in telomerase regulation has its effect on physiological systems like the cardiovascular function and development, tissue and tumour morphology. IPA also showed that inhibition of telomerase affects cellular and molecular functions like cellular assembly and organization, molecular transport, protein trafficking cell morphology, cell-to-cell signaling and interaction. The IPA library of canonical pathways indicated that proteins identified in this study are participants in regulation of actin-based motility by Rho, glycolysis, Integrin linked kinase (Ilk) signaling and actin cytoskeleton signaling. Several potential targets along this pathway might be useful for therapeutic intervention in the future. These results highlight the significant downstream effect of telomerase in different cellular functions besides its role in maintaining telomere length.

A functional protein association network for proteins that were differentially expressed due to silencing of *hTERT* was generated using IPA. Filters were adjusted to select molecules belonging to human species and affecting cancer. This network was overlayed to an inbuilt biomarker library generated in the IPA knowledgebase. A network was generated which involved Hsp90, telomerase, annexin 1, beta actin, vimentin, RAN and myosin regulatory light chain. The IPA analysis demonstrated that besides Hsp90 and hTERT, vimentin which is differentially regulated by

silencing regulatory mechanisms of telomerase is used as a biomarker in several cancers and hence, can be a potential biomarker in glioma cell lines whose activity can be modulated by telomerase.

Upregulation of proteins via telomerase inhibition

Inhibition of telomerase activity resulted in the upregulation of various proteins such as the eukaryotic elongation factor 2, albumin, annexin 1, ribosomal protein P0 variant (RRP0), GAPDH, 67kDA laminin receptor, and ras-related nuclear protein. These proteins are involved in various physiological and pathological pathways such as cell growth, membrane trafficking, phagocytosis, proliferation, inflammation, tumour suppression and apoptosis differentiation. Two differentially expressed spots were identified as EF2. EF2 plays a role in the polypeptide chain elongation step in the tumourigenesis. A high level protein synthesis is one of the characteristics of cancer cells. EF-2 is a 93 kDa monomeric guanine nucleotide-binding protein and is solely responsible for the translocation of codons from the A to P ribosomal positions and hence is an essential mediator of the ribosomal elongation step during mRNA translation (Py *et al*., 2009; Sivan *et al*., 2007). The phosphorylation of EF2 via EF2 kinase in response to elevation in intracellular calcium leads to the inactivation of this translation factor and protein synthesis is halted with mRNA-loaded ribosomes (Yang *et al*., 2001; Sivan *et al*., 2007). EF2 and EF2 kinase are thus, inversely related. EF2 protein is overexpressed in 92.9% of gastric and 91.7% of colorectal cancers with a knockdown of EF2 showing inhibition in cancer cells and activation of EF2 kinase in these cancer cells (Nakamura *et al*., 2009). EF2 kinase is markedly increased in human glioblastoma and is chaperoned by Hsp90α. EF2 kinase inhibitor, antisense RNA to calmodulin (Nairn *et al*., 1985) and EF2 kinase (Libermann *et al*., 1985) have been shown to be effective against cancer cells

in glioma. Glendamycin, an Hsp90α inhibitor, has been shown to disturb the chaperone pathway between the EF2 kinase and Hsp90α and thus inhibits EF2 kinase activity (Yang *et al*., 2001). These results are consistent with our data showing the use of si*hsp90α* results in upregulation of EF2 due to inhibition of EF2 kinase activity.

Albumin (ALB) is the most abundant plasma protein accounting for over 50% protein of the serum proteins. Its primary functions include transportation and maintenance of osmotic pressure cell metabolism (Nicholson *et al*., 2000). Albumin has been known to demonstrate an inverse relationship with mortality of cancer patients. Serum albumin has been described as an independent prognosticator of survival in lung cancer, pancreatic cancer, gastric cancer, colorectal cancer and breast cancer (Gupta *et al*., 2009). A clinical study on GBM tissues showed that serum albumin levels can be used as a prognostic marker for predicting patient survivals with higher serum albumin levels showing better survival rates (Schwartzbaum *et al*., 1999). However the mechanism still remains unknown.

Annexin 1 (ANXA1) belongs to the family of annexins which have calcium and phospholipid binding properties. It is involved in various physiological and pathological pathways like cell growth, membrane trafficking, phagocytosis, chaperone activity, proliferation, inflammation, tumour suppression and apoptosis differentiation (Lim *et al*., 2007). ANXA1 possesses phophorylation sites which play a vital role in proliferation of certain signaling molecules. It is strongly involved in the modulation of intracellular calcium release and by that mechanism interferes with processes that are calcium-dependent. ANXA1, N-terminal domain includes sites for protein kinase C (PKC) and tyrosine kinase phosphorylation, and for glycosylation, acetylation and proteolysis (John *et al*., 2004). ANXA1, thus, plays a

key role in certain signaling pathways important in cancer, however, the exact mechanism is not known.

ANXA1 may have important regulatory roles in tumour development and progression. Evidence for this lies in the clear observations that the expression of ANXA1 is reduced in certain cancers like esophageal cancers and prostate cancer. While it is increased in other cancers like head, neck and breast cancers (Lim and Parvaiz, 2007). Previous studies have reported over-expression of ANXA1 in some central nervous system (CNS) tumours (GBM, anaplastic astrocytoma and astrocytoma) wherein primary glioblastomas have a higher ANXA1 expression level compared with secondary glioblastomas (Schittenhelm *et al*., 2009). ANXA1 serves as a substrate for the epidermal growth factor receptor (EGFR), which is frequently amplified in primary gliomas and its expression profile is similar to its substrate, EGFR.

However, our results show that in glioma cell lines decreasing telomerase activity results in 5 fold increase in ANXA1 level. A possible explanation for this could be the antiproliferative and/or proapoptotic function of ANXA1. Reduction in telomerase results in an increase in cellular apoptosis as seen by the cell viability results. Also loss of ANXA1 has been shown to make cancer cell resistant to apoptosis via chemotherapeutic agents in several cancers (Zhang and Liu, 2007). However, no relationship between telomerase activity and ANXA1 has been reported so far and more detailed analysis is required to understand the role of ANXA1 in glioma development and progression.

The 67-kDa laminin receptor (67LR) is a nonintegrin cell surface receptor that binds laminin with high affinity. It is widely expressed in mammalian cells and is overexpressed in a variety of tumour cells and plays a significant role in tumour

invasion and metastasis (Sobel, 1993; Castronovo, 1993; Martignone *et al*., 1993). Though the exact mechanism of how this receptor plays a role in invasion is unclear. 67LR is known to promote adhesions of molecules which play a key role in the rearrangement of the extracellular matrix (ECM) around the tumour (Berno *et al*., 2005). It also facilitates the attachment and migration of endothelial cells. This receptor has been shown to be over expressed in glioma with down-regulation of 67LR by RNAi resulting in a decrease in its migratory and invasion activity.

While these studies showed the expression of these proteins in different cancer cell lines, namely, ovarian (67LR) and mesenchymal (ANXA1), using different methods and treatments, our studies utilised proteomic analysis and a high grade glioblastoma cell line after inhibiting the activity of telomerase.

However, our studies showed that inhibition of telomerase resulted in upregulation of this receptor. This contradicts the role of telomerase as a target to reduce glioma metastasis. The cause of the increase of the expression of this receptor remains unknown. This could be the reason why targeting telomerase alone is insufficient to kill tumour cells completely. Hence, though it is clear that telomerase plays a role in cellular apoptosis and tumour metastasis, the net effect of telomerase on the metastatic potential still remains unclear and more mechanistic insights are required to gain a complete understanding of the effect telomerase on tumour cell metastasis.

RAN (ras-related nuclear protein) is a small GTP binding protein belonging to the RAS superfamily. It plays a key role in the nucleus-cytosol exchange through the nuclear pore complex. It is involved in many other processes such as regulation of microtubule network during mitosis, cycle regulation, apoptotic response to a variety of conditions (Wong *et al*., 2009) as well as RNA and DNA synthesis. RAN has been found to be occasionally amplified in tumours and also in certain resistant cell

lines (Zhang and Liu, 2007). It has been suggested that its over-expression may cause drug resistance possibly by enhancing the survival of cells under drug attack. RAN over expression resulted in a decrease of paclitaxel-induced apoptosis and was hypothesized to act via downregulation of JNK-dependent signaling pathways in this glioblastoma cell line (Woo *et al*., 2008). Our data shows that siRNA targeted towards h*TERT* results in a 2 fold increase in the RAN protein, however si*hsp90α* resulted in 2 fold decrease. Hsp90α is a chaperone and assists in the maturation of diverse groups of proteins. Inhibiting the activity of Hsp90 affects various signaling pathways and hence, the decrease in the expression of RAN could be a result of diverse and complex regulatory mechanism affected by Hsp90. However, more research needs to be carried out in order to help explain how silencing *hTERT* gene results in an increased protein level of RAN.

An important consideration in cancer chemotherapy is the onset of cellular resistance to certain chemotherapies. For example, ribosomal activity has been shown to be increased in cells treated with antitumour agents (Grabowski *et al*., 1992). Alteration of ribosomal proteins influence protein translation processes, via upregulation of 37 kDA laminin receptor precursor which increases the quantity of 67LR molecules which consequently increases cell adhesion to extracellular matrix and enhances the survival of tumour cells during drug attack affecting the response of tumour cells to anticancer agents (Shi *et al*., 2002). In addition ANXA1 (Sinha *et al*., 1998; Zhang and Liu, 2007), RAN (Rush *et al*., 1996) and GAPDH (Shi *et al*., 2002) have been reported to be upregulated in various drug resistant cell lines. It is speculated that ANXA1 plays a role in drug resistance due to it being a stress protein, thereby protecting cells under therapeutic attack (Zhang and Liu, 2007). Thus, it can be inferred that inhibition of telomerase is sub-lethal and is not capable of solely inhibiting tumour progression and further research is necessary in order to

understand the complex regulation of the dynamic changes caused in cancer proteome due to the altered levels of telomerase. There are numerous established mechanisms that are responsible for acquired resistance of tumour cells to anticancer treatments (Shi *et al*., 2002). These include increased DNA repair mechanisms, drug efflux, altered survival and apoptotic signaling pathways. Hence, though it is clear that telomerase plays a role in cellular apoptosis and tumour metastasis, the net effect of telomerase on tumour formation and metastatic potential still remains unclear and more mechanistic insights are required to gain a complete understanding of the effect telomerase on tumour cells and its metastasis.

Besides these, other proteins such as cyclophilin and ribonuclease inhibitor (RNH1) exhibit downregulation when telomerase was inhibited. Cyclophilins are known as the target binding proteins for the immunosuppressive agent cyclosporin A (Handschumacher *et al*, 1984). Cyclophilin A has enzymatic peptidyl-prolyl cis–trans-isomerase (PPIase) activity necessary for protein binding *in vivo*. The enzymatic activity in cyclophilins is also involved in protein transport, mitochondrial function and pre-mRNA processing (Andreeva *et al*., 1999; Bourquin *et al*., 1997). Cyclophilin A has been reported to be overexpressed in many cancer cells. Its role in cancer cells remains unclear although a study showed that over expression of cyclophilin A renders cancer cells resistant to hypoxia and cisplatin-induced apoptosis (Choi *et al*., 2007). Over expression of cyclophilin A directly stimulates pancreatic cancer cell proliferation through its receptor CD147 (Li et al, 2006). The role of cyclophilin A in glioma cancer cells is not known although a has study shown that cyclophilins were among the up-regulated proteins found in human glioma cell lines treated with an experimental antiglioma agent suggesting that cyclophilin may also play a role in the resistance of glioma cancer cells to drug-induced apoptosis (Bian *et al*., 2008).

Telomerase inhibition also resulted in the down regulation of RNH1 which demonstrated several tumour suppressor properties by inhibiting tumour-induced angiogenesis tumour growth (Chen *et al*., 2005). It is unclear as to why telomerase inhibition would result in the down regulation of a protein with such properties and further investigations are necessary to address this issue.

Downregulation of cytoskeleton associated proteins

Inhibition of telomerase has led to a significant down regulation in the level of vimentin, cofilin 1 (CFL1), ACTB proteins and myosin regulatory light chain variant 3 (MRCL3). These proteins directly or indirectly affect the actin cytoskeleton regulation and are mainly upregulated in cancers (Condeelis *et al*., 2005). Changes in the regulation and expression of key molecules of the actin cytoskeleton contribute dramatically to the differences between metastatic and non-metastatic cancer cells (Dizhoor, 2002; Condeelis *et al*., 2005).

Myosin regulatory light chain 3 (MRCL3) is a subunit of the myosin regulatory light chain which is thought to play a specific role myosin regulation (Dizhoor, 2002). The literature suggests that MRCL3 may play a role in the regulation of the muscle filament assembly and reorganization in muscle cells (Tohtong *et al*., 2003). A study proposed that diphosphorylated MRCL3 is necessary for the organization of stress fibers and contractile rings during cell division (Iwasaki *et al*., 2001). The role of MRLC3 in cancer is not clear although studies suggest that the function of MRCL3 in cell migration may be involved in cell invasion in metastatic cancer (Nguyen *et al*., 1998; Tohtong *et al*., 2003). Cancer cell lines treated with inhibitors of myosin light chain kinase (MLCK), which regulates the phosphorylation of MRLC3, showed marked reduction of invasiveness in *in vitro* invasion assays (Tohtong *et al*., 2003). The reduction in tumour cell invasion was mainly due to impaired cellular motility.

This result is consistent with our results showing a 3 fold decrease in MRCL3 levels after targeting si*hTERT*, thereby leading to a decrease in the metastatic potential of cancer cells. However, this protein was upregulated by 1 fold when *hsp90α* was silenced.

Cofilin 1 is a small ubiquitous protein of approximately 19 kD and is one of the key regulators of actin dynamics of migrating cells, both *in vivo* and *in vitro* (Yamaguchi *et al*., 2007). Inhibition of cofilin 1 (CFL1) activity in carcinoma cells have shown to inhibit cell motility and invasiveness via actin depolymerisation resulting in an increase in disorganized actin microfilaments (Feldner and Brandt, 2002). Cofilin plays a key role in epithelial-mesenchymal transition (EMT), however, its net effect on EMT is yet to be determined (Keshamouni and Schiemann, 2009). In glioblastoma cells, cofilin 1 has been shown to be up regulated resulting in an increase in the velocity of cell migration (Yamaguchi *et al*., 2007).

Cytoplasmic isoactins β was also downregulated. β-actin plays a role in the "ameboidal" type of movement, which is a characteristic of intravassation of cancer cells through the vessel wall (Khatilina, 2001; Peckham *et al.*, 2001). The increased expression of cytoplasmic β-actin is found in some tumour cells (Le *et al.,* 1998; Nowak *et al.,* 2005; Nguyen *et al.,* 2000). The level of β-actin is higher in invasive cell lines of sarcoma compared with non-invasive ones. There is a distinct correlation between the metastatic capacity of cancer cells and the state of actin polymerization, actin cytoskeleton organization and the β-actin expression.

Four different proteins down regulated by a magnitude of 2.4-3.1 and 1.6-1.9 fold with si*hTERT* and si*hsp90α*, respectively, were identified as vimentin. These spots had the same theoretical molecular weights and pI values suggesting that there may be post translational modifications, degradation or cross-linking to other proteins.

Post translational modifications play an important role in regulating the expression of vimentin. Vimentin can exist in multiple phosphorylated and non-phosphorylated forms (Ando *et al*., 1989; Chou *et al*., 1991; Huang *et al*., 1994). Phosphorylated vimentin is suggested to be an indicator of non-aggressiveness and/or non-invasiveness in certain tumours. Studies on colorectal cancers have shown that vimentin proteins are present in highly methylated forms (Shirahata *et al*., 2009). In addition to the four identified vimentin, a fifth spot was identified as vimentin variant 3 which was significantly up regulated by a magnitude of 4 in U87-MG-si*hTERT* cell lines. Thus, these results open up new avenues for a possible involvement of telomerase in the regulation of the phosphorylated/ methylation status of these intermediatory filaments.

Vimentin is the major intermediate filament cytoskeletal protein and is involved in a wide range of cellular activities. Intermediate filaments play an important role in cell motility and movement (Katsumoto *et al*., 1990), responding to mechanical stresses (Thoumine *et al*., 1995) stabilising cytoskeletal interactions and maintaining the integrity of the cytoplasm. It also plays a role in mechanosensitive signaling, apoptosis, immune defence and regulation of genomic DNA (Wang *et al*., 1993; Ingber, 1997). Vimentin plays a role in tumour development, progression, and chemosensitivity (Ngan *et al*., 2007; Zajchowski *et al*., 2001; Penuelas *et al*., 2005). Vimentin belongs to glioma specific extracellular matrix components and is involved in both neo-vascularization and invasion of malignant glial cells (Zhang *et al*., 2006). Interestingly, vimentin is a novel client protein of Hsp90α and inhibition of Hsp90α-vimentin binding results in an increase in apoptosis-induced stimulus making the cells more chemosensitive (Trog *et al*., 2006). Vimentin distribution is specific for mesenchymal tissue, however, in epithelial cancer cells, there is an aberrant expression of vimentin. This phenomenon is referred, as EMT, which results in the

acquisition of migratory and/or invasive properties. In several cancers, increase in its expression has been associated with increased invasiveness and metastasis (Hendrix *et al*., 1996; Hu *et al*., 2004). However, the use of vimentin as a tumour marker is controversial since the expression of vimentin is not always proportional to invasiveness and it depends on the cell lines being tested.

The expression of vimentin in different grades of glioma cell lines was investigated. The results indicated that the expression of vimentin in glioma cell lines was directly proportional to its grade. Furthermore, si*hTERT* decreased vimentin expression in a grade specific manner. These results complement the bioinformatics' prediction for vimentin as a potential tumour marker in glioma. Thus, silencing telomerase, could results in a decreased metastatic potential of the cells via vimentin. To confirm this hypothesis the expression of vimentin in tissue samples was investigated and our results showed that 9/12 glioblastoma tissues were positive for its expression, while vimentin was absent in normal cells or lower grade gliomas. However, unlike the cell lines, the expression of vimentin in the tissue samples did not show any correlation with the grade of the tissue specimens used. Vimentin has been shown to be upregulated in glioma cells under irradiation and temozolomide treatment and has been associated with clinical tumour relapse and drug resistance (Trog *et al*., 2008). Hence, inhibition of telomerase could help to overcome the problem of drug resistance to some extent by decreasing the expression of vimentin and cyclophilins.

The expression of vimentin was checked in 15 tumour samples and 3 normal brain tisuue samples and with a view of establishing vimentin as a potential indicator of tumourogenesis in glioma its expression should be checked in a larger cohort of glioma tissue samples as well as normal brain samples.

CHAPTER 5

DISCUSSION

Multidrug resistance and tumour reoccurrence is very common in glioma in spite of the advances made in radiation therapy and chemotherapy. Advancement of telomerase as a therapeutic target has paved the way for taking this enzyme from *in vivo* and *in vitro* experiments to well designed clinical trials. Telomerase is an important molecular target of glioma due to its preferential expression in tumour cells. Although the importance of telomerase for tumour proliferation is well documented, very little is known about the downstream effect of telomerase on the various physiological and signaling pathways. The aim of this thesis was to silence telomerase at the genetic level with a view to highlight the changes caused in the cancer proteome and identify the potential downstream pathways controlled by telomerase in tumour progression and maintenance.

Human telomerase is a ribonucleoprotein complex composed of the catalytic subunit hTERT and the RNA component-hTR. Since *hTERT* is only found in telomerase positive cells, it is a precise measure of telomerase activity. The activity of telomerase can be regulated at multiple levels. One such aspect is the regulation of telomerase by various telomerase and/or telomere associated proteins which either mediate or regulate the association of telomerase with the telomere. Hsp90 is a key component of a multi chaperone complex. It is a significant target in the development of rational cancer therapy due to its role at the crossroads of multiple signaling pathways associated with cell proliferation and cell viability. Over-expression of Hsp90 is an important factor in the activation of telomerase via hTERT. Results from our laboratory have also shown that siRNA directed towards *hsp90α* not only completely silences *hsp90α* but results in almost 80% silencing of *hTERT*.

Hence, in this study two different approaches regulating telomerase activity were used in order to inhibit telomerase activity and to study the downstream effect of this

inhibition. Direct silencing of the catalytic subunit hTERT, by siRNA was used as the first regulatory mechanism to inhibit telomerase activity. The second approach involved an indirect mechanism of telomerase regulation by silencing the Hsp90α chaperone.

For over a decade genetic analysis has been an important tool in cancer research. The advent of proteomics can complement and contribute to the existing knowledge gained via these extensive genomic studies. Besides accurately identifying the cellular protein content in normal as well as diseased conditions, proteomics has the inherent advantage of identifying proteins that are the endpoints of various biological processes. This further emphasizes the importance of adapting high resolution proteomic studies to complement existing genomic data.

This is the first study which assessed the effect of inhibition of telomerase transcription (through RNAi) in glioma cell lines to understand its effect on the cancer proteome. It is evident from the results of this study that telomerase is involved in numerous cellular functions besides telomere maintenance. It is known that telomerase plays a role in tumour metastasis but the precise mechanism has still not been fully elucidated. Our study sheds a light on key role played by telomerase in glioma metastasis by affecting cytoskeletal molecules such as vimentin, CFL1, MRCL3 and ATCB. Novel data from this study suggest the potential involvement of telomerase in regulating the expression of vimentin at proteomic as well as genomic levels. This study reveals that telomerase plays a role in cellular metabolism as observed by the changes in the GAPDH, it is closely involved in post transcriptional mechanisms as observed by the change in the levels of elongation factors, ribosomal proteins and various other receptor proteins and hence plays a role in cellular fate making decisions. Telomerase also assists in decreasing the protein levels of vimentin and cyclophilins which contributes to cell

tumorigenicity. These findings also suggest that caution should be exercised regarding the use of GAPDH as a housekeeping gene. Proteomics is an important tool to study the downstream effect of telomerase and it will be interesting to further investigate the effect of telomerase on the cytoskeletal associated proteins reported in this study with a view to substantiate direct evidence.

Despite the upregulation of various proteins that might make the glioma cells chemoresistant, such as ANXA1, RAN and laminin receptor, the inhibition of telomerase could emerge as an effective anti-cancer therapy. Interestingly, green tea polyphenol, Epigallocatechin-3-gallate, has been shown to induce its anticancer activity via 67LR and vimentin (Higashi *et al*., 2005; Umeda *et al*., 2008). ECGC is known to reduce telomerase activity and increase cell viability in glioma cells (Shervington *et al*., 2009). ECGC can thus, chemosensitize glioma cells more effectively by affecting the 67LR and phosphorylating vimentin. This can be used as an adjuvant therapy along with silencing telomerase with a view of overcoming the side effects of inhibiting telomerase. Combining telomerase inhibition with natural products such ECGC or chemotherapeutic drugs like cisplatin, could help to overcome the shortcomings of telomerase inhibition and significantly decrease cell viability. Glioma is one of the most intricate cancers and it does not follow predictable and repeatable pathways. There is no single treatment effective against glioma. Phenomena like adeptness at rewiring molecular circuitry and development of multi-drug resistance, a deficiency of preclinical models and difficulties posed by the blood brain barrier, makes glioma one of the most complex cancers. Although, combination therapy has been proven to be successful for a number of cases, the quality of the patient's life may be compromised due to the high dose of toxic drugs. Thus, the enthusiasm for applying non toxic regimes like the inhibition of telomerase via RNAi technology and use of natural drugs

can be justified, especially when they can produce comparable results to those obtained by chemotherapeutic drugs.

This approach of of silencing telomerase at the genetic level, using two different regulatory mechanisms and studying its subsequent effect on the cancer proteome was novel and shed light on potentially new roles of telomerase in the regulation of tumour metastasis via cystoskeletal proteins. Progressing knowledge of the downstream pathways regulated by telomerase will be instrumental in building a network of complementary targets for intervention, biomarker discovery, patient selection and prognosis of glioma.

Future Work

It will be advantageous to study the relationship between telomerase and the cytoskeletal proteins identified in this study, especially vimentin. Morphological studies should be carried out on different grades of glioma cell lines after silencing *hTERT* individually as well as in combination with the silencing of vimentin.

With a view of establishing vimentin as a potential biomarker for glioma, the expression of vimentin should be checked in a larger cohort of glioma tissue samples as well as normal brain samples. The efforts of Brain Tumour Northwest (BTNW) in setting up a brain bank should enhance the availability of sample size and thus reduce these limitations.

The results obtained from this study have shown that the inhibition of telomerase via RNAi technology and natural drugs such as ECGC, produce comparable results to those obtained by chemotherapeutic drugs. To enhance the therapeutic potential of telomerase, a combinational approach of telomerase inhibition and natural drugs should

be studied in more detail. The possible implication of such methods as adjuvant therapy to overcome drug resistance in glioma will reduce the therapeutic side-effects in glioma and greatly improve the quality of life of the patient.

While studying the downstream effect of telomerase inhibition, a new mode of action of ECGC via *hTERT* and *hsp90α* was discovered. The alteration in the expression of 67LR and vimentin that are the key targets of ECGC as well as the effect of EGCG on the cell viability, telomerase expression and chemosensitivity in glioma led us to investigate the possible relationship between ECGC, *hTERT* and *hsp90α*. A preliminary bioinformatics analysis was carried out to confirm to this speculation. The promoter sequences of *hTERT* and *hsp90α* were retrieved using Transcriptional Regulatory Element Database (TRED). Using publically available signal scan program, AliBaba 2.1, these promoter sequences were analysed to identify the potential transcription factor binding sites present. The results indicated the presence of early growth response 1 (Egr-1) on both the promoter sequence (Fig 5.1). Egr-1, tumour suppressor protein has been reported to substantiate the effect of ECGC (Moon *et al.*, 2007; Cho *et al.*, 2007; Fu and Chen, 2006). However, the exact mechanism is unknown.

A.

B.

Figure 5.1. Potential transcription factor binding sites for Egr-1 present on the promoters of A) *hTERT* and B) *hsp90α* as generated by AliBaba 2.1.

These preliminary results have shed light on the mode of action of ECGC via the ribonucleoprotein enzyme telomerase and the molecular chaperone Hsp90α. However, a more thorough investigation is required to establish the concrete relationship between ECGC, hTERT, Hsp90α, vimentin, 67LR and Egr-1. Studying the interconnection between these molecules can lead to the development of a novel mechanistic pathway for the action of ECGC.

REFERENCES

Agrawal, N., Dasaradhi, P.V., Mohmmed, A., Malhotra, P., Bhatnagar, R.K., Mukherjee, S.K. RNA interference: biology, mechanism, and applications. Microbiol Mol Biol Rev. 2003;67(4):657-685.

Alaoui-Jamali, M.A. and Xu, Y.J. Proteomic technology for biomarker profiling in cancer: an update. J Zhejiang Univ Sci B. 2006;7(6):411-420.

Alban, A., David, S.O., Bjorkesten, L., Andersson, C., Sloge, E., Lewis, S., Currie, I. A novel experimental design for comparative two-dimensional gel analysis: two-dimensional difference gel electrophoresis incorporating a pooled internal standard. Proteomics. 2003;3(1):36-44.

Ando, S., Tanabe, K., Gonda, Y., Sato, C., Inagaki, M. Domain- and sequence-specific phosphorylation of vimentin induces disassembly of the filament structure. Biochemistry. 1989;28(7):2974-2979.

Andreeva, L., Heads, R., Green, C.J. Cyclophilins and their possible role in the stress response. Int J Exp Pathol. 1999;80(6):305-315.

Avilion, A.A., Piatyszek, M.A., Gupta, J., Shay, J.W., Bacchetti, S., Greider, C.W. Human telomerase RNA and telomerase activity in immortal cell lines and tumor tissues. Cancer Res. 1996;56(3):645-650.

Bagheri, S., Nosrati, M., Li, S., Fong, S., Torabian, S., Rangel, J., Moore, D.H., Federman, S., LaPosa, R.R., Baehner, F.L., Sagebiel, R.W., Cleaver, J.E., Haqq, C., Debs, R.J., Blackburn, E.H., Kashani-Sabet, M. Genes and pathways downstream of telomerase in melanoma metastasis. Proc Natl Acad Sci. 2006;103(30):11306-11311.

Baltimore, D. Our genome unveiled. Nature. 2001;409(6822):814-816.

Baumann, B., Berno, V., Porrini, D., Castiglioni, F., Campiglio, M., Casalini, P., Pupa, S.M., Balsari, A., Menard, S., Tagliabue, E. The 67 kDa laminin receptor increases tumor aggressiveness by remodeling laminin-1. Endocr Relat Cancer. 2005;12(2):393-406.

Behlke M A. Progress towards in vivo use of siRNAs. Mol Ther. 2006;13(4):644-670.

Bian, X.W., Xu, J.P., Ping, Y.F., Wang, Y., Chen, J.H., Xu, C.P., Wu, Y.Z., Wu, J., Zhou, X.D., Chen, Y.S., Shi, J.Q., Wang, J.M. Unique proteomic features induced by a potential antiglioma agent, Nordy (dl-nordihydroguaiaretic acid), in glioma cells. Proteomics. 2008;8(3):484-494.

Bourquin, J.P., Stagljar, I., Meier, P., Moosmann, P., Silke, J., Baechi, T., Georgiev, O., Schaffner, W. A serine/arginine-rich nuclear matrix cyclophilin interacts with the C-terminal domain of RNA polymerase II. Nucleic Acids Res. 1997;25(11):2055-2061.

Bradford, M.M. A rapid and sensitive method for the quantitation of microgram quantities of protein utilizing the principle of protein-dye binding. Anal Biochem. 1976;72:248-254.

Bradshaw, R.A. Revised draft guidelines for proteomic data publication. Mol Cell Proteomics. 2005;4(9):1223-1225.

Cairney, C. J. and Keith, W. N. Telomerase redefined: integrated regulation of hTR and hTERT for telomere maintenance and telomerase activity. Biochimie. 2008;90(1):13-23.

Calado, R.T. and Chen, J. Telomerase: not just for the elongation of telomeres. Bioessays. 2006;28(2):109-112.

Carr, S., Aebersold, R., Baldwin, M., Burlingame, A., Clauser, K., Nesvizhskii, A., The need for guidelines in publication of peptide and protein identification data: Working Group on Publication Guidelines for Peptide and Protein Identification Data. Mol Cell Proteomics. 2004;3(6):531-533.

Castronovo, V. Laminin receptors and laminin-binding proteins during tumor invasion and metastasis. Invasion Metastasis. 1993;13(1):1-30.

Cech, T.R. and Reddel, R.R. Human POT1 facilitates telomere elongation by telomerase. Curr Biol. 2003;13(11):942-946.

Chalmers, M.J. and Gaskell, S.J. Anvances in mass spectrometry for proteome analysis. Curr Opin Biotechnol. 2000;11(4):384-90.

Chandramouli, K. and Qian, P.Y. Proteomics: Techniques and Possibilities to Overcome Biological Sample Complexity. Human Genomics and Proteomics. 2009;2009:1-23.

Changa, M.W., Grillaria, J., Mayrhoferb, C., Fortscheggera, K., Allmaierb, G., Marzbana, G., Katingera, H., Voglauer, R. Comparison of early passage, senescent and hTERT immortalized endothelial cells. Exp Cell Res. 2005;309(1):121-136.

Chen, J.X., Gao, Y., Liu, J.W., Tian, Y.X., Zhao, J., Cui, X.Y. Antitumor effects of human ribonuclease inhibitor gene transfected on B16 melanoma cells. Int J Biochem Cell Biol. 2005;37(6):1219-1231.

Chen S M, Tao Z Z, Hua Q Q, Xiao B K, Xu Y, Wang Y, Deng Y Q. Inhibition of telomerase activity in cancer cells using short hairpin RNA expression vectors. Cancer Invest. 2007;25(8):691-698.

Chen, X.S., Zhang, Y., Wang, J.S., Li, X.Y., Cheng, X.K., Zhang, Y., Wu, N.H., Shen, Y.F. Diverse effects of Stat1 on the regulation of hsp90alpha gene under heat shock. J Cell Biochem. 2007;102(4):1059-1066.

Chen, Y., Hakin-Smith, V., Teo, M., Xinarianos, G., Jellinek, D., Carroll, T., McDowell, D., MacFarlane, M., Boet, R., Baguley, B.C., Braithwaite, A., Reddel, R., Royds, J. Association of mutant TP53 with alternative lengthening of telomeres and favourable prognosis in glioma. Cancer Res. 2006;66(13)6473-6476.

Chen S M, Tao Z Z, Hua Q Q, Xiao B K, Xu Y, Wang Y, Deng Y Q. Inhibition of telomerase activity in cancer cells using short hairpin RNA expression vectors. Cancer Invest. 2007;25(8):691-698.

Chi, J.T., Chang, H.Y., Wang, N.N., Chang, D.S., Dunphy, N., Brown, P.O. Genome-wide view of gene silencing by small interfering RNAs. Proc Natl Acad Sci U S A. 2003;100(11):6343-6346.

Cho, C.Y., Wang, J.H., Chang, H.C., Chang, C.K., Hung, W.C. Epigenetic inactivation of the metastasis suppressor RECK enhances invasion of human colon cancer cells. J Cell Physiol. 2007;213(1):65-69.

Choi, K.J., Piao, Y.J., Lim, M.J., Kim, J.H., Ha, J., Choe, W., Kim, S.S. Overexpressed Cyclophilin A in Cancer Cells Renders Resistance to Hypoxia- and Cisplatin-Induced Cell Death. Cancer Res. 2007;67(8):3654-3662.

Chou, Y.H., Ngai, K.L., Goldman, R. The regulation of intermediate filament reorganization in mitosis. p34cdc2 phosphorylates vimentin at a unique N-terminal site. J Biol Chem. 1991;266(12):7325-7328.

Cohen, S.B., Graham, M.E., Lovrecz, G.O., Bache, N., Robinson, P.J., Reddel, R.R. Protein Composition of Catalytically Active Human Telomerase from Immortal Cells. Science. 2007;315(5820):1850-1853.

Colgin, L., Baran, K., Colinge, J., Masselot, A., Giron, M., Dessingy, T., Magnin, J. OLAV: towards highthroughput tandem mass spectrometry data identification. Proteomics. 2003;3(8):1454-1463.

Condeelis, J., Singer, R.H., Segall, J.E. The great escape: when cancer cells hijack the genes for chemotaxis and motility. Annu Rev Cell Dev Biol. 2005;21:695-718.

Cong, Y., Wright, W.E., Shay, J.W. Human Telomerase and Its Regulation. Microbiol Mol Biol Rev. 2002;66(3):407-425.

Cong, Y.S., Wen, J., Bacchetti, S. The human telomerase catalytic subunit hTERT: organization of the gene and characterization of the promoter. Hum Mol Genet. 1998;8(1)137-142.

Cristea, I.M., Gaskell, S.J., Whetton, A.D. Proteomics techniques and their application to hematology. Blood. 2004;103(10):3624-3634.

Crowe, D.L., Nguyen, D.C., Tsang, K.J., Kyo, S. E2F-1 represses transcription of the human telomerase reverse transcriptase gene. Nucleic Acids Res. 2001;29(13):2789-2794.

Cruickshanks, N., Shervington, L., Patel, R., Munje, C., Thakkar, D., Shervington, A. Can hsp90alpha-Targeted siRNA Combined With TMZ Be a Future Therapy for Glioma? Cancer Invest. 2010. DOI: 10.3109/07357901003630967.

Cuthbert, A.P., Bond, J., Trott, D.A., Gill, S., Broni, J., Marriott, A., Khoudoli, G., Parkinson, E.K., Cooper, C.S., Newbold, R.F. Telomerase Repressor Sequences on Chromosome 3 and Induction of Permanent Growth Arrest in Human Breast Cancer Cells. J Natl Cancer Inst. 1999;91(1):37-45.

Dang, C. and Jayasena, S.D. Oligonucleotide Inhibitors of Taq DNA polymerase Facilitate Detection of Low Copy Number Targets by PCR. J Mol Biol. 1996;264(2):268-278.

de Fougerolles A, Vornlocher H P, Maraganore J, Lieberman J. Interfering with disease: a progress report on siRNA-based therapeutics. Nat Rev Drug Discov. 2007;6(6):443-453.

Dieffenbach, C.W., Lowe, T.M.J., Dveksler, G.S. General concepts for PCR primer design. PCR Methods Appl. 1993;3(3):S30-S37.

Dimri G P, Lee X, Basile G, Acosta M, Scott G, Roskelley C, Medrano E E, Linskens M, Rubelj I, Pereira-Smith O. A biomarker that identifies senescent human cells in culture and in aging skin in vivo. Proc Natl Acad Sci U S A. 1995;92(20):9363-9367.

Dizhoor, A. Site-directed and natural mutations in studying functional domains in guanylyl cyclase activating proteins (GCAPs). Adv Exp Med Biol. 2002;514:291-301.

Dome, J.S., Chung, S., Bergemann, T., Umbricht, C.B., Saji, M., Carey, L.A., Grundy, P.E., Perlman, E.J., Breslow, N.E., Sukumar, S. High telomerase reverse transcriptase (hTERT) messenger RNA level correlates with tumor recurrence in patients with favorable histology Wilms' tumor. Cancer Res. 1999;59(17):4301-4307.

Domon, B. and Aebersold, R. Mass spectrometry and protein analysis. Science. 2006;312(5771):212-221.

Dubey, H. and Grover, A. Current initiatives in proteomics research: the plant perspective. Current Science. 2001;80(2): 262-269.

Duncan, M.W. and Hunsucker, S.W. Proteomics as a tool for clinically relevant biomarker discovery and validation. Exp Biol Med. 2005;230:808-817.

Eaton, L. World cancer rates set to double by 2020. BMJ. 2003;326(7392):728.

Elbashir SM, Lendeckel W, Tuschl T. RNA interference is mediated by 21- and 22-nucleotide RNAs. Genes Dev. 2001;15(2):188-200.

Elenitoba-Johnson, K.S.J. Complex Regulation of Telomerase: Activity Implications for Cancer Therapy. 2001;159:405-410.

Essader, A. S., Cargile, B. J., Bundy, J. L., Stephenson, J. L., Jr., A comparison of immobilized pH gradient isoelectric focusing and strong-cation-exchange chromatography as a first dimension in shotgun proteomics. Proteomics. 2005;5(1):24-34.

Fan, X., Wang, Y., Kratz, J., Brat, D.J., Robitaille, Y., Moghrabi, A., Perlman, E.J., Dang, C.V., Burger, P.C., Eberhart, C.G. hTERT Gene Amplification and Increased mRNA Expression in Central Nervous System Embryonal Tumours. Am J Pathol. 2003;62(6):1763-1769.

Fenstermacher, D. Introduction to Bioinformatics. JASIST. 2005;56(5):440-446.

Florens, L. and Washburn, M. P. Proteomic analysis by multidimensional protein identification technology. Methods Mol Biol. 2006;328:159-175.

Flores, I., Benetti, R., Blasco, M.A. Telomerase regulation and stem cell behaviour. Curr Opin Cell Biol. 2006;18(3):254-260.

Ford, L.P., Shay, J.W., Wright, W.E. The La antigen associates with the human telomerase ribonucleoprotein and influences telomere length in vivo. RNA. 2001;7(8):1068-1075.

Forsythe, H.L., Jarvis, J.L., Turner, J.W., Elmore, L.W., Holt, S.E. Stable association of hsp90 and p23, but Not hsp70, with active human telomerase. J Biol Chem. 2001;276(19):15571-15574.

Freshney, R. Culture of Animal Cells: A Manual of Basic Technique. Alan R. Liss, Inc., New York. 1987; pp 117.

Fu, Y. and Chen, A. The phyto-chemical (-)-epigallocatechin gallate suppresses gene expression of epidermal growth factor receptor in rat hepatic stellate cells in vitro by reducing the activity of Egr-1. Biochem Pharmacol. 2006;72(2):227-238.

Fujimoto, K., Kyo, S., Takakura, M., Kanaya, T., Kitagawa, Y., Itoh, H., Takahashi, M., Inoue, M. Identification and characterization of negative regulatory elements of the human telomerase catalytic subunit (hTERT) gene promoter: possible role of MZF-2 in transcriptional repression of hTERT. Nucleic Acids Res. 2000;28(13):2557-2562.

Geer, L.Y., Markey, S.P., Kowalak, J.A., Wagner, L., Xu, M., Maynard, D.M., Yang, X., Shi, W., Bryant, S.H. Open mass spectrometry search algorithm. J Proteome Res. 2004;3(5):958-964.

Godovac-Zimmermann, J. and Brown, L.R. Perspectives for mass spectrometry and functional proteomics. Mass Spectrom Rev. 2001;20(1):1-57.

Grabowski, D.T., Pieper, R.O., Futscher, B.W., Deutsch, W.A., Erickson, L.C., Kelley, M.R. Expression of ribosomal phosphoprotein PO is induced by antitumor agents and increased in Mer-human tumor cell lines. Carcinogenesis. 1992;13(2):259-263.

Griffith J D, Comeau L, Rosenfield S, Stansel R M, Bianchi A, Moss H, de Lange T. Mammalian telomeres end in a large duplex loop. Cell. 1999;97(4):503-514.

Guilleret, I. and Benhattar, J. Demethylation of the human telomerase catalytic subunit (hTERT) gene promoter reduced hTERT expression and telomerase activity and shortened telomeres. Exp Cell Res. 2003;289(2):326-334.

Gupta, D., Lammersfeld, C.A., Vashi, P.G., Dahlk, C., Grutsch, J.F., Lis, C.G. Is Serum Albumin an Independent Predictor of Survival in Ovarian Cancer? Clin Ovarian Cancer. 2009;2(1):52-56.

Gygi, S.P., Rist, B., Gerber, S.A., Turecek, F., Gelb, M.H., Aebersold, R. Quantitative analysis of complex protein mixtures using isotope-coded affinity tags. Nat Biotechnol. 1999;17(10):994-999.

Hanahan, D. and Weinberg, R.A. The hallmarks of cancer. Cell. 2000;100(1):57-70.

Handschumacher, R.E., Harding, M.W., Rice, J., Drugge, R.J., Speicher, D.W. Cyclophilin: a specific cytosolic binding protein for cyclosporin A. Science. 1984;226(4674):544-547.

Harada, K., Kurisu, K., Tahara, H., Tahara, E., Ide, T., Tahara, E. Telomerase activity in primary and secondary glioblastomas multiforme as a novel molecular tumour marker. J Neurosurg. 2000;93(4):618-625.

Harrington, L. A mammalian telomerase-associated protein. Science. 1997;275(5302): 973-977.

Hendrix, M.J., Seftor, E.A., Chu, Y.W., Trevor, K.T., Seftor, R.E. Role of intermediate filaments in migration, invasion and metastasis. Cancer Metastasis Rev. 1996;15(4):507-525.

Henson, J.D., Hannay, J.A., McCarthy, S.W., Royds, J.A., Yeager, T.R., Robinson, R.A., Wharton, S.B., Jellinek, D.A., Arbuckle, S.M., Yoo, J., Robinson, B.G., Learoyd, D.L., Stalley, P.D., Bonar, S.F., Yu, D., Pollock, R.E., Reddel R.R. A robust assay for alternative lengthening of telomeres in tumours shows the significance of alternative lengthening of telomeres in sarcomas and astrocytomas. Clin Cancer Res. 2005;11(1):217-225.

Henson, J.D., Neumann, A.A., Yeager, T.R., Reddel, R.R. Alternative lengthening of telomeres in mammalian cells. Oncogene. 2002;21(4):598-610.

Herms, J.W., Von Loewenich, F.D., Behnke, J., Markakis, E., Kretzschmar, H.A. c-myc oncogene family expression in glioblastoma and survival. 2005;27(1):131-141.

Higashi, N., Kohjima, M., Fukushima, M., Ohta, S., Kotoh, K., Enjoji, M., Kobayashi, N., Nakamuta, M. Epigallocatechin-3-gallate, a green-tea polyphenol, suppresses Rho signaling in TWNT-4 human hepatic stellate cells. J Lab Clin Med. 2005;145(6):316-322.

Hiyama, E. and Hiyama, K. Telomerase as tumor marker. Cancer Lett. 2003;194(2):221-233.

Hodes, R.J., Hathcock, K.S., Weng, N.P. Telomeres in T and B cells. Nat Rev Immunol. 2002; 2(9):699-706.

Holt, S.E. and Shay, J.W. Role of telomerase in cellular proliferation and cancer. J Cell Physiol. 1999;180(1):10-18.

Holt, S.E., Aisner, D.L., Baur, J., Tesmer, V.M., Dy, M., Ouellette, M., Trager, J.B., Morin, G.B., Toft, D.O., Shay, J.W., Wright, W.E., White, M.A. Functional requirement of p23 and Hsp90 in telomerase complexes. Genes & Dev. 1999;13(7):817-826.

Horikawa, I. and Barrett, J.C. Transcriptional regulation of the telomerase hTERT gene as a target for cellular and viral oncogenic mechanisms. Carcinogenesis. 2003;24(7):1167-1176.

Horikawa, I., Cable, P.L., Afshari, C., Barrett, J.C. Cloning and Characterization of the Promoter Region of Human Telomerase Reverse Transcriptase. Cancer Res. 1999;59(4):826-830.

Horikawa, I. and Barrett, J.C. Transcriptional regulation of the telomerase hTERT gene as a target for cellular and viral oncogenic mechanisms. Carcinogenesis. 2003;24(7):1167-1176.

Hu, L., Lau, S.H., Tzang, C.H., Wen, J.M., Wang, W., Xie, D., Huang, M., Wang, Y., Wu, M.C., Huang, J.F., Zeng, W.F., Sham, J.S., Yang, M., Guan, X.Y. Association of Vimentin overexpression and hepatocellular carcinoma metastasis. Oncogene. 2004;23(1):298-302.

Huang, G.P., Pan, Z.J., Huang, J.P., Yang, J.F., Guo, C.J., Wang, Y.G., Zheng, Q., Chen, R., Xu, Y.L., Wang, G.Z., Xi, Y.M., Shen, D., Jin, J., Wang, J.F. Proteomic analysis of human bone marrow mesenchymal stem cells transduced with human telomerase reverse transcriptase gene during proliferation. Cell Prolif. 2008;41:625-644.

Huang, T.J., Lee, T.T., Lee, W.C., Lai, Y.K., Yu, J.S., Yang, S.D. Autophosphorylation-dependent protein kinase phosphorylates Ser25, Ser38, Ser65, Ser71, and Ser411 in vimentin and thereby inhibits cytoskeletal intermediate filament assembly. J Protein Chem. 1994;13(6):517-525.

Ingber, D. Tensegrity I. Cell structure and hierarchical systems biology. J Cell Sci. 2003;116:1157-1173.

Inha, P., Hutter, G., Kottgen, E., Dietel, M., Schadendorf, D., Lage, H. Increased expression of annexin I and thioredoxin detected by two-dimensional gel electrophoresis of drug resistant human stomach cancer cells. J Biochem Biophys Methods. 1998;37(3):105-116.

Iwasaki ,T., Murata-Hori, M., Ishitobi, S., Hosoya, H. Diphosphorylated MRLC is required for organization of stress fibers in interphase cells and the contractile ring in dividing cells. Cell Struct Funct. 2001;26(6):677-683.

Janknecht, R. On the road to immortality: hTERT upregulation in cancer cells. FEBS Lett. 2004;564(1-2):9-13.

Jarvis R. and King A. Optimising chemical transfection and electroporation of siRNAs. Ambion TechNotes. 2003;10:12-15.

Jeyapalan, J.N., Varley, H., Foxon, J.L., Pollock, R.E., Jeffreys, A.J., Henson, J.D., Reddel, R.R., Royle, N.J. Activation of the ALT pathway for telomere maintenance can affect other sequences in the human genome. Hum Mol Genet. 2005;14(13):1785-1794.

Jiang, W.Q., Zhong, Z.H., Henson, J.D., Neumann, A.A., Chang, A.C.M., Reddel, R.R. Suppression of alternative lengthening of telomeres by Sp100-mediated sequestration of MRE11/RAD50/NBS1 complex. Mol Cell Biol. 2005;25(7):2708-2721.

Jimenez-Marin, A., Collado-Romero, M., Ramirez-Boo, M., Arce, C., Garrido, J.J. Biological pathway analysis by ArrayUnlock and Ingenuity Pathway Analysis. BMC Proc. 2009;3(4):S6.

Kang, S.S., Kwon, T., Kwon, D.Y., Do, S.I. Akt Protein Kinase Enhances Human Telomerase Activity through Phosphorylation of Telomerase Reverse Transcriptase Subunit. J Biol Chem. 1999;274(19):13085-13090.

Karlseder, J.D., Broccoli, Y., Dai, S., Hardy, S., de Lange, T. p53-and ATM-dependent apoptosis induced by telomeres lacking TRF2. Science. 1999;283(5406):1321-1325.

Katsumoto, T., Mitsushima, A., Kurimura, T. The role of the vimentin intermediate filaments in rat 3Y1 cells elucidated by immunoelectron microscopy and computer-graphic reconstruction. Biol Cell. 1990;68(2):139-146.

Keith, W.N., Bilsland, A., Evans, T.R., Glasspool, R.M. Telomerase-directed molecular therapeutics. Expert Rev Mol Med. 2002;4(10):1-25.

Keith, W.N., Thomson, C.M., Howcroft, J., Maitland, N.J., Shay, J.W. Seeding drug discovery: integrating telomerase cancer biology and cellular senescence to uncover new therapeutic opportunities in targeting cancer stem cells. Drug Discov Today. 2007;12(15-16):611-21.

Keshamouni, V.G. and Schiemann, W.P. Epithelial-mesenchymal transition in tumor metastasis: a method to the madness. Future Oncol. 2009;5(8):1109-1111.

Khalil, A.A. and Madhamshetty, J. Proteome Analysis of Whole-cell Lysates of Human Glioblastoma Cells During Passages. Res J Med Med Sci. 2006;1(4):120-131.

Khatilina, S. Functional specificity of actin isoforms. Int Rev Cytol. 2001;202:35-98.

Kilian, A., Bowtell, D.D., Abud, H.E., Hime, G.R., Venter, D.J., Keese, P.K., Duncan, E.L., Reddel, R.R., Jefferson, R.A. Isolation of a candidate human telomerase catalytic subunit gene, which reveals complex splicing patterns in different cell types. Hum Mol Genet.1997;6(12):2011-2019

Kim, S.H., Kaminker, P., Campisi, J. Telomeres, aging and cancer: in search of a happy ending. Oncogene. 2002;21(4):503-511.

Kim, T.D. PCR primer design: an inquiry-based introduction to bioinformatics on the World Wide Web. Biochem. Mol. Biol. Educ. 2000;28(5):274-276.

Kiyozuka, Y., Yamamoto, D., Yang, J., Uemura, Y., Senzaki, H., Adachi, S., Tsubura, A. Correlation of chemosensitivity to anticancer drugs and telomere length, telomerase activity and telomerase RNA expression in human ovarian cancer cells. Anticancer Res. 2000;20(1A):203-212.

Klose, J. Protein mapping by combined isoelectric focusing and electrophoresis of mouse tissues. A novel approach to testing for induced point mutations in mammals. Humangenetik. 1975;26(3):231-243.

Koller E. Competition for RISC binding predicts in vitro potency of siRNA. Nucleic Acids Res. 2006;34(16):4467-4476.

Komata, T., Kanzawa, T., Kondo, Y., Kondo, S. Telomerase as a therapeutic target for malignant gliomas. Oncogene. 2002;21(4):656-663.

Komata, T., Kondo, Y., Koga, S., Ko, S.C., Chung, L.W., Kondo, S. Combination therapy of malignant glioma cells with 2-5A-antisense telomerase RNA and recombinant adenovirus p53. Gene Ther. 2000;7(24):2071-2079.

Kondo, S., Tanaka, Y., Kondo, Y., Hitomi, M., Barnett, G.H., Ishizaka, Y., Liu, J., Haqqi, T., Nishiyama, A., Villeponteau, B., Cowell, J.K., Barna, B.P. Antisense telomerase treatment: induction of two distinct pathways, apoptosis and differentiation. FASEB J. 1998;12(10):801-811.

Kondo, T. and Hirohashi, S. Application of highly sensitive fluorescent dyes (CyDye DIGE Fluor saturation dyes) to laser microdissection and two-dimensional difference gel electrophoresis (2D-DIGE) for cancer proteomics. Nat. Protoc. 2007;1(6):2940-2986.

Kosciolek B A, Kalantidis K, Tabler M, Rowley P T. Inhibition of telomerase activity in human cancer cells by RNA interference. Mol Cancer Ther. 2003;2(3):209-216.

Kyo, S., Takakura, M., Fujiwara, T., Inoue, M. Understanding and exploiting hTERT promoter regulation for diagnosis and treatment of human cancers, Cancer Sci, 2008;99: 1528-1538.

Langford, L.A., Piatyszek, M.A., Xu, R., Schold, S.C.Jr., Shay, J.W. Telomerase activity in human brain tumours. Lancet. 2005;346 (8985):1267-1268.

Le, P.U., Nguyen, T.N., Drolet-Savoie, P., Leclerc, N., Nabi, I.R. Increased beta-actin expression in an invasive moloney sarcoma virus-transformed MDCK cell variant concentrates to the tips of multiple pseudopodia. Cancer Res. 1998;58(8):1631-1635.

Le, S., Sternglanz, R., Greider, C.W. Identification of two RNA-binding proteins associated with human telomerase RNA. Mol Biol Cell. 2000;11(13):999-1010.

Lee, G.E., Yu, E.Y., Cho, C.H., Lee, J., Muller, M.T., Chung, I.K. DNA-protein kinase catalytic subunit-interacting protein KIP binds telomerase by interacting with human telomerase reverse transcriptase. J Biol Chem. 2004;279(33):34750-34755.

Lee, M.K., Hande, M.P., Sabapathy, K. Ectopic mTERT expression in mouse embryonic stem cells does not affect differentiation but confers resistance to differentiation- and stress-induced p53-dependent apoptosis. J Cell Science. 2005,118(4):819-829.

Li, M., Zhai, Q., Bharadwaj, U., Wang, H., Li, F., Fisher, W.E., Chen, C., Yao, Q. Cyclophilin A is overexpressed in human pancreatic cancer cells and stimulates cell proliferation through CD147. Cancer. 2006;106(10):2284-2294.

Libermann, T.A., Nusbaum, H.R., Razon, N., Kris, R., Lax, I., Soreq, H., Whittle, N., Waterfield, M.D., Ullrich, A., Schlessinger, J. Amplification, enhanced expression and possible rearrangement of EGF receptor gene in primary human brain tumours of glial origin. Nature. 1985;313(5998):144-147.

Lim, L.H. and Pervaiz, S. Annexin 1: the new face of an old molecule. FASEB J. 2007;21(4):968-975.

Liu, J. Studies of the molecular mechanisms in the regulation of telomerase activity. FASEB Journal. 1999;13(15):2091-2104.

Liu, Y., Snow, B., Hande, M., Baerlocher, G., Yeung, D., Wakeham, D., Itie, A., Siderovski, D., Landsdorp, P.M., Robinson, M.O., Harrington, L. Telomerase-Associated Protein TEP1 Is Not Essential for Telomerase Activity or Telomere Length Maintenance In Vivo. Mol Cell Biol. 2000;20(21):8178-8184.

Loeffler-Ragg, J., Sarg, B., Mueller, D., Auer, T., Lindner, H., Zwierzina, H. Proteomics, a new tool to monitor cancer therapy? Memo. 2008;1(3):129-136.

Long, X., Olszewski, M., Huang, W., Kletzel, M. Neural cell differentiation in vitro from adult human bone marrow mesenchymal stem cells. Stem Cells Dev. 2005;14(1):65-69.

Mann, M. and Pandey, A. Use of mass spectrometry-derived data to annotate nucleotide and protein sequence databases. Trends Biochem Sci. 2001;26(1):54-61.

Mann, M., Hendrickson, R. C., Pandey, A. Analysis of proteins and proteomes by mass spectrometry. Annu Rev Biochem. 2001;70:437-473.

Mann, M., Hojrup, P., Roepstorff, P. Use of mass spectrometric molecular weight information to identify proteins in sequence databases. Biol Mass Spectrom. 1993;22(6):338-345.

Marouga, R., David, S., Hawkins, E. The development of the DIGE system: 2D fluorescence difference gel analysis technology. Anal Bioanal Chem. 2005;382(3):669-678.

Martignone, S., Menard, S., Bufalino, R., Cascinelli, N., Pellegrini, R., Tagliabue, E., Andreola, S., Rilke, F., Colnaghi, M.I. Prognostic significance of the 67-kilodalton laminin receptor expression in human breast carcinomas. J Natl Cancer Inst. 1993;85(5):398-402.

Martinez M. RNA interference and viruses: current innovations and future trends. Horizon Scientific Press. ISBN1904455565.

Mattei, T.A., Ramina, R., Tatagiba, M., Aguiar, P.H. Past, present and future perspectives of genetic therapy in gliomas. Indian J Hum Genet. 2005;11(1):4-13.

Mazzucchelli, G.D., Gabelica, V., Smargiasso, N., Fleron, M., Ashimwe, W., Rosu, F., Pauw-Gillet, M.D., Riou, J., Pauw, E.D. Proteome alteration induced by hTERT transfection of human fibroblast cells. Proteome Sci. 2008;6(12):1-13.

McClintock, B. The Behavior in Successive Nuclear Divisions of a Chromosome Broken at Meiosis. Proc Natl Acad Sci U S A. 1939;25(8):405-416.

Medzihradszky, K. F., Campbell, J. M., Baldwin, M. A., Falick, A.M., Juhasz, P., Vestal, M.L., Burlingame, A.L. The characteristics of peptide collision-induced dissociation using a high-perfformance MALDI-TOF/TOF tandem mass spectrometer. Anal Chem. 2000;72(3):552-558.

Minden, J. Comparative proteomics and difference gel electrophoresis. Biotechniques. 2007;43(6):739-745.

Mohammed, K. A study of gene expression in human normal and carcinogenic cell lines using qRT-PCR. Theses Collection 572.865/MOH University of Central Lancashire theses collection. 2007.

Mohammed, K. and Shervington, A. Can CYP1A1 siRNA be an effective treatment for lung cancer? Cell Mol Biol Lett. 2008;13(2):240-9.

Moller, H., Fairley, L., Coupland, V., Okello, C., Green, M., Forman, D., Moller, B., Bray, F. The future burden of cancer in England: incidence and numbers of new patients in 2020. Br J Cancer. 2007;96(9):1484-1488.

Moon, H.S., Lee, H.G., Choi, Y.J., Kim, T.G., Cho, C.S. Proposed mechanisms of (-)-epigallocatechin-3-gallate for anti-obesity. Chem Biol Interact. 2007;167(2):85-98.

Morii, K., Tanaka, R., Onda, K., Tsumanuma, I., Yoshimura, J. Expression of Telomerase RNA, Telomerase Activity, and Telomere Length in Human Gliomas. Biochem Biophys Res Commun. 1997;239(3):830-834.

Muller, H.J. The remaking of chromosomes. Collecting Net. 1938;13:181-195.

Nairn, A.C., Bhagat, B., Palfrey, H.C. Identification of calmodulin-dependent protein kinase III and its major Mr 100,000 substrate in mammalian tissues. Proc Natl Acad Sci U S A. 1985;82(23):7939-7943.

Nakamura, J., Aoyagi, S., Nanchi, I., Nakatsuka, S., Hirata, E., Shibata, S., Fukuda, M., Yamamoto, Y., Fukuda, I., Tatsumi, N., Ueda, T., Fujiki, F., Nomura, M., Nishida, S., Shirakata, T., Hosen, N., Tsuboi, A., Oka, Y., Nezu, R., Mori, M., Doki, Y., Aozasa, K., Sugiyama H., Oji, Y., Overexpression of eukaryotic elongation factor eef2 in gastrointestinal cancers and its involvement in g2/m progression in the cell cycle. Int J Oncol. 2009;34(5):1181-1189.

Nakamura M, Masutomi K, Kyo S, Hashimoto M, Maida Y, Kanaya T, Tanaka M, Hahn W C, Inoue M. Efficient inhibition of human telomerase reverse transcriptase expression by RNA interference sensitizes cancer cells to ionizing radiation and chemotherapy. Hum Gene Ther. 2005 ;16(7):859-868.

Ngan, C.Y., Yamamoto, H., Seshimo, I., Tsujino, T., Man-i, M., Ikeda, J.I., Konishi, K., Takemasa, I., Ikeda, M., Sekimoto. M., Matsuura, N., Monden, M. Quantitative evaluation of vimentin expression in tumour stroma of colorectal cancer. Br J Cancer. 2007;96(6):986-992.

Nguyen, T.N., Wang, H.J., Zalzal, S., Nanci, A., Nabi, I.R. Purification and characterization of beta-actin-rich tumor cell pseudopodia: role of glycolysis. Exp Cell Res. 2000;258(1):171-183.

Nicholson, J.P., Wolmarans, M.R., Park, G.R. The role of albumin in critical illness. Br J Anaesth. 2000;85(4):599-610.

Nittis, T., Guittat, L., Stewart, S.A. Alternative lengthening of telomeres (ALT) and chromatin: Is there a connection? Biochimie. 2008;90(1):5-12.

Novobrantseva T I, Akinc A, Borodovsky A, De Fougerolles A. Delivering silence: advancements in developing siRNA therapeutics. Curr Opin Drug Discov Devel. 2008;11:217–224.

Nowak, D., Skwarek-Maruszewska, A., Zemanek-Zboch, M., Malicka-Błaszkiewicz, M. Beta-actin in human colon adenocarcinoma cell lines with different metastatic potential. Acta Biochim Pol. 2005;52(2):461-468.

O'Farrell, P.H. High resolution two-dimensional electrophoresis of proteins. J Biol Chem. 1975;250(10):4007-4021.

Oh, S., Song, Y., Yim, J., Kim, T.k. The Wilms' tumor 1 tumor suppressor gene represses transcription of the human telomerase reverse transcriptase gene. J Biol Chem. 1999;274(52):37473-37478.

Ohgaki, H. and Kleihues, P. Epidemiology and etiology of gliomas. Acta Neuropathol. 2005;109(1):93-108.

Olovnikov, A.M. A theory of marginotomy. The incomplete copying of template margin in enzymic synthesis of polynucleotides and biological significance of the phenomenon. J Theor Biol. 1973;41(1):181-190.

Olsen, J.V., Ong, S.E., Mann, M. Trypsin cleaves exclusively C-terminal to arginine and lysine residues. Mol Cell Proteomics. 2004;3(6):608-614.

Ong, S.E., Blagoev, B., Kratchmarova, I., Kristensen, D.B., Steen, H., Pandey, A., Mann, M. Stable isotope labeling by amino acids in cell culture, SILAC, as a simple and accurate approach to expression proteomics. Mol Cell Proteomics. 2002;1(5):376-386.

Pardridge W M. shRNA and siRNA delivery to the brain. Adv Drug Deliv Rev. 2007;59(2-3):141-152.

Pappin, D.J., Hojrup, P., Bleasby, A.J. Rapid identification of proteins by peptide-mass fingerprinting. Curr Biol. 1993;3(6):327-332.

Patel, R., Shervington, L., Lea, R., Shervington, A. Epigenetic silencing of telomerase and a non-alkylating agent as a novel therapeutic approach for glioma. Brain Res. 2008;1188:173-181.

Peckham, M., Miller, G., Wells, C., Zicha, D., Dunn, G.A. Specific changes to the mechanism of cell locomotion induced by overexpression of beta-actin. J Cell Sci. 2001;114:1367-1377.

Pellish R S, Nasir A, Ramratnam B, Moss S F. RNA interference--potential therapeutic applications for the gastroenterologist. Aliment Pharmacol Ther. 2008;27(9):715-723.

Pendino, F., Tarkanyi. I., Dudognon, C., Hillion, J., Lanotte, M., Aradi, J., Segal-Bendirdjian, E. Telomeres and telomerase: Pharmacological targets for new anticancer strategies? Curr Cancer Drug Targets. 2006;6(2):147-180.

Penuelas, S., Noe, V., Ciudad, C.J. Modulation of IMPDH2, survivin, topoisomerase I and vimentin increases sensitivity to methotrexate in HT29 human colon cancer cells. FEBS J 2005; 272(3):696-710.

Phatak, P. and Burger, A.M. Telomerase and its potential for therapeutic intervention. Br J Pharmacol.. 2007;152(7):1003-1011.

Pillai, A.A., Bhattacharya, R.N., Radhakrishnan, V.V., Banerjee, M. Molecular signatures of cell cycle transcripts in the pathogenesis of Glial tumours. J Carcinog. 2004;3(1):11-17.

Pouratian, N., Asthagiri, A., Jagannathan, J., Shaffrey, M.E., Schiff, D. Surgery Insight: the role of surgery in the management of low-grade gliomas Nat Clin Pract Neurol. 2007;3(11):628-639.

Pulkkanen, K.J. and Yla-Herttuala, S. Gene therapy for malignant glioma: current clinical status. Mol Ther. 2005;12(4):585-598.

Py, B.F., Boyce, M., Yuan, J. A critical role of eEF-2K in mediating autophagy in response to multiple cellular stresses. Autophagy. 2009;5(3):393-396.

Robinson R. RNAi therapeutics: how likely, how soon? PLoS Biol. 2004;2(1):E28.

Ross, P.L., Huang, Y.N., Marchese, J.N., Williamson, B., Parker, K., Hattan, S., Khainovski, N., Pillai, S., Dey, S., Daniels, S., Purkayastha, S., Juhasz, P., Martin, S., Bartlet-Jones, M., He, F., Jacobson, A., Pappin, D.J. Multiplexed protein quantitation in

Saccharomyces cerevisiae using amine-reactive isobaric tagging reagents. Mol Cell Proteomics. 2004;3(12):1154-1169.

Rush, M.G., Drivas, G., D'Eustachio, P. The small nuclear GTPase Ran: how much does it run? Bioessays. 1996;18(2):103-112.

Schittenhelm, J., Trautmann, K., Tabatabai, G., Hermann, C., Meyermann, R., Beschorner, R. Comparative analysis of annexin-1 in neuroepithelial tumors shows altered expression with the grade of malignancy but is not associated with survival. Mod Pathol. 2009;22(12):1600-1611.

Schwartzbaum, J.A., Lal, P., Evanoff, W., Mamrak, S., Yates, A., Barnett, G.H., Goodman, J., Fisher, J.L. Presurgical serum albumin levels predict survival time from glioblastoma multiforme. J Neurooncol. 1999;43(1):35-41.

Seimiya, H. The telomeric PARP, tankyrases, as targets for cancer therapy. Br J Cancer. 2006;94(3):341-345.

Shaw, J., Rowlinson, R., Nickson, J., Stone, T., Sweet, A., Williams, K., Tonge, R. Evaluation of saturation labelling two-dimensional difference gel electrophoresis fluorescent dyes. Proteomics. 2003;3(7):1181-1195.

Shay, J.W. and Gazdar, A.F. Telomerase in the early detection of cancer. J. Clin. Pathol. 1997;50:106-109.

Shay J W, Roninson I B. Hallmarks of senescence in carcinogenesis and cancer therapy. Oncogene. 2004;23(16):2919-233.

Shervington, A. and Patel, R. Silencing DNA methyltransferase (DNMT) enhances glioma chemosensitivity. Oligonucleotides 2008;18(4):365-374.

Shervington, A., Cruickshanks, N., Wright, H., Atkinson-Dell, R., Lea, R., Roberts, G., Shervington, L. Glioma: What is the role of c-Myc, hsp90 and telomerase? Mol Cell Biochem. 2006;283(1-2):1-9.

Shervington, A., Mohammed, K., Patel, R., Lea, R. Identification of a novel co-transcription of P450/1A1 with telomerase in A549. Gene. 2007;388(1-2):110-116.

Shervington, A., Patel, R., Lu, C. Telomerase subunits expression variation between biopsy samples and cell lines derived from malignant glioma. Brain Research. 2007;11(34):45-52.

Shervington, A., Pawar, V., Menon, S., Thakkar, D., Patel, R. The sensitization of glioma cells to cisplatin and tamoxifen by the use of catechin. Mol. Biol. Rep. 2009;36(5):1181-1186.

Shi, Y., Zhai, H., Wang, X., Wu, H., Ning, X., Han, Y., Zhang, D., Xiao, B., Wu, K., Fan, D. Multidrug-resistance-associated protein MGr1-Ag is identical to the human 37-kDa laminin receptor precursor. Cell Mol Life Sci. 2002;59(9):1577-1583.

Shirahata, A., Sakata, M., Sakuraba, K., Goto, T., Mizukami, H., Saito, M., Ishibashi, K., Kigawa, G., Nemoto, H., Sanada, Y., Hibi, K. Vimentin methylation as a marker for advanced colorectal carcinoma. Anticancer Res. 2009;29(1):279-281.

Shmueli, O., Horn-Saban, S., Chalifa-Caspi, V., Shmoish, M., Ophir, R., Benjamin-Rodrig, H., Safran, M., Domany, E., Lancet, D. GeneNote: whole genome expression profiles in normal human tissues. C R Biol. 2003;326(10-11):1067-1072.

Sivan, G., Kedersha, N., Elroy-Stein, O. Ribosomal slowdown mediates translational arrest during cellular division. Mol Cell Biol. 2007;27(19):6639-6646.

Skynner, H.A., Amos, D.P., Murray, F., Salim, K., Knowles, M.R., Munoz-Sanjuan, I., Camargo, L.M., Bonnert, T.P., Guest, P.C. Proteomic analysis identifies alterations in cellular morphology and cell death pathways in mouse brain after chronic corticosterone treatment. Brain Res. 2006;1102(1):12-26.

Smogorzewska, A., Van., Steensel, B., Bianchi, A., Oelmann, S., Schaefer, M.R., Schnapp, G., de Lange, T. Control of human telomere length by TRF1 and TRF2. Mol. Cell. Biol. 2000;20(5):1659-1668.

Sobel, M.E. Differential expression of the 67 kDa laminin receptor in cancer. Semin Cancer Biol. 1993;4(5):311-317.

Srinivas, P.R., Verma, M., Zhao, Y., Srivastava, S. Proteomics for Cancer Biomarker Discovery. Clin Chem. 2002;48(8):1160-1169.

Sun, W., Xing, B., Sun, Y., Du, X., Lu, M., Hao, C., Lu, Z., Mi, W., Wu, S., Wei, H., Gao, X., Zhu, Y., Jiang, Y., Qian, X., He, F. Proteome Analysis of Hepatocellular Carcinoma by Two-dimensional Difference Gel Electrophoresis Novel Protein Markers in Hepatocellular Carcinoma Tissues. Mol Cel Proteomics. 2007;6(10):1798-1808.

Takakura, M., Kya, S., Kanaya, T., Hirano, H., Takeda, J., Yutsudo, M., Inoue, M. Cloning of Human Telomerase Catalytic Subunit (hTERT) Gene Promoter and Identification of Proximal Core Promoter Sequences Essential for Transcriptional Activation in Immortalized and Cancer Cells . Cancer Res. 1999;59(3):551-557.

Terrin, L., Trentin, L., Degan, M., Corradini, I., Bertorelle, R., Carli, P., Maschio, N., Bo, M.D., Noventa, F., Gattei, V., Semenzato, G., De Rossi, A. Telomerase expression in B-cell chronic lymphocytic leukemia predicts survival and delineates subgroups of

patients with the same igVH mutation status and different outcome. Leukemia. 2007;21(5):965-972.

Thakkar, D. and Shervington, A. Proteomics: the tool to bridge the gap between the facts and fables of telomerase. Crit Rev Oncog. 2008;14(4):203-215.

Thoumine, O., Ziegler, T., Girard, P.R., Nerem, R.M. Elongation of confluent endothelial cells in culture: the importance of fields of force in the associated alterations of their cytoskeletal structure. Exp Cell Res. 1995;219(2):427-441.

Timms, J.F. and Cramer, R. Difference gel electrophoresis. Proteomics. 2008;8(23-24):4886-4897.

Tohtong, R., Phattarasakul, K., Jiraviriyakul, A., Sutthiphongchai, T. Dependence of metastatic cancer cell invasion on MLCK-catalyzed phosphorylation of myosin regulatory light chain. Prostate Cancer Prostatic Dis. 2003;6(3):212-216.

Tonge, R., Shaw, J., Middleton, B., Rowlinson, R., Rayner, S., Young, J., Pognan, F., Hawkins, E., Currie, I., Davison, M. Validation and development of fluorescence two-dimensional differential gel electrophoresis proteomics technology. Proteomics. 2001;1(3):377-396.

Tomari Y, Zamore P. Perspective: machines for RNAi, Genes Dev. 2005;19(5):517-529.

Toogun, O.A., Dezwaan, D.C., Freeman, B.C. The hsp90 molecular chaperone modulates multiple telomerase activities. Mol Cell Biol. 2008;28(1):457-467.

Trog, D., Fountoulakis, M., Friedlein, A., Golubnitschaja, O. Is current therapy of malignant gliomas beneficial for patients? Proteomics evidence of shifts in glioma cells

expression patterns under clinically relevant treatment conditions. Proteomics. 2006;6(9):2924-2930.

Trog, D., Yeghiazaryan ,K., Schild, H.H., Golubnitschaja, O. Up-regulation of vimentin expression in low-density malignant glioma cells as immediate and late effects under irradiation and temozolomide treatment. Amino Acids. 2008;34(4):539-545.

Tuschl T, Zamore P D, Lehmann R, Bartel D P, Sharp P A. Targeted mRNA degradation by double-stranded RNA in vitro. Genes Dev. 1999;13(24):3191-3197.

Tzukerman, M., Shachaf, C., Ravel, Y., Braunstein, I., Cohen-barak, O., Yalon-hacohen, M., Skorecki, K.L. Identification of a Novel Transcription Factor Binding Element Involved in the Regulation by Differentiation of the Human Telomerase (hTERT) Promoter. Mol Bio Cell. 2000;11(12):4381-4391.

Ulaner, G.A., Hu, J., Vu, T.H., Giudice, L.C., Hoffman, A.R. Telomerase Activity in Human Development Is Regulated by Human Telomerase Reverse Transcriptase (hTERT) Transcription and by Alternate Splicing of hTERT Transcripts. Cancer Res. 1998;58(18):4168-4172.

Umeda, D., Yano, S., Yamada, K., Tachibana, H. Green tea polyphenol epigallocatechin-3-gallate signaling pathway through 67-kDa laminin receptor. J Biol Chem. 2008;283(6):3050-3058.

Unlu, M., Morgan, M.E., Minden, J.S. Difference gel electrophoresis: a single gel method for detecting changes in protein extracts. Electrophoresis. 1997;18(11):2071-2077.

Van den Bergh, G. and Arckens, L. Recent advances in 2D electrophoresis: an array of possibilities. Expert Rev Proteomics. 2005;2(2):243-252.

Venteicher, A.S., Abreu, E.B., Meng, Z., McCann, K.E., Terns, R.M., Veenstra, T.D., Terns, M.P., Artandi, S.E. A human telomerase holoenzyme protein required for Cajal body localization and telomere synthesis. Science. 2009;323(5914):644-648.

Venteicher, A.S., Meng, Z., Mason, P.J., Veenstra, T.D., Artandi, S.E. Identification of ATPases pontin and reptin as telomerase components essential for holoenzyme assembly. Cell. 2008;132(6):945-957.

Vestling, M.M. and Fenselau, C. Polyvinylidene difluoride (PVDF): an interface for gel electrophoresis and matrix-assisted laser desorption/ionization mass spectrometry. Biochem Soc Trans. 1994;22(2):547-551.

Walsh, C.T., Garneau-Tsodikova, S., Gatto, G.J. Jr. Protein posttranslational modifications: the chemistry of proteome diversifications. Angew Chem Int Ed Engl. 2005;44(45):7342-7372.

Wang, N., Butler, J.P., Ingber, D.E. Mechanotransduction across the cell surface and through the cytoskeleton. Science 1993;260(5111):1124-1127.

Wheeler, J.X., Wait, R., Stone, T., Wootton, L., Lewis, S., Fowler, S., Cummins, W.J. Mass spectrometric analysis of maleimide CyDye labelled model peptides. Rapid Commun Mass Spectrom. 2003;17(22):2563-2566.

Whiteley, G. Proteomic patterns for cancer diagnosis-promise and challenges. Mol Biosys. 2006;2:358-363.

Wilkins, M.R., Sanchez, J.C., Gooley, A.A., Appel, R.D., Humphery-Smith, I., Hochstrasser, D.F., Williams, K.L. Progress with proteome projects: why all proteins expressed by a genome should be identified and how to do it. Biotechnol Genet Eng Rev. 1996;13:19-50.

Wittwer, C., Hahn, M. and Kaul, K. Rapid cycle real-time PCR: methods and applications: quantification. Berlin; New York: Springer. 2004.

Wong, C.H., Chan, H., Ho, C.Y., Lai, S.K., Chan, K.S., Koh, C.G, Li, H.Y. Apoptotic histone modification inhibits nuclear transport by regulating RCC1. Nat Cell Biol. 2009;11(1):36-45.

Woo, I.S., Jang, H.S., Eun, S.Y., Kim, H.J., Ham, S.A., Kim, H.J., Lee, J.H., Chang, K.C., Kim, J.H., Han, C.W., Seo, H.G. Ran suppresses paclitaxel-induced apoptosis in human glioblastoma cells. Apoptosis. 2008;13(10):1223-1231.

Workman, P., Burrows, F., Neckers, L., Rosen, N. Drugging the cancer chaperone HSP90: combinatorial therapeutic exploitation of oncogene addiction and tumor stress. Ann N Y Acad Sci. 2007;1113:202-216.

Wright, W.E. and Shay W.J. Cellular senescence as a tumour-protection mechanism: the essential role of counting. Curr Opin Genet Dev. 2001;11(1):98-103.

Xu, W. and Neckers, L. Targeting the molecular chaperone heat shock protein 90 provides a multifaceted effect on diverse cell signaling pathways of cancer cells. Clin Cancer Res. 2007;13(6):1625-1629.

Yamaguchi, H. and Condeelis, J. Regulation of the actin cytoskeleton in cancer cell migration and invasion. Biochim Biophys Acta 2007; 1773(5):642-652.

Yang, J., Yang, J.M., Iannone, M., Shih, W.J., Lin, Y., Hait, W.N. Disruption of the EF-2 kinase/Hsp90 protein complex: a possible mechanism to inhibit glioblastoma by geldanamycin. Cancer Res. 2001;61(10):4010-4016.

Yates , J.R. 3rd., Carmack, E., Hays, L., Link, A.J., Eng, J.K. Automated protein identification using microcolumn liquid chromatography-tandem mass spectrometry. Methods Mol Biol. 1999;112:553-569.

Yates, J. R. 3rd., Speicher, S., Griffin, P. R, Hunkapiller, T. Peptide mass maps: A highly informative approach to protein identification. Anal Biochem. 1993;214(2):397-408.

Yates, J.R. 3rd., McCormack, A.L, Schieltz, D., Carmack, E., Link, A. Direct analysis of protein mixtures by tandem mass spectrometry. J Protein Chem. 1997;16(5):495-497.

Yi, X., Shay, J.W., Wright, W.E. Quantitation of telomerase components and hTERT mRNA splicing patterns in immortal human cells. Nucleic Acids Res. 2001;29(23):4818-4825.

Yin, L.T., Fu, Y.J., Xu, Q.L., Yang, J., Liu, Z.L., Liang, A.H., Fan, X.J., Xu, C.G. Potential biochemical therapy of glioma cancer. Biochem Biophys Res Commun. 2007;362(2):225-229.

You, Y., Pu, P., Huang, Q., Xia, Z., Wang, C., Wang, G., Yu, C., Yu, J.J., Reed, E., Li, Q.Q. Antisense telomerase RNA inhibits the growth of human glioma cells in vitro and in vivo. Int J Oncol. 2006;28(5):1225-1232.

Zajchowski, D.A., Bartholdi, M.F., Gong, Y., Webster, L., Liu, H.L., Munishkin, A., Beauheim, C., Harvey, S., Ethier, S.P., Johnson, P.H. Identification of gene expression profiles that predict the aggressive behavior of breast cancer cells. Cancer Res. 2001;61(13):5168-5178.

Zhang, J.T. and Liu, Y. Use of comparative proteomics to identify potential resistance mechanisms in cancer treatment. Cancer Treat Rev. 2007;33(8):741-756.

Zhang, M.H., Lee, J.S., Kim, H.J., Jin, D.I., Kim, J.I., Lee, K.J. Seo, J.S. HSP90 protects apoptotic cleavage of vimentin in geldanamycin-induced apoptosis. Mol Cell Biochem. 2006;281(1-2):111-121.

Zhou J, Rossi J J, Aptamer-targeted cell-specific RNA interference. Silence. 2010;1(1):4.

APPENDIX

1. 2D-DIGE spot Analysis report for U87-MG-si*hTERT*/U87-MG

Protein ID	Abundance	Volume Ratio	Max Slope	Area	Max Peak Height	Max Volume
1	Decreased	-1.66	0.74	408	3746	3.64E+05
2	Similar	1.49	0.69	467	2931	3.77E+05
3	Increased	2.83	0.82	522	4416	7.42E+05
4	Increased	2.81	0.70	554	10749	1.96E+06
5	Decreased	-1.52	0.89	198	1709	9.99E+04
6	Similar	1.34	0.70	342	2397	2.31E+05
7	Decreased	-1.57	0.48	418	1876	3.68E+05
8	Increased	1.55	0.50	286	868	6.70E+04
9	Increased	1.79	0.30	422	4309	6.52E+05
10	Increased	2.10	0.37	523	5376	9.24E+05
11	Increased	1.53	0.57	702	4909	7.51E+05
12	Increased	1.66	0.23	437	1496	3.30E+05
13	Decreased	-2.85	0.40	491	2342	4.91E+05
14	Decreased	-2.35	0.57	740	10020	2.60E+06
15	Increased	2.02	0.71	596	12676	2.77E+06
16	Increased	4.25	0.92	436	34704	3.39E+06
17	Decreased	-2.45	0.66	431	1576	2.00E+05
18	Decreased	-2.29	0.31	871	9284	2.47E+06
19	Decreased	-3.10	0.37	812	10228	2.71E+06
20	Increased	1.93	0.17	903	1586	4.59E+05
21	Decreased	-1.92	0.35	614	1472	3.74E+05
22	Similar	-1.50	0.22	491	746	3.77E+05
23	Decreased	-1.76	0.26	712	2634	6.94E+05
24	Increased	2.87	0.22	185	1119	1.18E+05
25	Increased	1.54	0.31	344	2109	3.47E+05
26	Decreased	-1.96	0.43	464	4277	5.02E+05
27	Decreased	-1.50	0.28	466	705	1.00E+05
28	Increased	1.53	0.45	471	1202	2.36E+05
29	Similar	-1.41	0.34	652	10801	2.31E+06
30	Similar	-1.38	0.19	813	2095	7.34E+05
31	Increased	2.01	0.18	335	1216	1.93E+05
32	Increased	2.54	0.28	557	728	1.28E+05
33	Increased	1.51	0.44	643	4720	1.34E+06
34	Decreased	-1.57	0.19	500	2429	5.44E+05
35	Increased	5.26	0.34	491	1198	2.15E+05
36	Increased	3.10	0.36	386	1222	2.35E+05
37	Similar	-1.46	0.16	672	1632	5.45E+05
38	Increased	2.74	0.20	492	391	8.73E+04
39	Decreased	-1.88	0.18	663	527	1.32E+05
40	Similar	1.21	0.14	771	517	1.15E+05
41	Increased	1.71	0.32	1302	5184	1.73E+06
42	Decreased	-1.51	0.17	984	1390	4.98E+05
43	Decreased	-3.22	0.17	518	754	1.60E+05
44	Decreased	-1.50	0.09	1057	480	1.84E+05
45	Decreased	-1.78	0.11	1100	700	2.63E+05
46	Decreased	-2.35	0.09	1117	375	1.91E+05
47	Increased	1.88	0.16	570	777	2.05E+05
48	Increased	1.70	0.12	697	422	9.68E+04
49	Decreased	-1.75	0.08	659	136	3.28E+04
50	Increased	1.54	0.19	1720	4546	1.73E+06
51	Similar	-1.17	0.36	549	17967	3.19E+06
52	Similar	-1.24	0.41	585	8516	2.29E+06
53	Decreased	-1.51	0.30	772	21263	4.49E+06
54	Increased	2.09	0.29	516	2793	5.66E+05

2. 2D-DIGE spot Analysis report for U87-MG- si *Hsp90α/* U87-MG

Protein ID	Abundance	Volume Ratio	Max Slope	Area	Max Peak Height	Max Volume
1	Similar	1.22	0.74	408	3746	3.64E+05
2	Similar	1.29	0.69	467	2931	3.77E+05
3	Increased	1.61	0.82	522	4416	7.42E+05
4	Increased	2.00	0.70	554	10749	1.96E+06
5	Similar	-1.15	0.89	198	1709	9.99E+04
6	Increased	1.65	0.70	342	2397	2.31E+05
7	Decreased	-1.50	0.48	418	1876	3.68E+05
8	Similar	1.19	0.50	286	868	6.70E+04
9	Increased	1.90	0.30	422	4309	6.52E+05
10	Increased	2.34	0.37	523	5376	9.24E+05
11	Similar	-1.26	0.57	702	4909	7.51E+05
12	Increased	1.67	0.23	437	1496	3.30E+05
13	Decreased	-1.89	0.40	491	2342	4.91E+05
14	Decreased	-1.60	0.57	740	10020	2.60E+06
15	Similar	1.34	0.71	596	12676	2.77E+06
16	Increased	1.81	0.92	436	34704	3.39E+06
17	Decreased	-1.65	0.66	431	1576	2.00E+05
18	Decreased	-1.57	0.31	871	9284	2.47E+06
19	Decreased	-1.71	0.37	812	10228	2.71E+06
20	Similar	-1.06	0.17	903	1586	4.59E+05
21	Decreased	-2.64	0.35	614	1472	3.74E+05
22	Decreased	-2.52	0.22	491	746	3.77E+05
23	Similar	-1.26	0.26	712	2634	6.94E+05
24	Similar	1.13	0.22	185	1119	1.18E+05
25	Similar	1.07	0.31	344	2109	3.47E+05
26	Similar	-1.37	0.43	464	4277	5.02E+05
27	Similar	-1.30	0.28	466	705	1.00E+05
28	Similar	1.00	0.45	471	1202	2.36E+05
29	Decreased	-1.62	0.34	652	10801	2.31E+06
30	Decreased	-1.67	0.19	813	2095	7.34E+05
31	Increased	1.83	0.18	335	1216	1.93E+05
32	Increased	2.14	0.28	557	728	1.28E+05
33	Similar	1.02	0.44	643	4720	1.34E+06
34	Similar	-1.47	0.19	500	2429	5.44E+05
35	Similar	1.17	0.34	491	1198	2.15E+05
36	Increased	1.78	0.36	386	1222	2.35E+05
37	Decreased	-1.62	0.16	672	1632	5.45E+05
38	Increased	2.25	0.20	492	391	8.73E+04
39	Similar	-1.45	0.18	663	527	1.32E+05
40	Increased	1.56	0.14	771	517	1.15E+05
41	Increased	1.67	0.32	1302	5184	1.73E+06
42	Similar	1.00	0.17	984	1390	4.98E+05
43	Similar	1.31	0.17	518	754	1.60E+05
44	Decreased	-1.92	0.09	1057	480	1.84E+05
45	Decreased	-2.14	0.11	1100	700	2.63E+05
46	Decreased	-2.20	0.09	1117	375	1.91E+05
47	Increased	1.97	0.16	570	777	2.05E+05
48	Similar	1.25	0.12	697	422	9.68E+04
49	Similar	-1.44	0.08	659	136	3.28E+04
50	Similar	1.10	0.19	1720	4546	1.73E+06
51	Similar	1.06	0.36	549	17967	3.19E+06
52	Similar	-1.22	0.41	585	8516	2.29E+06
53	Similar	-1.10	0.30	772	21263	4.49E+06
54	Decreased	-2.44	0.29	516	2793	5.66E+05

3. 2D-DIGE spot Analysis report volume/ratio summary

Spot No.	U87-MG-si*hTERT*/ U87-MG	U87-MG- si *Hsp90α*/ U87-MG
1	-1.66	1.22
3	2.83	1.61
4	2.81	2.00
5	-1.52	-1.15
6	1.34	1.65
7	-1.57	-1.50
8	1.55	1.19
9	1.79	1.90
10	2.10	2.34
11	1.53	-1.26
13	-2.85	-1.89
14	-2.35	-1.60
15	2.02	1.34
16	4.25	1.81
17	-2.45	-1.65
18	-2.29	-1.57
19	-3.10	-1.71
20	1.93	-1.06
21	-1.92	-2.64
22	-1.50	-2.52
24	2.87	1.13
25	1.54	1.07
26	-1.96	-1.37
27	-1.50	-1.30
28	1.53	1.00
29	-1.41	-1.62
30	-1.38	-1.67
31	2.01	1.83
32	2.54	2.14
33	1.51	1.02
34	-1.57	-1.47
35	5.26	1.17
36	3.10	1.78
37	-1.46	-1.62
38	2.74	2.25
39	-1.88	-1.45
40	1.21	1.56
41	1.71	1.67
42	-1.51	1.00
43	-3.22	1.31
44	-1.50	-1.92
45	-1.78	-2.14
46	-2.35	-2.20
47	1.88	1.97
48	1.70	1.25
49	-1.75	-1.44
50	1.54	1.10
51	-1.17	1.06
52	-1.24	-1.22
53	-1.51	-1.10
54	2.09	-2.44